Understanding the mechanisms and consequences of double-strand breaks induced by palindromic DNA sequences

A Dissertation
Presented to
The Academic Faculty

by

Ziwei Sheng

In Partial Fulfillment
of the Requirements for the Degree

Doctor of Philosophy
in the
School of Biological Sciences

Georgia Institute of Technology
May, 2017

Copyright © Ziwei Sheng

Understanding the mechanisms and consequences of DSB induced by palindromic DNA sequences

Approved by:

Dr. Kirill S. Lobachev, Advisor
School of Biological Sciences
Georgia Institute of Technology

Dr. Harold Kim
School of Physics
Georgia Institute of Technology

Dr. Yury Chernoff
School of Biological Sciences
Georgia Institute of Technology

Dr. Fredrik Vannberg
School of Biological Sciences
Georgia Institute of Technology

Dr. Francesca Storici
School of Biological Sciences
Georgia Institute of Technology

Date Approved: Mar 31st, 2017

ACKNOWLEDGEMENTS

I would like to express my heartfelt gratitude towards my advisor Dr. Kirill Lobachev. I have very high regard for him as he introduced me to the stimulating field of DNA repair, educated and supported me so many years. I would also want thank Dr. Natasha Degtyareva for her kind, valuable help and suggestions during my study.

I am also highly thankful to all my committee members, Dr. Yuri Chernoff, Dr. Francesca Storici, Dr. Harold Kim and Dr. Fredrik Vannberg for their valuable suggestions during the course of Ph.D.

I would like to thank all the members of my lab. Their constant help and support were extremely valuable in both my research and my life. I hold their friendship in high esteem and will be forever grateful to them.

I would like to extend a special thanks to my husband, my family and my friends for always supporting me.

TABLE OF CONTENTS

LIST OF TABLES

LIST OF FIGURES

LIST OF SYMBOLS AND ABBREVIATIONS

Alu-QP	Inverted *Alu* Repeats
Alu-PAL	*Alu* perfect palindrome
BIR	Break-induced replication
CAN	L-Canavanine
CHEF	Contour-clamped Homogeneous Electric Field
CDK	Cyclin-dependent kinase
CP	Centromere-proximal
DSB	Double Strand Break
FACS	Fluorescence-activated cell sorting
GCR	Gross Chromosomal Rearrangement
IS50-PAL	Palindromic *IS50* repeats
MMS	Methyl-methane Sulfonate
MRX	Mre11-Rad50-Xrs2
PCR	Polymerase Chain Reaction
SDSA	Synthesis Dependent Strand Annealing
SSA	Single-Strand Annealing

ssDNA	Single-stranded DNA
TD	Telomere-distal
TLS	Translesion Synthesis
TP	Telomere-proximal
URA3-PAL	*URA3* perfect palindrome
URA3-QP	*URA3*-quasi-palindrome
2D gel	Two-dimensional Gel Electrophoresis

SUMMARY

Palindromic DNA sequences, capable of forming hairpin or cruciform structures, are often a potent sources of genome instability by inducing double strand breakage (DSB).

Studies on palindrome-induced instability have proposed several mechanisms in which different nucleases, responsible for inducing DSBs at the repeats, are involved. The lack of consensus from the conclusions drawn from these studies can be attributed to a variety of factors, such as using different model organisms and repeats with various features. Here, I systematically demonstrate that there are three pathways governing the instability at palindromic repeats. Sae2-MRX nuclease plays a dual role of recognizing and attacking structures forming at perfect palindromic repeats during replication and processing and opening hairpin-capped ends for resection. However, Sae2-MRX does not affect quasi-palindrome fragility. Structure-specific endonuclease Mus81-Mms4 is responsible for inducing DSB at transcription-active palindromes in G2 stage of cell cycle and results in hairpin-capped breaks. The third pathway, which is Sae2-MRX- and Mus81-Mms4-independent, also happens in G2 stage and is under control of cell cycle kinase Cdc28 and LSm proteins that are involved in mRNA degradation.

Moreover, I demonstrated that palindromes induce mutagenesis in the surrounding regions and Sae2-MRX-induced DSBs are channeled into break-induced replication (BIR). The synthesis intermediate with BIR characteristics, 'bubble'-shape, was detected at both sides of breakage and at distances over 100kb

away, indicating that the broken ends can anneal to the complementary strand on both Watson and Crick strands using repeat's homology and initiate bidirectional BIR. The progression of BIR is stable and bypasses replication origins and the centromere. We also analyzed the players involve in palindrome-induced BIR and found that Pif1 helicase and Rad52 recombinase are required during the process. This study provides a systematic and mechanistic insight into the palindrome-induced genome instability.

In another study, I participated in collaboration study with Dr. Anna Malkova's laboratory in University of Iowa, we demonstrated that Srs2 helicase is involved in resolving toxic recombination intermediates during HO endonuclease-induced BIR. I showed that complex DNA structures other than 'bubble'-like BIR structures are accumulated in *srs2Δ* mutants by two-dimensional gel electrophoresis. In *srs2Δ mus81Δ* double mutant, we can observe structures resemble 'X'-shape recombination intermediates, indicating that Mus81/Mms4 is involved in resolving the recombination intermediates in the absence of Srs2. This study proposed the important role of the Srs2 helicase in break-induced repair.

Chapter 1 Introduction

1.1 Introduction and literature review

1.1.1 Palindromic Sequences can adopt non-B DNA structures

Human genome is affected consistently by exogenous DNA damaging agents, such as chemical mutagens, radiation, and reactive oxygen species. The effects of these agents on chromosomal integrity, such as generation of double-strand breakage (DSB) and mutagenesis, have been identified and well characterized. Besides exogenous factors, genomic stability is also under the threat of endogenous ones, for example, unstable DNA repeats. More than 50% of human genome consists of repetitive sequences, a subset of which can adopt different classes of non-canonical structures, such as hairpin, cruciform, G-quadruplex, triplex and Z-DNA (Lander et al., 2001)(Sinden et al., 1994).

One class of the repetitive sequences, DNA palindromes, are capable of forming hairpin or cruciform structures. Perfect DNA palindromes contain perfectly symmetrical sequences that are identical when read from both 5' to 3' in corresponding strands. In quasi-palindromes, the two symmetrical arms are separated by a spacer.

A hairpin is formed when palindrome repeat is present in form of single stranded DNA, which allow for random intrastrand collision. The generation of single-stranded DNA is common during lagging strand synthesis in replication; single-stranded DNA is coated by RPA during Okazaki fragment synthesis. The length of spacer also affects the formation of the hairpin. Palindromes with long spacers that exceed the length of the Okazaki fragments have a lower probability of

self-annealing. The length of the pair arms and divergence of sequence composition between them might also be factors of structure stability.

Cruciform formation, however, is more complicated process, compared to hairpin formation since the initiation of an extrusion requires dissociation of the hydrogen bonds and forming new ones after self-annealing. The negative supercoiling generated during DNA metabolism can facilitate this process. In *E.coli*, extrusion of cruciform at a loci containing a 322 base-pair, imperfect palindromic insert can be detected on the plasmids (Dickie et al., 1987). In eukaryotes, DNA is wrapped around nucleosomes which relax the negative supercoiling. However, supercoiling forces can be generated during transcription to an extent that they impair the progression of RNA polymerases through rDNA in absence of topoisomerases in yeast (French et al., 2011). Negative DNA supercoiling driving cruciform formation in a chromosomal context, can be also generated by chromatin remodeling complexes (Havas et al., 2000).

1.1.2 Palindromic sequences and genome instability

Palindromic sequences, with their predisposition to form non-B DNA structures, are often a potent sources of genome instability. It has been shown that in *E. coli*, palindromes cannot be propagated in the wild-type strains on the plasmids (reviewed in Leach 1994). When palindromes are inserted into *E. coli* chromosome, they are often deleted, and induce DSBs and homologous recombination (Connelly and Leach, 1996; Cromie et al., 2000; Darmon et al., 2010; Eykelenboom et al., 2008). and mitotic recombination. Palindromes and long

inverted repeats were shown to induce allelic and ectopic recombination, crossing-overs and GCRs in baker and fission yeast, and mice (Gordenin et al., 1993; Lemoine et al., 2005; Lobachev et al., 2002; Lobachev et al., 1998b; Lobachev et al., 2000; Narayanan et al., 2006; Ruskin and Fink, 1993; St Charles and Petes, 2013; Waldman et al., 1999).

In human genome, the palindromic AT-rich repeats(PATRRs) were shown to induce recurrent constitutional translocations involving chromosome 8, 11, 17 and 22. The most frequent non-Robertsonian translocation, t(11;22)(q23;q11), leads to Emanuel syndrome (Kehrer-Sawatzki et al., 1997; Kurahashi et al., 2003; Sheridan et al., 2010). It was also shown that large deletions mediated by palindromes can lead to εγδβ thalassemia (Rooks et al., 2012), X-linked congenital hypertrichosis syndrome (Zhu et al., 2011) and hereditary renal cell carcinoma (Kato et al., 2014). Palindromic sequences were also implicated in promoting tumorigenesis in colon and breast cancer, medulloblastoma and lymphoma by triggering gene amplification in the manner of recombination-dependent amplification and/or breakage-fusion-bridge cycles (Amler and Schwab, 1989; Guenthoer et al., 2012; Kuwahara et al., 2004; Mangano et al., 1998; Murnane, 2006; Neiman et al., 2006; Neiman et al., 2008; Tanaka et al., 2005, 2006; Tanaka et al., 2007)

1.1.3 Mechanisms of palindrome-induced instability

Mechanisms of palindrome-induced instability are explored in different model organisms, both prokaryotic and eukaryotic and many conclusions have been

drawn. However, some results contradict each other, possibly due to differences in the mechanisms of maintenance of genomic instability in different species, as well as different structural feature of studied palindromes. Additionally, it is clear that the list of factors involved in the regulation of palindrome-induced instability has not been fully explored yet.

Experiments done in *E.coli* have shown that DNA palindromes inserted into the bacterial chromosome can form hairpin structures on lagging strand during replication. Such structures are the targets for SbcCD nuclease that generates DSBs leading to palindrome instability. Consequently, long palindromes can be stably propagated on the plasmids in sbcCD mutants (reviewed in Leach 1994). Similarly to bacteria, Mre11/Rad50/Nbs1, the SbcCD homolog in *S. pombe*, has been shown to be responsible for the mitotic recombination at a short 160bp perfect palindrome (Farah et al., 2002) and DSB formation at repeats during premeiotic stage (Joseph et al., 2004). Conversely, in yeast *S. cerevisiae*, Mre11/Rad50/Xrs2 (MRX), together with another structure-specific nuclease, Pso2, has hairpin-opening endonuclease activity when processing hairpin-capped breaks; however, MRX has no effect on generating DSBs at the loci of quasi-palindromes (Lobachev et al., 2002; Tiefenbach and Junop, 2012). Moreover, SbcCD homolog in human, MRN, together with the protein CtIP, was suggested to process DSB ends generated at common fragile sites (CFSs) and at palindromic repeats which are mitotic recombination hotspots (Wang et al., 2014)

Structure-specific nucleases that are involved in processing of the Holliday junction (HJ) during DNA repair are also suggested to play a role in DSB

formation at loci containing palindromic repeats since the cruciform resembles HJ structurally. Gen1, the homolog of Yen1 in yeast, exhibits the activity of symmetrical cleavage at synthetic HJ (Ip et al., 2008) and four-way junctions (Blanco et al., 2010). When GEN1 is knocked down in HEK293 cells by siRNA, cleavage at the palindromic AT-rich repeats (PATRRs) loci on plasmids decreases while other structure-specific nuclease complexes such as Slx1-Slx4 and Mms4-Mus4 had no effect (Inagaki et al., 2013). Slx1-Slx4, belonging to URI-YIG family of endonucleases, was tested and shows some activity towards mobile HJs and lower activity on fixed HJ substrate; however, the cleavage pattern is asymmetric across all arms and the breaks are not suitable for ligation (Fricke and Brill, 2003). Another structure-specific nuclease complex Mus81-Mms4, conserved in multiple organisms (Mus81-Eme1 in *S.pombe*, *D. melanogaster*, and human), is involved in resolving branched molecules during stalled replication and meiotic recombination (Schwartz and Heyer, 2011). Cote et al. suggest that Mus81-Mms4 is able to recognize extruded cruciform structure formed on plasmids by palindrome (Cote and Lewis, 2008) however the exact nature of the structure formed was not determined. Biochemical analysis of Mus81-Mms4/Eme1 shows that, regardless of the organisms the complex was purified from, it prefers DNA structure with a nick in proximity to branch point over cruciform or HJ structures with four contiguous strands (Ciccia et al., 2003). There is some disagreement about the activity of Mus81-Mms4 on HJs. One study shows that full-length protein has no role in cleavage of HJs (Chang et al., 2008) while the other one demonstrates that it has low activity on extruded cruciforms when given an excess amount of proteins and

substrates (Taylor and McGowan, 2008). Mlh1-Mlh3 complex is known for its activity in resolving crossover intermediates with Mus81-Mms4 and HJ-like molecules to generate crossovers in meiosis (de los Santos et al., 2003). The other meiosis-related nuclease, Spo11, attacks exclusively hairpin and cruciform structures formed during meiotic recombination (Keeney et al., 1997; Klapholz et al., 1985; Wagstaff et al., 1985). Cce1, known as *in vitro* cruciform-cutting-enzyme and residing on mitochondrial inner membrane recognizes and cleaves HJ formed during mitotic recombination of mitochondrial DNA (Ezekiel and Zassenhaus, 1993; Kleff et al., 1992).

1.1.4 Repair of palindrome-mediated DSB

Studies on palindrome-mediated DSB suggested multiple pathways of repair. In, E. coli, palindrome-mediated breaks occurring on the lagging strand are repaired via recBCD-depenedent and independent repair involving undamaged leading strand (Connelly and Leach, 1996; Eykelenboom et al., 2008). As a consequence, palindromes are maintained in chromosomal context. Alternatively, resected breaks can be repaired vis single-stranded annealing leading to palindrome deletion (Bzymek and Lovett, 2011). In yeast, it has been shown that broken ends at palindromic loci are protected by covalent hairpins which can be recognized and opened by MRX complex and Sae2 (Lobachev et al., 2002) and Pso2 (Tiefenbach and Junop, 2012). The role of Pso2 in opening hairpin structures generated by palindrome-induced DSB is auxiliary to that of MRX-Sae2 since hairpin structures are well preserved in *Δsae2* background (Lobachev et al., 2002). In the presence of

MRX-Sae2 complex, exposed ends might be recognized by telomerase followed by de novo telomere addition to establishing a shorter but stable chromosome (Kramer and Haber, 1993; Narayanan et al., 2006; Pennaneach et al., 2006). The broken end can also be repaired by break-induced replication (Malkova et al., 1996) in this pathway of the repair, resection of one strand of the DNA leads to generation of long single-stranded DNA which utilizes microhomology or repetitive sequence as the repair template (Narayanan et al., 2006). In the absence of the opening activity of MRX-Sae2, the hairpins are preserved until the intrastrand base pairings are removed by replication machinery and the hairpins are fully replicated into a new palindrome. There are two outcomes of the replication of the palindrome in absence of MRX-Sae2. When replication of the palindrome located at the end of the chromosome is directed towards and encounters the centromere such process results in appearance of the dicentric chromosome. When replication is directed towards telomere, such repair yields an extrachromosomal acentric fragment. The later cannot be maintained stably in dividing cells. The dicentric chromosome is prone to breakage during anaphase when two centromeres are drawn to opposite spindle poles The broken ends resulting from this breakage are subject to telomere addition, BIR or are engaged in the next cycle of breakage-fusion-bridge (Lobachev et al., 2002; Narayanan et al., 2006).

1.1.5 Break-induced replication is one of the error-prone DNA repair pathways

One of the pathways to repair DSB is through BIR in which one broken end of DSB invades into homologous sequences and copy DNA by the template. BIR

can stably proceeds hundreds of kbs on the donor chromosome to the telomere end. However, unlike *bona fide* S-phase replication, DNA synthesis through BIR leads to a great cost to the cell, such as mutagenesis, translocations, loss of heterozygosity, and copy number variations, which are hallmarks of carcinogenesis (Deem et al., 2008; Llorente et al., 2008; Malkova and Haber, 2012). It is demonstrated that, instead of employing a replication fork producing two semi-conservatively replicated DNA molecules, BIR proceeds through a D-loop that results in conservative inheritance of DNA. During BIR progression, long single-stranded DNA molecules identified by two dimensional gel electrophoresis are prone to damage which are responsible for BIR-associated mutations (Malkova and Ira, 2013; Saini et al., 2013a; Wilson et al., 2013).. In study using the site-specific recombinase Flp1H305L, a step arrest mutant form of Flp, to induce single strand nick that is later converted to DSB by replication fork, it is shown that BIR is involved to repair the DSB generated in S phase (Mayle et al., 2015).

1.2 Overview of dissertation

Palindromic DNA sequences that can form non-B DNA structures are potent DSBs inducers. Since breakage and imprecise repair events can hamper genome integrity, leading to genome rearrangements and mutagenesis, understanding of the mechanisms of DSB formation and repair at palindromic sequences is very important. *In vivo* and *in vitro* studies, employing different model organisms and focusing on different palindromic repeats have yielded many explanations on how DSBs are generated in the region containing the repeats;

however, very often conclusions of these studies contradict each other. Moreover, the repertoire of proteins involved in regulation of the genome stability at palindromic repeats is not fully explored since there is a class of DSBs that cannot be attributed to activity of any known nucleases. Recent studies suggest that break-induced repair is one of the outcomes of palindrome fragility. It persists for long distance and can be mutagenic. It remains unclear what factors are involved to ensure the progression of BIR and affect the accuracy of synthesis. This dissertation focuses on understanding the mechanisms by presenting three distinct pathways that regulate the DSB formation at different palindromic repeats which helps to understand the discrepancy of conclusions drawn from previous studies. Additionally, this study presents the evidence that BIR can be initiated at a breakpoint where palindrome resides, describes the features of this palindrome-induced BIR and compares it to BIRs in other studies.

To be more specific, this study presents an analysis of DSB formation at quasi- and perfect palindromes. We show that structure-specific nuclease MRX-Sae2 is partially accountable for generating DSBs at loci containing perfect palindromes while it is not responsible for breakage at quasi-palindromes. Structure-specific nuclease Mus81-Mms4 can recognize and attack structures formed by palindromic sequences consisted of two *URA3* genes with active transcription initiated at the center of symmetry. Aside from MRX-Sae2 and Mus81-Mms4 pathways, DSB formation is under control of another pathway in strains containing quasi-palindromes or perfect palindromes with deletion of Sae2 and Mus81.

This study also demonstrates that repair synthesis surrounding perfect palindrome is highly error prone and the mutagenesis is dependent on the nuclease MRX-Sae2 and translesion synthesis polymerase Polζ. The structural analysis reveals that the repair progresses as a typical bubble-like replication fork structure as seen in other break-induced replication studies. Moreover, such structures could be detected at a distance farther than 100 kb away from the initial break point, indicating that BIR proceeds even beyond replication origins and the centromere.

Chapter 2 Results and Discussion

2.1 Experimental system

The experimental system used to assess frequencies or rates of gross chromosomal rearrangements and mutations in strains containing inverted repeats in this study is based on the GCR assay described in several papers (Kim et al., 2008; Narayanan et al., 2006; Saini et al., 2013b; Zhang et al., 2013). The *LYS2* gene containing the inverted repeats is located 43kb away from the left arm telomere on chromosome V in haploid strains. *CAN1* gene is 8kb telomere-proximal to *LYS2* gene. *ADE2* is located between *CAN1* and *LYS2*. GCRs lead to loss of *ADE2* and *CAN1* so GCR events can be scored by counting of Can^R red colonies on canavanine-containing medium with low concentration of adenine. Mutations in *CAN1* gene produce Can^R white cells. There are no essential genes between *LYS2* gene and the left arm telomere. (Figure 1).

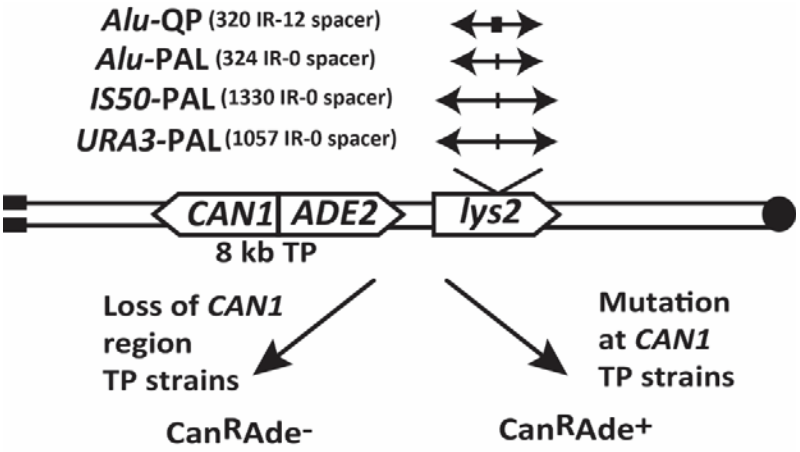

Figure 1. System to study gross chromosomal rearrangement events induced by various types of quasi- and perfect palindromes inserted into the *LYS2* gene. The size of the repeats ranges from 320bp to 2667bps. They are separated by 12bp spacer (*Alu*-QP) or no spacer.

In our work we utilized the following palindromic and quasi-palindromic insertions placed into the *LYS2* locus of our reporter system. The quasi-palindrome referred to as *Alu*-QP comprised of 100% homologous inverted *Alu* repeats (320bp) with a 12bp spacer. The perfect palindromes referred to as *Alu*-PAL, IS50-PAL, and *URA3*-PAL are comprised of inverted *Alu*, IS50 (1.3 kb), *URA3* (1.0kb) repeats, respectively (Figure 1).

2.2 MRX and Sae2 target non-B DNA structures formed at perfect palindromes and induce DSB formation

Lobachev et al. 2002 demonstrated that Sae2 or MRX complex does not induce DSBs at the quasi-palindrome formed by *Alu* repeats separated by a 12bp-spacer on chromosome II, but is responsible for opening the hairpin-capped breaks generated by DSBs at this locus for the later repair process. To address the question whether the same is true for perfect palindrome, we deleted Sae2 protein in the strains containing *Alu* quasi-palindromes and perfect palindromes, performed contour-clamped homogeneous electric field (CHEF) and Southern blotting using radio-labelled probe targeting telomere-proximal *HPA3* gene (Figure 2A). Upon deletion of Sae2, resection of DSBs in all strains is eliminated which confirms the previous finding that MRX-Sae2 is responsible for opening the hairpin-capped breaks. DSBs in *Alu*-QP *Δsae2* remain at the same level as in *Alu*-QP *SAE2* background. Interestingly, in *Δsae2* background, DSB decreases approximately 3-fold in *Alu*-PAL, 4-fold in IS50-PAL and *URA3*-PAL compared to *SAE2*

background (Figure 2B and 2D). Deletion of Mre11, the nuclease component of MRX complex, and the *mre11-DD56N*, allele of Mre11 specifically deficient in nuclease activity leads to same level of decrease in breakage in perfect palindrome *URA3*-PAL (Figure 2C and 2E), suggesting that MRX-Sae2 functions in both generating DSBs and break resection in strains with perfect palindromes. However, the level of GCRs in *Δsae2* background is not significantly lower than in *SAE2* background. GCR level in *URA3*-PAL strain is not significantly higher than *Alu*-QP even though Southern blotting reveals that DSB level in *URA3*-PAL strain is over 30-fold higher than in *Alu*-QP strain. Deletion of Sae2 in *URA3*-PAL strain increases rates of GCRs by 15-fold (Table 1). Combined the data from GCR assay and direct detection of DSBs suggest that DSBs created by MRX-Sae2 are not repaired as efficiently as DSBs resulting from hairpin-capped breaks. It is possible that in the *URA3*-PAL strain, the specific secondary structure targeted by MRX-Sae2 is formed more efficiently (potentially due to transcription initiation) and thus the majority of DSBs are generated by MRX-Sae2 and fail to be repaired. Lobachev et al. 2002 and Saini et al. 2013 suggested that hairpin-capped breaks are opened by MRX-Sae2 and repaired using sister chromatid as the template. Since the MRX-Sae2-dependent DSBs are not recovered, it is plausible that they are generated in G1 or early S phase when a sister chromatid is not available for repair.

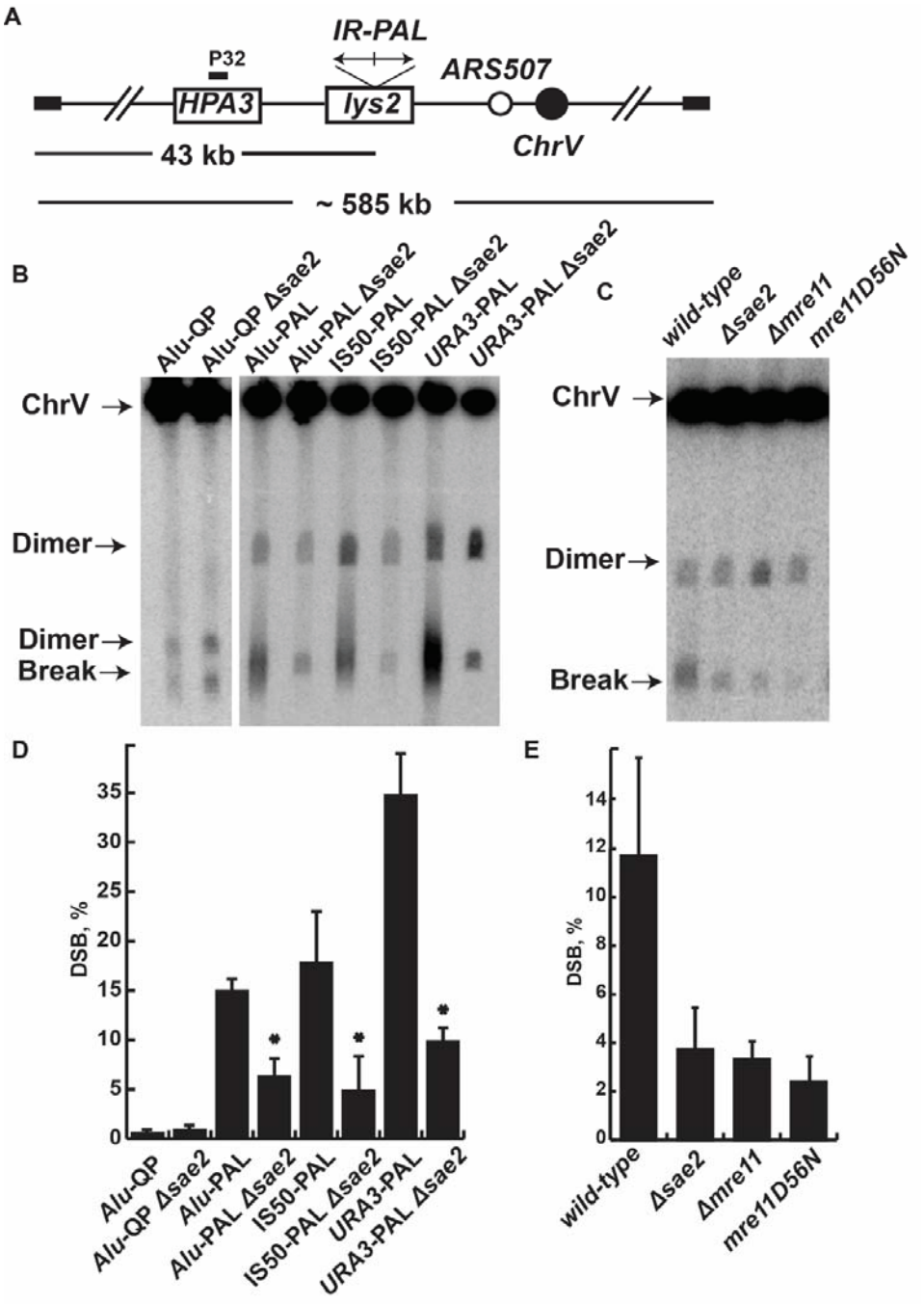

Figure 2. MRX-Sae2 induce DSBs at locus containing perfect palindromes. (A) Probe targeting *HPA3* gene telomeric-proximal to repeats detects 43kb broken fragment from 585kb intact chromosome V. (B) Detection of DSB formation by CHEF gel electrophoresis in strain containing *Alu*-QP, *Alu*-PAL, IS50-PAL or *URA3*-PAL with wild-type or deletion of Sae2. (C) Detection of DSB formation in *URA3*-PAL with mutations in MRX-Sae2. (D) Quantification of MRX-Sae2-

induced DSB at different repeats. (E) Quantification of DSB in *URA3*-PAL with different mutations in MRX-Sae2.

Transient or stable replication intermediates can be analyzed by DNA two-dimensional (2D) gel electrophoresis. Using 2D gel electrophoresis, intermediates of DNA synthesis can be separated based on the differences in size and complexity (Figure 3A). Replication fork stalling at repeats was observed in strains containing perfect palindromes with *sae2Δ* (Figure 3B), while in strains with quasi-palindrome fork stalling was only observed in replication-defective background and not in wild-type (Zhang et al., 2013). These data indicate that compared to quasi-palindrome which is likely to be attacked in G2 (Saini et al., 2013b; Zhang et al., 2013), perfect palindromes, especially *URA3*-PAL, might form structures which blocks replication and is attacked during S phase. In *SAE2* background, in strains containing *Alu*-PAL, IS50-PAL, and *URA3*-PAL., a bubble-shape structure is also present which resembles that of previously reported to be characteristic for break-induced replication (Saini et al., 2013a). It indicates that MRX-Sae2-induced DSBs are probably repaired through break-induced replication using homology in repeats as the point of invasion. Another prominent intermediate located below the replication fork stalling was detected. Its migration pattern suggests that MRX-Sae2 generates DNA intermediate similar in size to structure formed at the site of replication fork stalling but with lower complexity. This intermediate is absent in *sae2*□ strains. This result suggests that this structure presents a collapsed o replication fork which comes from MRX-Sae2 attack.

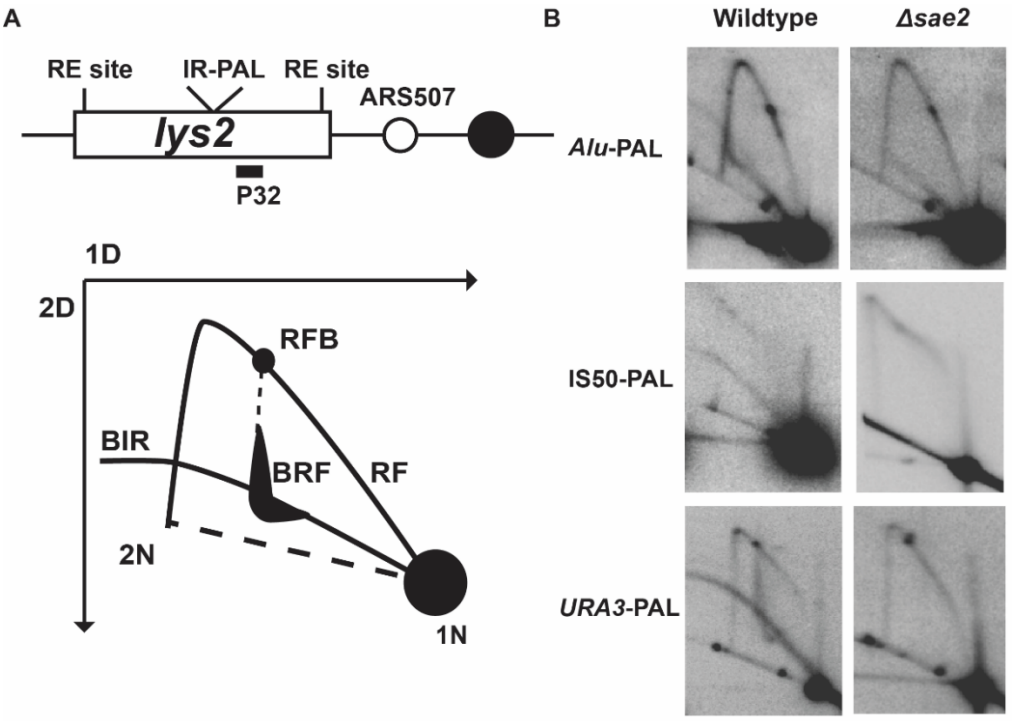

Figure 3. 2D gel electrophoresis reveals Sae2-depedent intermediates in strains containing perfect palindromes. (A) Position of probe-targeting region and restriction enzyme sites. (B) Illustration of 2D gel electrophoresis and position of various complex DNA structures. RF-replication fork; RFB-replication fork blockage; BIR-break-induced replication; BRF-broken replication fork. (C) 2D gel analysis of synthesis intermediates in wild-type and *Δsae2* strains with perfect palindromes.

To address the dynamics of the DSBs induction and replication fork progression throughout the cell cycle, I constructed a conditional Sae2 system in which endogenous Sae2 is fused with estradiol binding domain and placed under control of non-leaky GAL1-v10 promoter (Figure 4A). Induction of Sae2 can effectively reverse the MMS sensitivity of Δ*sae2* background upon addition of galactose and estradiol (Figure 4B). This system allows to tightly regulate the expression of Sae2 at different stages of cell cycle. In this experiment, Sae2 is induced when cells are arrested at G1 stage and released into medium containing

galactose and estradiol. Samples collected at different time-points are subjected to 2D gel electrophoresis analysis (Figure 4C). I found that the replication forks as well as replication fork stalling start to appear at 60min after cells are released from G1 arrest which corresponds to S phase (Figure 4D). The collapse of replication fork can be observed at the same time suggesting that MRX-Sae2 complex recognizes and attacks the secondary structures formed at S phase by replication fork. At 150min, replication fork fades away as replication process passes this region and broken forks are processed; however, arrested forks persist. In the later timepoints, as the population enters asynchronized stage, more replication forks and broken forks are generated. The repair through BIR is initiated hours later (at 4hr timepoint) after the attack. This finding is in a good agreement with finding in Saini et al. 2013 that BIR events initiated by HO endonuclease start hours after DNA breakage. The intensity of the signal corresponding to BIR bubble structures becomes even higher at 5.5hr after releasing. The delay in the appearance of the structures, indicative of BIR, could reflect the necessity for resection and search for homologous template, which implies that palindrome-induced BIR happens when cells are not replicatingand arrested by checkpoint. To analyze the resolution of the palindromes in non-dividing cells, in another experiment, I prevent the replication by arresting cells in G2/M stage: the cells are released to nocodazole-containing medium after G1 arrest so that the population are synchronized in G2/M and does not enter next cell cycle (Figure 4E). Replication fork, blockage, and breakage are observed after 60min in a pattern similar to what was going on in the experiment when cells

are released into medium without nocodazole (Figure 4F). At the later timepoints, replication fork fades away, while the signals for broken forks and replication blockage persist. The BIR structures are observed at the timepoint of 5.5hr when replication is absent, indicating that occurrence of BIR events does not require S phase replication. Overall, using conditional Sae2 system, I was able to monitor events occurring at palindromic regions and conclude that-1) replication fork arrests at *URA3*-PAL happens prior to breakage and BIR starts several hours after breakage; 2) BIR occurs when cells are arrested by checkpoint and do not go through the replication. This conclusion is consistent with previous finding that HO-induced BIR synthesis generates long single-stranded DNA and takes hours to finish (Saini et al., 2013a).

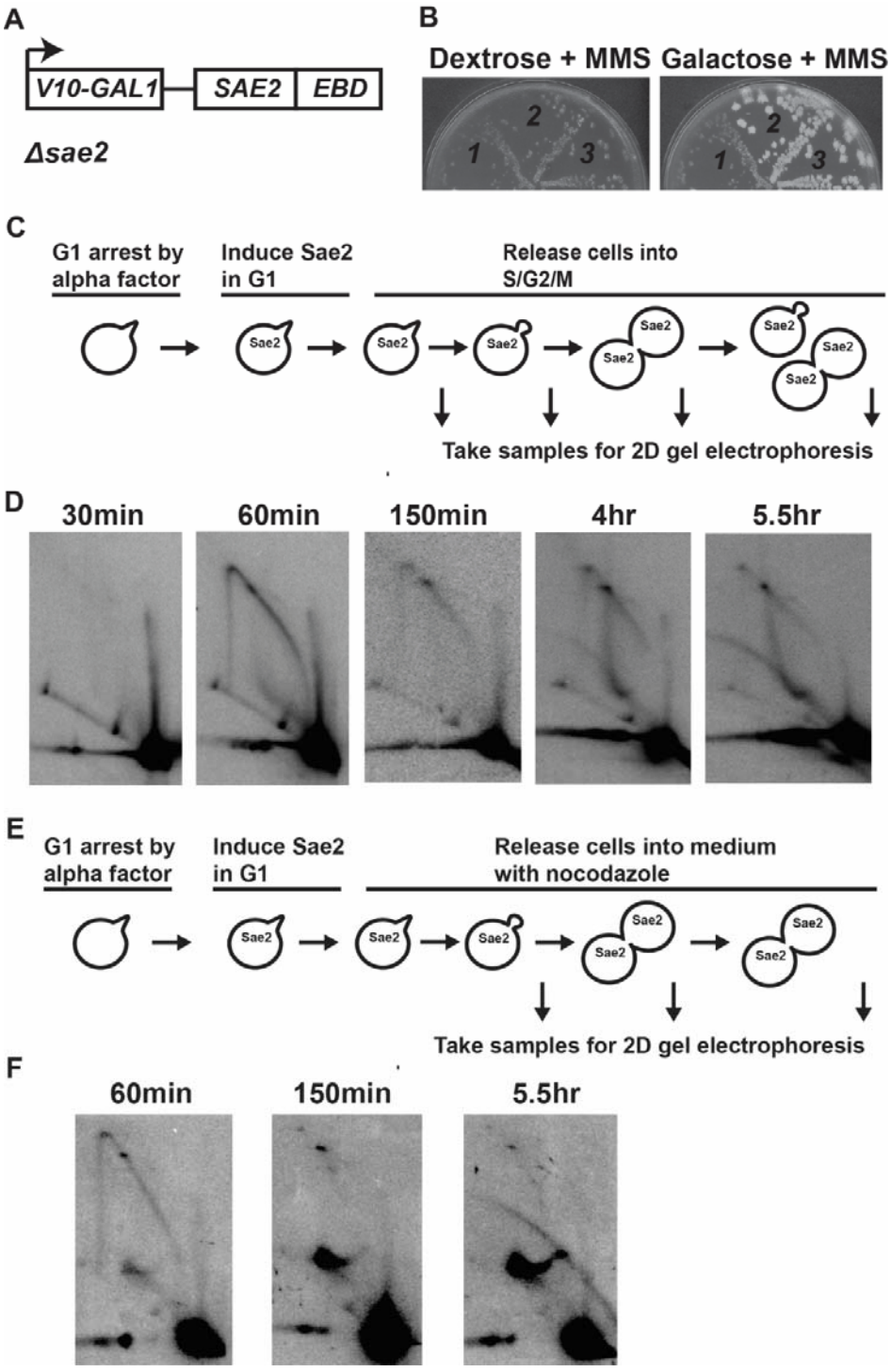

Figure 4. Sae2-inducible system reveals timing of fork breakage and initiation of BIR process. (A) Illustration of the construct of inducible Sae2 system. (B) Induction of Sae2 reverses the phenotype of MMS sensitivity of *Δsae2* strain. (C) Scheme of time-point experiment releasing cells into synchronously to monitor breakage and BIR structures occurring at palindromic region. (D) 2D gel

electrophoresis analysis to reveal events happening in strains containing *URA3*-PAL. (E) Scheme of time-point experiment arresting cells in G2/M by nocodazole. (F) 2D gel electrophoresis analysis to reveal events happening in strains containing *URA3*-PAL arrested by nocodazole.

2.3 Structure-specific nuclease Mus81-Mms4 generates breaks at *URA3*-PAL

I observed a robust DSB formation in strains lacking MRX or Sae2. In the attempt to identify a nuclease responsible for MRX-Sae2-independent breaks, I analyzed the activity of several currently known nucleases that have been shown to target HJ or HJ-like structures, Mlh1-Mlh3, Yen1, Slx1-Slx4 and Mus81-Mms4 towards different palindromic structures in *Δsae2*strains. GCR rates decreased 2-fold in *URA3*-PAL *Δmus81* strains while deletion of other nucleases in *URA3*-PAL strains did not affect GCR events. Southern blotting reveals that DSB also decreases by 50% in *Δmus81* background compared to *MUS81* indicating that Mus81-Mms4 is accountable for resolving 50% the secondary DNA structures at *URA3*-PAL (Figure 5). Notably, deletion of Mus81, Mlh1, Yen1, Slx1 in *Alu*-PAL and IS50-PAL strains did not affect either GCR rates or DSB formation (Table 2, Figure 5).

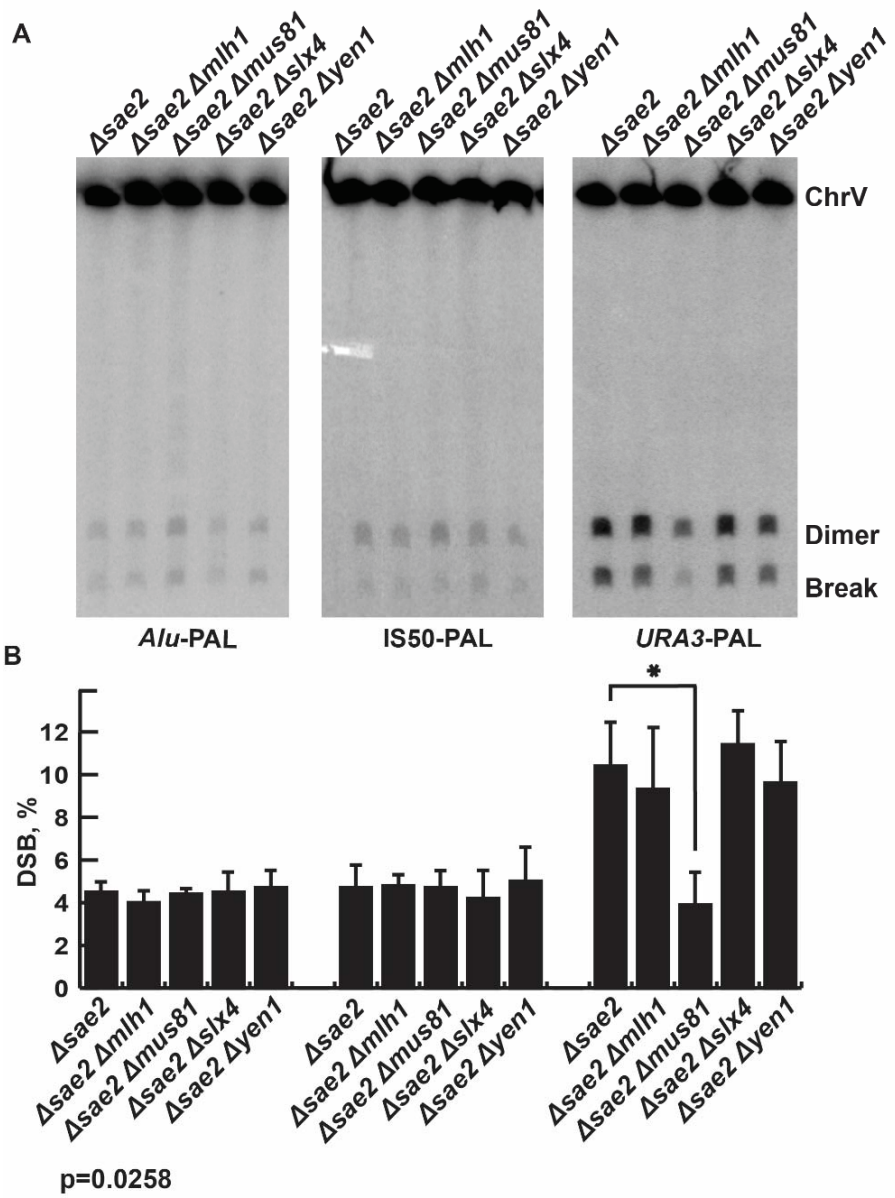

Figure 5. Mus81-Mms4 induces DSBs in strain containing *URA3*-PAL. (A) DSB detection in strains containing perfect palindromes with deletion of structure-specific nucleases. (B) Quantification of breakage in different backgrounds.

In previous study of the mechanism underlying the genomic instability triggered by *Alu* quasi-palindrome, it had been shown that during abnormal replication, recombinase Rad51, stimulates increase in secondary structure

formation at the quasi-palindrome which is later channeled into replication blockage and DSBs. Deletion of Rad51 decreases DSBs as well as replication fork blockage in these mutant strains. To test whether the effect of *Δmus81* mutant is as same as that of *Δrad51* mutant, I performed 2D gel electrophoresis on *Δsae2Δmus81* strain and found that replication blockage is not affected by *Δmus81* mutation, suggesting that Mus81-Mms4 induces DSB at *URA3*-PAL in a replication-independent manner (Figure 6A).

The difference between *URA3*-PAL and the other two types of perfect palindromes is that the *URA3* repeats are actively transcribed from the center where the two promoters are positioned. Thus, transcription might facilitate the formation of cruciform or hairpin structures. I investigated how transcription affects the DSB level in *URA3*-PAL by culturing *Δsae2* and *Δsae2 Δmus81* strains in medium with different levels of uracil. It is shown and confirmed by RT-PCR in this study that transcription of the auxotrophic marker is elevated upon amino acid starvation and deletion of *Mus81* does not affect *URA3* transcription (Figure 6C). DSB detection shows that the level of breakage is significantly increased when uracil is absent in the medium indicating that transcription plays a role in DSB formation at palindromes (Figure 6B). Transcription-related DSB induction is eliminated in *Δmus81 Δsae2* background suggesting that Mus81-Mms4 alone is responsible for attacking the structures facilitated by transcription. It has been demonstrated previously by alkaline gel electrophoresis in *Δsae2* strain that *Alu*-QP-mediated breaks are hairpin-capped (Lobachev et al., 2002; Zhang et al., 2013). By running DNA first in the neutral running buffer and then in the second dimension in

alkaline buffer, hairpin-capped breaks can be distinguished from same-size open-ended double strand breaks. In this work, alkaline gel electrophoresis reveals that DSBs generated in *Δsae2* strain by *URA3*-PAL perfect palindrome are also hairpin-capped (Figure 6D). The rest of breaks that are Mus81-Mms4-independent are also protected by hairpin caps. In summary, in this work I discovered that transcription-promoted secondary structures formed by *URA3*-PAL are recognized and processed by Mus81-Mms4; and that such processing leads to formation of covalently closed hairpin-capped breaks.

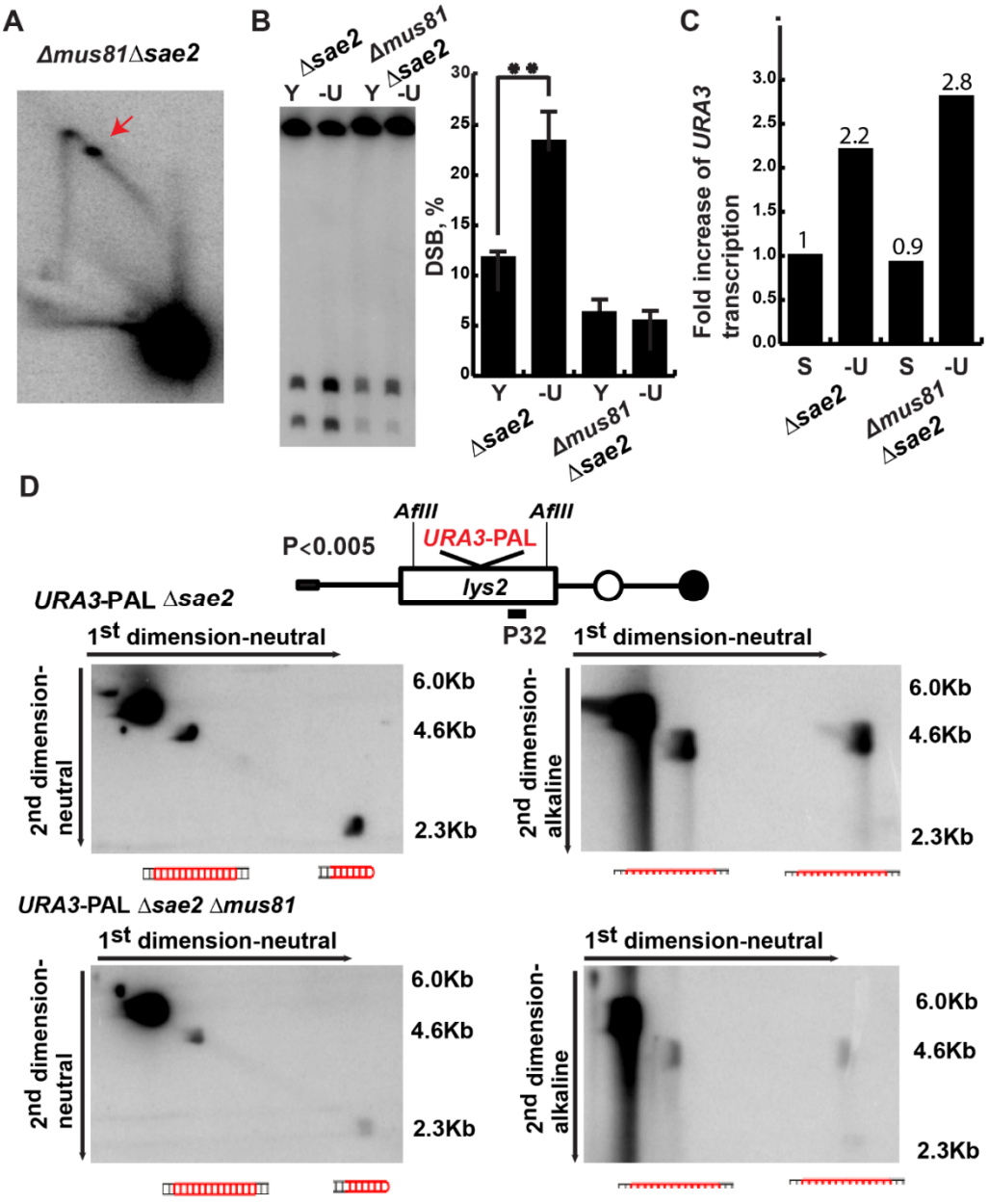

Figure 6. Mus81-Mms4 induces hairpin-capped DSBs at transcription-active palindromic locus. (A) DSB detection in *Δsae2* or *Δsae2Δmus81* strains with *URA3*-PAL cultured in YPD(Y) or uracil-depleted (-U) medium. (B) RT-PCR analysis of *URA3* transcription level. (D) 2D gel electrophoresis analysis reveals deletion of Mus81-Mms4 does not affect palindrome-induced replication fork blockage. (E) Neutral-Alkaline 2D gel electrophoresis reveals the hairpin-capped nature of DSB in in *Δsae2* and *Δsae2Δmus81* strains.

2.4 Sae2-independent DSBs are formed in G2-stage of cell cycle

From previous lab studies (Narayanan et al., 2006; Zhang et al., 2013), it is suggested that hairpin-capped breaks are generated in late S or G2/M stages in cell cycle. However it is difficult to evaluate the hypothesis using current system due to the presence of pre-existing breaks. To monitor the DSB formation during cell cycle with elimination of pre-existing breaks, we constructed a conditional DSB system in which the formation of a quasi-palindrome is induced at any stage of cell cycle. The arms of *URA3* repeats were separated by two direct repeats of 34bp loxP sites flanking *KanMX4* gene, resulting *URA3*-inverted repeats with approximately 1.7kb spacer. The long spacer efficiently prevents the formation of structure and DSB (Lobachev et al., 1998a). The construct also includes a gene coding for site-specific recombinase Cre under control of GAL1 promoter and fused with estradiol-binding domain. Induction of the Cre recombinase led to the excision of the *loxP-KanMX4-loxP* construct, leaving one loxP site between two arms (Figure 7A). Each loxP site is a quasi-palindrome with two 13bp-arms and a spacer of 8bp, thus after induction, the construct of inverted repeats with 1.7kb spacer became quasi-palindromes with a short 8bp spacer which were able to form cruciform and hairpin structures and induce fragility. To study the DSB generated during cell cycle, the strains with the conditional DSB construct and *SAE2* deletion were arrested in G1 by alpha factor (G1-S experiment) or in G2/M by nocodazole (G2/M experiment) prior to induction of Cre recombinase. After 3hr of induction of Cre, for G1-S experiment, cells were released into S and G2 phases to take time-points for DSB detection and FACS analysis.

DSB detection in both conditional *URA3*-repeat constructs confirmed that DSB does not occur in the strain without induction of Cre recombinase (Figure 7B) in G1 or G2/M stage. Signal for DSB can be observed after induction though intensity is weak using probes targeting region ARS507-distal or -proximal to the *URA3*-quasi-palindrome. It was clear that DSB accumulated in 50min (late S) and 70 and 90min (G2/M stages) at both sides. In the experiment in which cells are arrested in G2/M stage using nocodazole to evaluate replication -independent DSB, the signal for DSB was even stronger than that at 90min in G1-S experiment, indicating that at G2/M stage DSB formation is promoted at repeats in non-dividing cells. Moreover, in comparison, I also performed the experiment in which cells are treated in the same manner as G1-S experiment but released into fresh YPD containing alpha factor to prolong the arrest in G1 and found no increase in DSB (Figure 8B), confirming that cells need to enter S and G2/M stages to induce the majority of DSB.

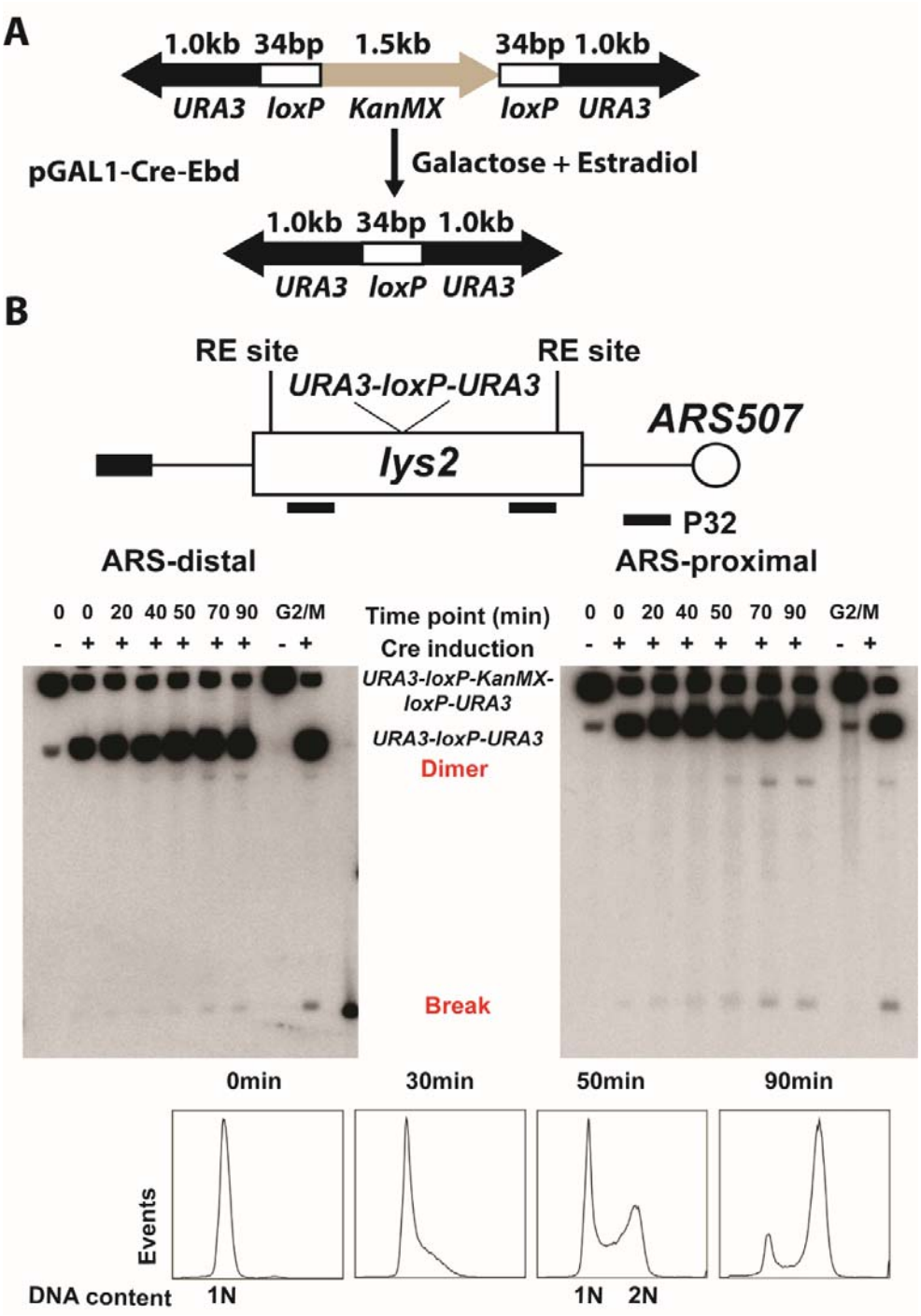

Figure 7. Conditional system to detect DSBs along cell cycle. (A) Diagram of the Cre-loxP system. (B) Illustration of DSB detection scheme and results. Southern blotting hybridization using radioactive-labelled probes targeting ARS507-distal or ARS507-proximal *lys2* region revealed that DSB accumulated in late S and G2/M stages of cell cycle at both ends. FACS analysis confirmed the cell cycle progression.

Using this conditional DSB system, I was able to evaluate the timing of the attack on Mus81-Mms4. I deleted *MUS81* in the strain containing conditional *URA3*-repeat system. Since it is reported that Mus81-Mms4 complex is phosphorylated in G2 stage (Gallo-Fernandez et al., 2012; Saugar et al., 2013; Schwartz et al., 2012), I performed G2/M experiment on wild-type and *Δmus81* strain and found that DSB level decreased significantly in mutant background (Figure 8A), indicating Mus81-Mms4 complex is accountable for a part of DSB in the G2/M stage. Moreover, it is interesting to note that, even though the level of DSB is low in G1 stage, the presence of breakage is confirmed by several experiment using conditional *URA3*-repeats system (Figure 8B). However, G1-stage-DSB was not observed in conditional *Alu*-repeats system (data not shown). I suggest that it is due to the active transcription of *URA3*-repeats in G1 that might lead to formation of structures attacked by active Mus81-Mms4 complex in G1 and result in DSB formation. In the study using conditional Sae2-induction system, I demonstrated that though Sae2 phosphorylation by Cdc28 which is required for Sae2 activity is conventionally recognized as a late S to G2 event (Huertas et al., 2008), induced Sae2 protein in G1 was still active (data not shown). Therefore, it is possible that a low amount of active Mus81-Mms4 is responsible for the DSB in G1.

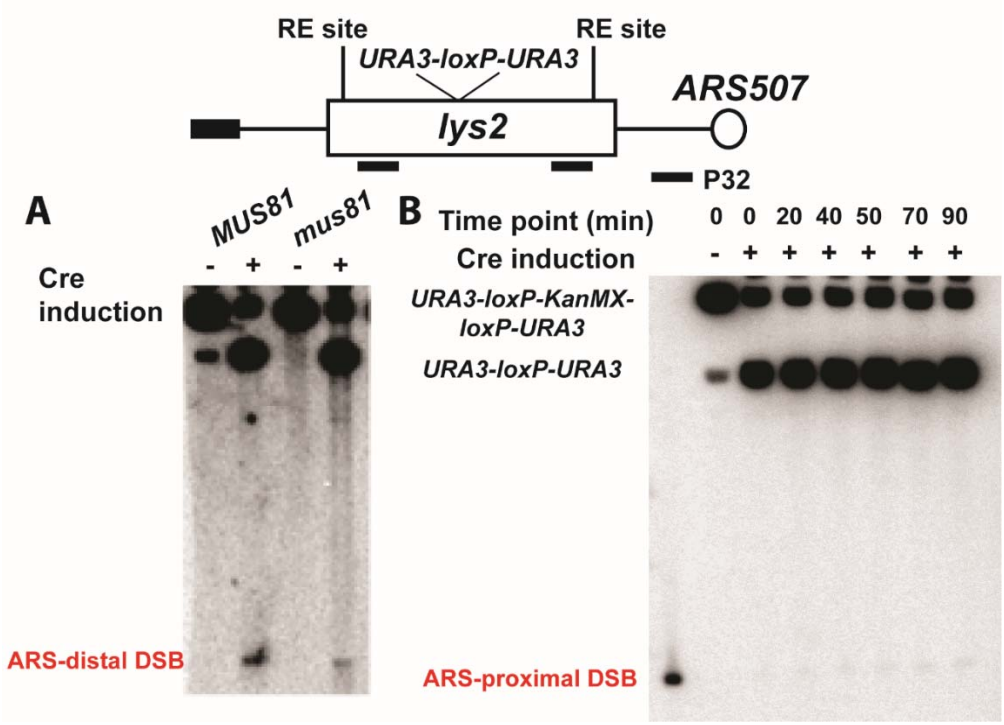

Figure 8. Conditional system for DSB detection in *Δmus81* background. (A) G2/M experiment revealed that DSB decreased in *Δmus81* strain after induction of Cre recombinase. (B) Cells were arrested by alpha factor in G1 along the time-points. DSB level remained the same as a function to time. At time-points of 70 and 90mins, DSB level were significantly lower than those time-points taken from samples which were released into S, G2/M stages.

2.5. Cdc28 is involved in DSB formation in G2 stage

Despite the activity of Mus81-Mms4, there is a part of DSBs that are Mus81-Mms4-independent and occur in G2 stage (Figure 7B). Based on this finding, I introduced a mutant form of Cdc28 in the conditional DSB system in pursuit to identify the player that is responsible for the DSB. Cdc28 is the yeast catalytic subunit of cyclin-dependent kinase (CDK) which serves as the master

regulator of mitotic and meiotic cell cycles (Mendenhall and Hodge, 1998) . It provides substrate specificity by alternatively forms complex with cyclins of G1, S, G2/M phase. Since the repertoire of the substrates have been published (Li et al., 2014), it was tempting to test whether a putative nuclease is under control of Cdc28.

The mutant form of Cdc28, Cdc28-as1, is sensitized to the cell-permeable molecules, 1-NM-PP-1, that has no effect on wild-type. With the addition of different concentration of the inhibitor, the level of functional Cdc28 can be controlled and thus cells can be arrested in different cell cycle stages (Bishop et al., 2000). The allele was introduced into conditional DSB system by the method of pop in-pop out.

First, I performed the experiments using nocodazole to arrest cells in G2/M prior to the addition of 1-NM-PP-1 followed by induction of Cre recombinase (Figure 9A). I found that DSB formation was not affected if inhibition of Cdc28 happens after cells finishing entering G2/M stage. It is expected since the Cdk kinase phosphorylates most of the substrate before cells entering G2/M and is inhibited by the dephosphotase Cdc14. (Reviewed in (Bloom and Cross, 2007)). Then I used the inhibitor to arrest cells in G2/M without adding nocodazole to inactivate Cdc28 before the formation of DSBs (Figure 9B). DSB detection revealed that the majority of DSB was eliminated in this treatment. The residual level of DSBs was even lower than that in *Δmus81* background, indicating that both Mus81-Mms4-induced DSB and the third currently unidentified pathway were affected. It is likely that Cdc28 phosphorylates both Mus81-Mms4 and a putative

nuclease or its regulators in that pathway when cells enter G2/M. In *Δsae2* strains containing *URA3*-PAL or *URA3*-quasi-palindrome, the non-B DNA structures are under attack by both nucleases, while in the strains with IS50-PAL, *Alu*-PAL and *Alu*-QP, structures formed at the repeats are only by a putative nuclease alone, leading to fragility in 5% of population (Figure 5).

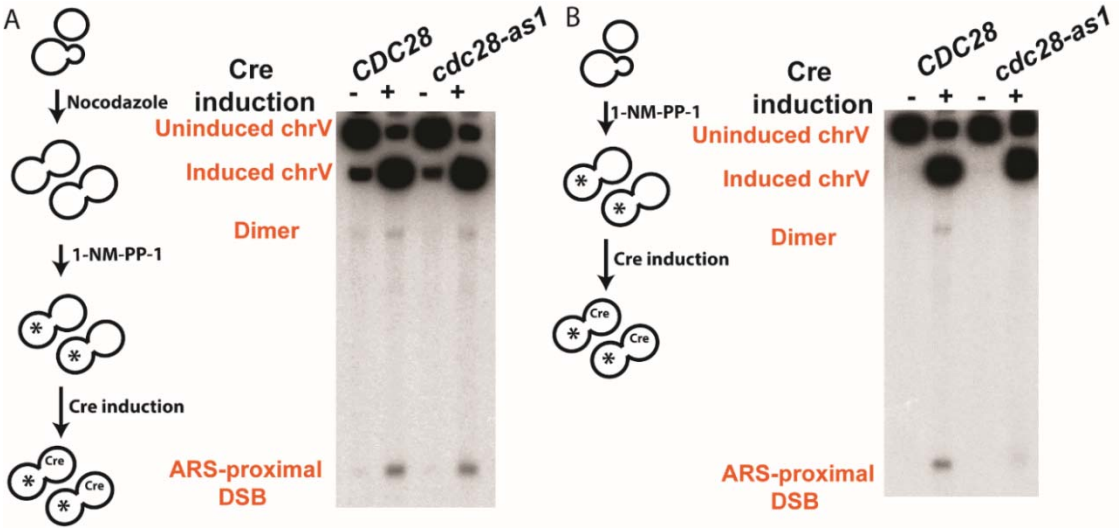

Figure 9. DSB formation in G2 is dependent on functional cell-cycle kinase Cdc28. * indicates the defective Cdc28 upon inhibition by 1-NM-PP-1. (A) Cells were arrested by Nocodazole in G2/M prior to the addition of kinase inhibitor 1-NM-PP-1. (B). Cells were arrested by 1-NM-PP-1 in G2/M.

2.6 The third pathway is under regulation of Lsm-like protein involved in mRNA decay.

DSB detection of strains with *Alu*-PAL, IS50-PAL and *URA3*-PAL revealed the presence of Sae2- and Mus81-independent breaks (~5%). Also, fragility in the strain containing *Alu*-QP occurs independently of Sae2 and Mus81, indicating that there is another pathway that induces DSB at the palindromic repeats. From the

previous publication (Lobachev et al., 2002) and the finding from this work (Figure 6), it is clear that this pathway produces hairpin-capped breaks in both the strain containing quasi-palindrome and those with perfect palindromes. To elucidate the players involved in this pathway, we performed EMS mutagenesis screen in the strain containing *Alu*-PAL with double deletion of *SAE2* and *MUS81* to get low-breakage mutants. GCR level was evaluated for colonies from cells after EMS-treatment. There were 33 out of 5000 colonies from cells after the EMS-treatment exhibiting low GCR rate. These colonies were then subject to DSB analysis by Southern blotting. DSB detection revealed that 7 cultures showed lower events of DSB (Figure 10A). Genomic DNA of these 7 cultures were then send together with untreated *Δsae2 Δmus81* strain with *Alu*-PAL for whole genome sequencing. The sequencing result revealed the presence of several mutations which I recreated in strain containing *Alu*-PAL to confirm their effects. Among those mutations, I found that deletion of *LSM6* in *Alu*-PAL with *SAE2* or *sae2* background resulted in a significant decrease of DSB in both backgrounds (Figure 10B). This data suggests that Lsm6 is involved in the third pathway that is independent on Sae2 and Mus81-Mms4. Lsm6 is a Sm-like protein that serves a part of the heteroheptameric complexs, Lsm2-8 or Lsm1-7 (Beggs, 2005; Mayes et al., 1999). Lsm1-7 complex, involved in mRNA decay, localizes in cytoplasm while the nuclear Lsm2-8 complex is proposed to play role in processing tRNA, rRAN and snoRNA. Subunits of the complex form a heteroheptameric ring with a small hole and it is suggested that RNA pass through the hole during mRNA processing (Kambach et al., 1999; Pomeranz Krummel et al., 2009; Stark et al., 2001). Among these

subunits, Lsm 1, Lsm 6 and Lsm7 are nonessential proteins. Lsm2-5 and Lsm8 are essential, depletion of any of which leads to the delay of pre-rRNA processing and the accumulation of many aberrant processing intermediates ((Kufel et al., 2003). It is plausible that mutation in Lsm6 destabilizes the ring structure, even though it does not completely inactivate the complex, resulting in aberrant RNA processing. The nuclease or the regulator of the nuclease that is responsible for creating the DSB is one of the protein whose mRNA processing is affected. Alternatively, RNA coding for protein(s) that promote(s) cruciform structure formation is hampered, thus less substrates for the nuclease were formed in the Lsm-mutant background.

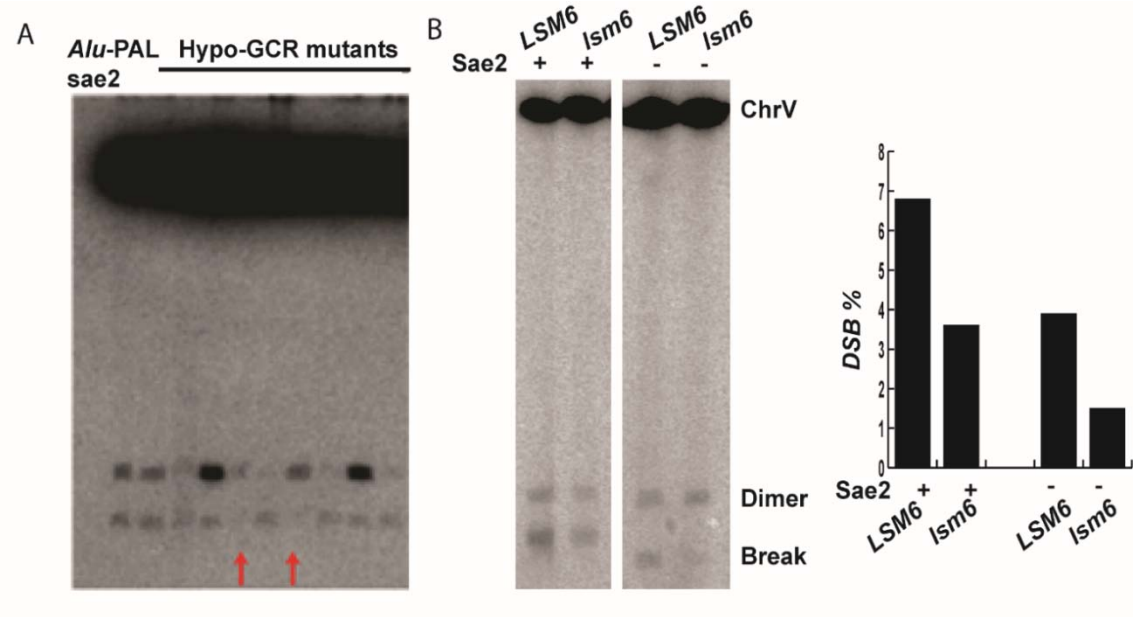

Figure 10. DSB detection in mutants exhibiting low GCR levels. (A) DSB formation in hypo-GCR mutants obtained from EMS-mutagenesis experiment and. Red arrow indicates mutants with lower DSB formation. (B) DSB detection in *Δlsm6* mutant showed a decrease in fragility.

2.7 Palindromic sequences trigger endogenous and radiation-induced mutagenesis at distant loci

It has been reported previously (Saini et al., 2013b) that regions surrounding *Alu*-QP in replication-defective mutants are a subject to higher mutation rates and that such increased mutagenesis is dependent on Sae2 and translesion DNA polymerase polζ. I also observed the similar effects in the strains with perfect palindromes *URA3*-PAL; it exhibits a significant 7-fold increase in mutation rate in comparison to the strain without repeats (Table 1). The assay I used to evaluate mutation rate utilizes the reporter system in which *CAN1* gene is placed approximately 8kb telomere-proximal to repeats. In experiments involving irradiation, cells were exposed to UV light at as does of 50J/m^2. I found that the frequencies of mutations in the region surrounding IS50-PAL and *URA3*-PAL are significantly increased compared to strains without exposure and the strain without repeats (Table 3), suggesting that region surrounding palindromic repeats is highly sensitive to exogenous damage such as radiation (Table 3). By placing *CAN1* gene at distance approximately 8kb, 15kb, and 33kb centromere- or telomere-proximal to repeats, I was able to follow the frequency of mutations as a function of the distance between the repeats and the insertion of the reporter gene (Figure 11). Mutation level decreases as *CAN1* moved further away from repeats and at a distance of approximately 33kb reaches the same level of that in the strain containing no repeats. These data are in agreement with previous reports that an efficient resection resulting in persistence of long single-stranded DNA can be detected at a distance up to 30kb from the site of break (Zhu et al., 2008) Together

with the data that palindrome-induced mutagenesis is dependent on Sae2, these findings allows us to suggest that ssDNA serves as an intermediate for mutagenesis.

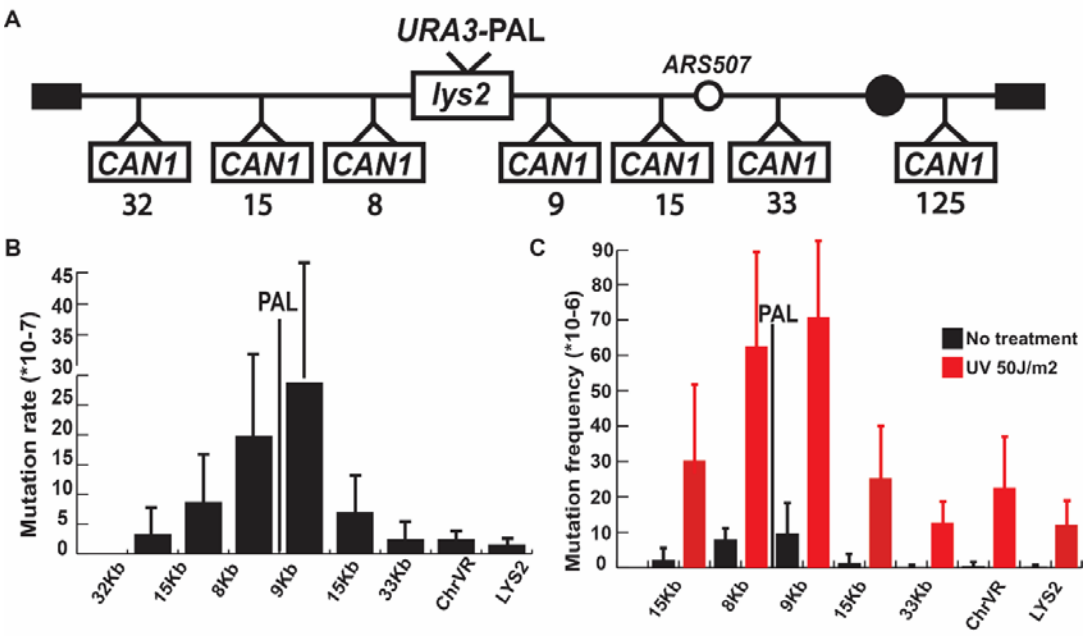

Figure 11. Mutation rates in regions surrounding *URA3* palindromic repeats. (A) Experimental system to study *URA3*-PAL-induced mutagenesis. Positions of *CAN1* as reporter inserted in telomere-proximal or centromere-proximal to the palindrome are shown. (B) Mutagenesis by *URA3*-PAL depends on the distance of *CAN1* to the repeats. (C) Mutation frequency of *URA3*-PAL-containing strain irradiated by 50J/m2 UV light.

Translesion polymerase Polζ is shown to be responsible for mutagenesis induced by fragile motifs and Ho-endonuclease-induced breaks (Holbeck and Strathern, 1997; Rattray et al., 2002; Saini et al., 2013b). To assess if mutagenesis id induced by perfect palindromes depends on Polζ, I disrupted *REV1, REV3*, and *REV7* in *URA3*-PAL strains. Rev1 forms a complex with subunits of Polζ, Rev3 and Rev7, involving in translesion synthesis (Prakash et al., 2005). Deletion of

Rev1, Rev3, and Rev7 significantly decreases mutagenesis at *CAN1* 8kb telomere-proximal to repeats down 7-, 3- and 5–fold, correspondingly (Table 5). Polη is also involved in translesion DNA synthesis during postreplication repair, especially repair at sites of cyclobutane pyrimidine dimers (McDonald et al., 1997; Prakash et al., 2005). Deletion of *Rad30* that codes for *S. cerevisiae* polη does not affect mutation level in strain containing *URA3*-PAL, suggesting that Polζ alone converts damages generated on ssDNA to mutations.

It has been previously reported that BIR mutagenesis is limited to few kb away from the break by Mus81-Mms4. It has been shown that when BIR collides with a replication fork, Mus81-Mms4 induces D-loop cleavage and thus suppresses BIR progression and the mutagenic synthesis by Pol32 (Mayle et al., 2015). These findings were obtained in the system where DSB is induced by mutated site-specific recombinase FLP to create a nick at one strand which is converted into DSB later by replication. Pol32 and Rad51 were found to be required in BIR events following the DSB. The decrease in mutagenesis was also observed with a reporter placed distal to nick and this reduction wasalso Mus81-dependent. To test if palindrome-induced mutagenesis at a farther distance is also dependent on Mus81-Mms4, I deleted *MUS81* and *YEN1* in the strain containing *URA3*-PAL and used *CAN1* as mutagenesis reporter located either close to (8kb telomere-proximal to repeat) or far from (33kb centromere-proximal to repeat-CP33kb) palindrome. *CAN1* CP33kb reporter flanks the active replication origin ARS507. The frequency of mutations in *CAN1* remained the same in *Δmus81*, *Δyen1* and *Δmus81 Δyen1* strains compared to wild-type regardless of *CAN1* position (Table 5). Considering

the difference in requirement of components for the synthesis between FLP-induced and palindrome-induced BIR (see below), and the observation that the most of BIR events in palindrome-containing strains happen outside of S phase, it is likely that during palindrome-mediated BIR, there is no substrate for Mus81-Mms4 complex.

In strains containing perfect palindromes with intact MRX-Sae2, "migrating bubble" structure characteristic to BIR can be detected by probing of the region in close proximity to repeats. However, how BIR proceeds to repair broken chromosome was not clear yet. To understand this process, I performed 2D gel electrophoresis using different probes that target regions approximately 1, 10, 30 kb centromeric- or telomeric-proximal to repeats and region 12 5kb away and residing across centromere on the right arm of chromosome V. The bubble-like BIR structure can be observed at nearby regions centromeric- and telomeric-proximal to repeats indicating that BIR events initiated by DSB at palindromes can proceed bidirectionally towards centromere or telomere (Figure 8A). It is possible that BIR synthesis can progress in both directions simultaneously in one cell or the observation of bidirectionality comes from mix events in the population. Unexpectedly, I found that BIR can steadily persist 30 kb and as far as 12 5kb and bypass the active replication origins ARS507, ARS508 and ARS510 and centromere CEN5 which indicates that it happens outside of normal replication cycle.

It is interesting that BIR intermediates can be observed at positions far away from palindromes where mutation rates drop significantly. This observation differs

from the conclusion drawn from the study of mutagenesis triggered by HO-induced BIR using the *LYS2* reporter containing homonucleotide runs of four adenines (A4), seven adenines (A7), or 14 adenines (A14) (Deem et al., 2011). In HO-induced BIR, the nucleotide slippage rate at 36 kb away from BIR invasion point remains as high as that at invasion point, leading to the conclusion that persistent BIR is highly inaccurate. It is possible that in palindrome-induced BIR, polζ is responsible for converting the damages to mutations at the ssDNA generated from resection. While as BIR progresses away from the breakage, ssDNA generated along synthesis is protected and not prone to mutation, which also suggests that the replication machinery of palindrome-induced BIR might differ from that of HO-endonuclease-induced BIR.

2.8 MRX-Sae2-dependent BIR initiated at *URA3*-PAL is Rad51- and Pol32-independent.

I decided to further investigate how the mechanism of palindrome-induced BIR is different from the "classic" BIR described in previous publications (Malkova and Haber, 2012; Saini et al., 2013a; Wilson et al., 2013). To do that I examined the contribution of the factors involved in HO-induced BIR events and gene conversion in this process. Pif1 helicase is believed to play a key role in BIR by driving the migration of synthesis structure 'bubble' along (Chung et al., 2010; Saini et al., 2013a; Wilson et al., 2013). Studies show that Rad52 is also essential for BIR: Rad52 catalyzes annealing of complementary ssDNA and promote strand-invasion by Rad51 (Mortensen et al., 1996; Symington, 2002). As has been shown

previously, the lagging strand DNA polymerases ol□ and polδ are required for BIR initiation and progression in the system in which a homologous sequence inserted into nonhomologous chromosome serves as a point of invasion (Lydeard et al., 2007). The currently published systems share some similarities in BIR studies—1) in some of them, exogenous endonuclease under inducible promoter makes double-stranded DSB directly (HO endonuclease) or in another produces nick which is converted to DSB by replication fork later (mutant Flp1H305L); 2) in many studies the cells are tightly arrested in G2 to eliminate the effect of replication; 3) most of the constructs employ homologous sequences placed on nonhomologous or disomic chromosomes; such sequences are essential for successful completion of the BIR. The distinct features of palindrome-induced BIR events are: they are initiated by endogenous nuclease; they are not restricted to cells arrested in G2/M stage of cell cycle; moreover, the template for repair is very likely a sister chromatid that is in a close proximity.

To examine whether the palindrome-induced BIR shares the same machinery and mechanism as the other systems for studying BIR, I checked the effect of deletion of several currently-known essential components on palindrome-induced BIR by2D gel electrophoresis. Depletion of Rad52 and Pif1 helicase led to significantly decrease in BIR structures at close proximity to palindromes, indicating that Rad52 and Pif1 play an important role in the initiation of BIR event (Figure 12B). However, ‘bubble’ structures with much lower amount can be

observed at the initiation point and along the progression of the synthesis. Surprisingly, BIR structures are not affected when Pol32 is depleted suggesting that Pol32 is nonessential for BIR initiation or progression, which diverges from conclusions made from the previous studies. The Rad51 is also dispensable for strand invasion in palindrome-induced BIR. Taking into account the data that deletion of Rad52 induces a dramatic decrease in BIR events, it is possible that strand-annealing but not strand invasion serves as an important step for BIR initiation. Rad51-independent BIR events have been reported in some studies of BIR. In diploid cells with deletion of Rad51, BIR induced by HO-induced DSB at Mat locus can occur by strand invasion with help of a two hundred bp sequence called facilitator of Rad51-independent BIR (FBI) located close to ARS310 (Malkova et al., 1996; Malkova et al., 2001). In the study by Galgoczy and Toczyski, Rad51-independent BIR was observed when cells were treated with X-ray radiation and was found to be dependent on checkpoint adaptation. This pathway is not detected in HO-induced BIR in the same study (Galgoczy and Toczyski, 2001). In the study of BIR at Y' sequence, the efficiency of BIR was reduced about 200-fold in *Δrad52* strain and 20-fold in *Δrad51* strain, indicating a group of Rad51-independent BIR events. It is hypothesized that Rad51-independent BIRs are dependent on the DNA sequence context; the presence of repetitive elements proximal to DSBs might decrease the necessity of searching for homology to initiate BIR (Davis and Symington, 2004).

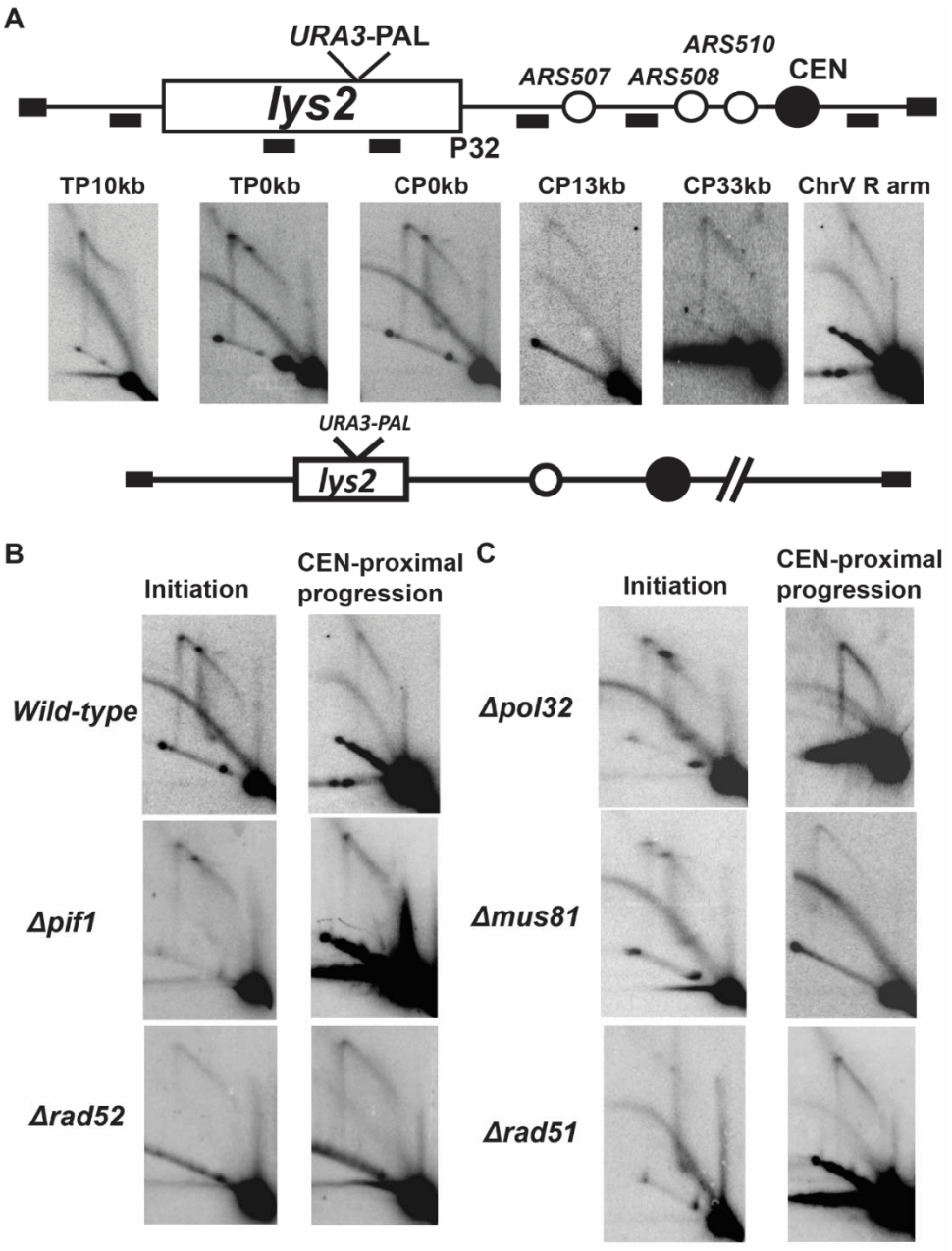

Figure 12. Bubble-like BIR structures present on chr V at surrounding and far away regions from *URA3*-PAL are dependent on Pif1 and Rad52. (A) Probe position on Chromosome V to detect the presence of BIR structure. CP probes probe region 0, 13 or 33 kb centromere-proximal to *URA3*-PAL; TP probes probe 0 or 10kb telomere-proximal to the palindrome. ChrV R arm probe targeting region that locates on right arm of ChrV and 125kb away from the palindrome. (B) Detection of BIR in *URA3*-PAL-containing strain with mutations in reported components of BIR machinery. Initiation probe targets 0 kb region centromere-proximal to *URA3*-PAL. CEN-proximal progression probe targets regions on the way of BIR progression to centromere (CP13kb, CP33kb, or ChrV R arm).

Chapter 3 Conclusions and future directions

The conclusions from this study have been summarized below.

1. MRX-Sae2 complex induces DSBs at perfect-palindromic regions but not at quasi-palindrome.
2. In the presence of MRX-Sae2, palindrome-induced DSBs, trigger BIR that likely occurs when cells are arrested by checkpoint and not during S-phase of the cell cycle.
3. Structure-specific endonuclease Mus81-Mms4 is responsible for the transcription-induced instability at the palindromic repeat.
4. There is a third pathway for breakage at palindromes which happens at G2 and is under regulation of Cdc28 and Lsm6.
5. Mutagenesis at regions surrounding palindrome is dependent on translesion polymerases polζ and the distance between reporter and repeats. Persistent presence of single-strand DNA is likely underlies the high level of mutagenesis at the sites surrounding the initial break.
6. BIR induced by palindrome can progress over a hundred kb away from DSB site. Chromosomal regions with complex architecture, such as active replication origins and centromere do not impede the progress of palindrome-induced BIR that is error-free.
7. Palindrome-induced BIR is dependent on Rad52 and Pif1, but not on Pol32, Rad51 or Mus81-Mms4, and thus its mechanism is different from that induced by different types of DSBs.

Model of palindrome-induced DSB is presented in Figure 13. Non-B structures formed at perfect palindromes are under attack by Sae2-MRX complex during replication leading to broken replication fork. Transcription-active palindromic locus is also a target for attack by Mus81-Mms4 complex which leads to hairpin-capped breaks. Besides these two pathways, there is another mechanism responsible for the genomic instability in the wild-type strains containing quasi-palindrome and strains with *Δsae2 Δmus81* background containing perfect palindromes.

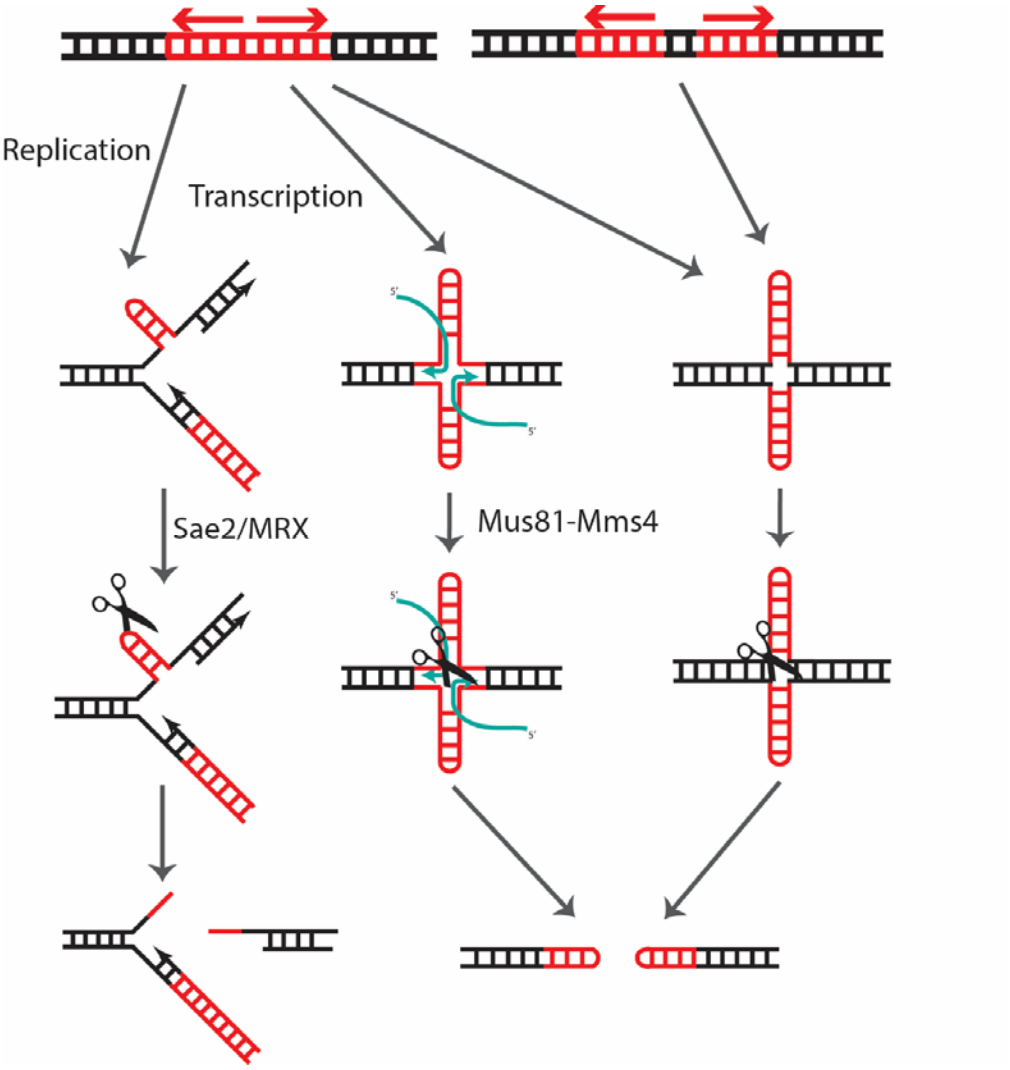

Figure 13. Model for DSB formation at quasi- and perfect palindromes

Model of palindrome-induced BIR is shown in Figure 14. The Sae2-MRX-induced DSBs in strains containing perfect palindromes lead to resection at the locus and generation of single-stranded DNA. Rad52 is involved in anneal the single-stranded DNA ends to the homology on the newly synthesized sister

chromatid which is possibly held close to the broken one by cohesion rings. Pif1 helicase is indispensable in BIR progression by unwinding DNA strands.

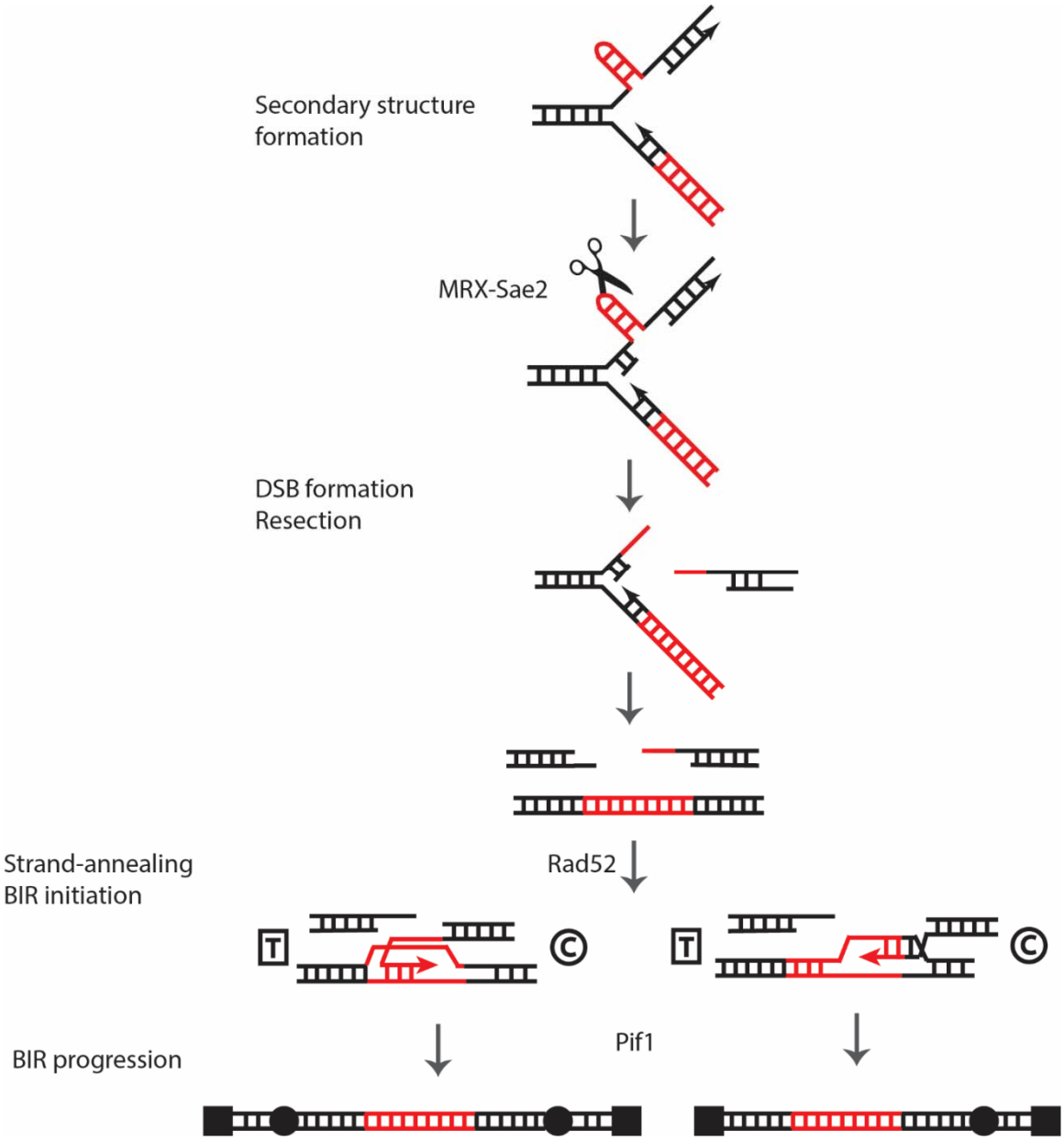

Figure 14. Model for palindrome-induced break-induced replication.

Future directions:

This study has provided insights into the mechanisms of palindrome-induced DSB and characterized the BIR events as a consequence of the palindrome fragility. Below are future directions that might help us gain an in-depth understanding of players involved in either DSB formation and BIR events occurring at palindromic repeats.

1. **What protein(s) other than MRX-Sae2 and Mus81-Mms4 initiate DSB in strains containing *Alu*-QP, IS50-PAL, *Alu*-PAL or *URA3*-PAL insertions?**

   Despite the role of MRX-Sae2 and Mus81-Mms4 in attacking the structures at the palindromic regions, a significant level of GCRs (25000-fold higher than that in the strain without repeat) and DSBs (1% in *Alu*-QP strain and 5% in IS50-PAL *Δsae2*, *Alu*-PAL *Δsae2*, and *URA3*-PAL *Δmus81 Δsae2* background) are induced by repeats. It is known from this study that the nucleases or regulators are under regulation of Cdc28 and Lsm6. It is of great importance to continue the study to reveal the components of this pathway. The importance to identify these proteins is not limited to understand genomic instability triggered by palindrome. Due to the structural similarity between palindrome-formed cruciform and Holliday junction, the research might also elucidate the role of these proteins in recombination and other DNA repair process.

2. **Is palindrome-induced BIR sequence-specific?**

It is shown by this study that palindrome-induced BIR has a different repertoire of factors compared to that of BIR induced by other types of breaks. From previous publications and this study, it is clear that the presence of homologous sequence adjacent to the breakage site can dictate the necessity of Rad51 recruitment. I hypothesize that if homology sequence is intrachromosomal and in close proximity to DSB, Rad51 is dispensable and Rad52 plays an important role in the strand annealing for BIR initiation. To test this hypothesis we can place *Alu*-QP, the repeat that does not induce BIR, close to HO site, and test if BIR will be driven into the Rad51-independent pathway.

3. **How does cell cycle correspond to BIR events? How does BIR influence the progression of the cells through the cell cycle?**

The results from this study imply that BIR events induced by the palindrome likely happen when cells are out of normal replicating cell cycle and arrested by checkpoint. To test this hypothesis, we can test the effect of checkpoint mutations or cell cycle regulator mutations on BIR synthesis by performing 2D gel electrophoresis on strains with mutations of Rad53 and Chk1.

This study using yeast as a model organism provide a foundation that can be extended to the understanding of the pathways leading to genomic instability induced by repetitive DNA sequences in normal human cells and cancer cells and

would potentially contribute to translational medicine by proposing protein targets for the drug design.

Table 1. Effect of palindromic sequences on GCRs and mutations

Insertion into *LYS2*	Rate of GCRs (X 10^{-7})		Rate of mutations (X 10^{-7})	
	wild-type	*Δsae2*	wild-type	*Δsae2*
Alu direct repeats	0.03 (0.02-0.04)	0.4 (0.3-0.6)	3 (1-6)	2 (1-3)
Alu-QP	310 (270-320)	1600 (1100-2200)	5 (3-7)	3 (2-4)
Alu-PAL	3050 (2540-3700)	4090 (2960-4450)	5 (4-9)	1 (1-3)
IS50-PAL	8600 (4190-8620)	5930 (4930-7230)	13 (10-19)	3 (2-5)
URA3-PAL	850 (680-960)	13460 (11090-15570)	23 (15-71)	2 (1-4)

Table 2. Effect of deficiency in structure-specific nucleases on palindrome-induced GCRs

		Rate of GCRs (X 10-5)	Fold of rate over wild type
Alu-PAL *Δsae2*	Wild type	40.9 (29.6-44.5)	1.0
	Δmlh1	30.1 (26.0-39.8)	0.7
	Δmus81	31.0 (26.8-52.1)	0.8
	Δslx4	35.9 (29.9-57.6)	0.9
	Δyen1	39.9 (25.7-69.5)	1.0
IS50-PAL *Δsae2*	Wild type	59.3 (49.3-72.3)	1.0
	Δmlh1	65.8 (45.4-13.5)	1.1
	Δmus81	39.7 (33.2-48.0)	0.7
	Δslx4	55.8 (47.9-83.7)	0.9
	Δyen1	58.7 (42.2-59.6)	1.0

Table 2 continued

URA3-PAL *Δsae2*	Wild type	134.6 (110.9-155.7)	1.0
	Δmlh1	154.7 (118.1-186.2)	1.1
	Δmus81	64.1 (45.9-74.3)	0.5
	Δslx4	130.7 (115.1-153.4)	1.0
	Δyen1	110.3 (102.6-144.3)	0.8

Table 3. Spontaneous and UV-induced mutagenesis by fragile perfect palindrome depends on the distance of *CAN1* from the DSB site.

		CAN1 mutation frequency X10^{-6} (Can^{R} Ade^{+})							
		No repeats		*URA3*-PAL		*Alu*-PAL		IS50-PAL	
			UV		UV		UV		UV
TP construct	8kb	0.2(0.1-0.3)	12.1(8.4-15.8)	7.9(5.6-10.9)	62.7(41.3-89.2)	1.9(0.7-2.7)	16.5(13.6-19.3)	2.7(1.2-3.5)	23.1(17.0-25.7)
	15kb	0.6(0.4-1.6)	ND	2.1(1.3-5.7)	30.3(15.0-52.0)				
	32kb	ND	ND	0.4(0.3-0.7)	ND				
CP construct	9kb	0.3(0.2-0.6)	ND	9.6(7.0-18.6)	70.9(62.4-92.0)				
	15kb	0.3(0.1-1.2)	ND	1.2(0.8-3.3)	25.3(20.1-39.8)				
	33kb	ND	ND	0.3(0.2-0.8)	12.8(9.8-16.7)				
	125kb	0.3(0.2-1.3)	ND	0.2(0.2-0.3)	22.6(16.3-37.0)				

Table 4. Mutation spectrum analysis of UV-irradiated strains containing *URA3*-PAL

	Number of mutations in a stretch of 1.7 kb in *CAN1* region			
	1		2	
	Number	Percentage in mutated population	Number	Percentage in mutated population
No repeat	16	100	0	0
No repeat 50J/m^2 UV	29	100	0	0
URA3-PAL	26	100	0	0
URA3-PAL 50J/m^2 UV	37	84	7	16

Table 5. Mutation rates in strains containing *URA3*-PAL using *CAN1* reporter

CAN1 located telomere-proximal 8kb to repeats		
Wildtype	20.7 (17.1-39.7)	1
Δ*rev1*	3.1 (1.9-3.9)	Decrease 6.7-fold
Δ*rev3*	6.6 (4.2-16.1)	Decrease 3.1-fold
Δ*rev7*	3.8 (2.3-5.3)	Decrease 5.4-fold
Δ*rad30*	36.6 (23.9-49.1)	Increase 1.8-fold
Δ*rad30*Δ *rev3*	4.9 (2.4-9.4)	Decrease 4.2-fold
Δ*pif1*	8.1 (4.5-41.4)	Decrease 2.6-fold
Δ*mus81*	26.4 (14.9-71.7)	Increase 1.3-fold
Δ*yen1*	23.2 (15.3-44.4)	Increase 1.1-fold
Δ*yen1*Δ *mus81*	19.7 (13.6-23.0)	Decrease 1.1-fold
Δ*pol32*	10.7 (8.2-18.1)	Decrease 1.9-fold

Table 5 continued

Δ*rad52*	40.3 (25.6-74.6)	Increase 2-fold
CAN1 located centromere-proximal 33kb to repeats		
Wildtype	2.4 (1.4-9.7)	1
Δ*mus81*	2.7 (2.2-3.7)	Increase 1.1-fold
Δ*mus81*Δ *yen1*	3.3 (1.6-6.6)	Increase 1.4-fold

Appendix A

Materials and Methods

Yeast Strains

The yeast strains use in this study were derivatives of KT19 strain (*MATa, bar1*-Δ, *his7-2, trp1*-Δ, *URA3*-Δ, *leu2-3,112, ADE2*-Δ, *LYS2*-Δ, *cup1*-Δ, *yhro54c*-Δ, *cup2*-Δ, *V34205::ADE2, V29616::CUP1*). *Alu*-QP and *Alu*-PAL are inserted into the BamHI site, *IS50*-PAL into the HpaI site and *URA3*-PAL into the XhoI. The strains without repeats contain an intact and functional *LYS2*.

Estimation of GCR and mutation frequencies and rates

Standard fluctuation tests were used to assay the frequencies and rates of mutations or GCRs in various background. Strains were cultured on YPD agar plate for 3 days in 30˚C. 14 individual colonies were picked and suspended in 0.25ml water and serial dilutions were performed to $1:10^5$. The dilutions were plated on YPD agar plate and on selection medium -- synthetic medium containing L-canavanine (60mg/L) and low concentration of adenine (5mg/L). Plates were incubated in 30˚C for 3 days before the number of white colonies or red colonies on selection medium were assayed for frequency/rate of mutation or GCR correspondingly. Frequency/rate and 95% confidence intervals were calculated according to the previous publication (Lobachev et al., 2002).

DSB detection and quantification

For DSB detection, yeast cells were inoculated in 5ml YPD liquid and incubated in 30˚C for overnight. Cells were then harvested and washed before embedded into low-melt agarose plugs at a concentration of $5*10^9$ cells/ml. For detecting DSB in *Alu*-QP, the concentration is increased to 7*109 cells/ml. The plugs were treated in 0.5M EDTA 10mM Tris solution containing 1.5mg/ml lyticase for 2hr in 37 degree or overnight in 30 degree followed by incubating in 1mg/ml Proteinase K solution overnight. For DSB detection by contour-clamped homogeneous electric field (CHEF) gel, plugs were equilibrated in CHEF running buffer 0.5*TBE for 10min before loaded and embedded in 1% CHEF agarose. Chromosomes were separated in CHEF machine at 14 degree for 28hr at 6V/cm, with angle of 120 degree. The initial and final switching time were 12.56s and 17.35s. The gel was treated with 500ml 0.25N HCl for 30min, 500ml alkaline buffer (1.5M NaCl, 0.5M NaOH) for 40min, and 500ml neutralization buffer (1.5M NaCl, 1M Tris, pH7.5) for 40min. DNA was transferred to charged nylon membrane for 2hr in 10*SSC by Posiblotter (Stratagene). Probe labeled with P32 was used in Southern hybridization at 65 degree overnight. The membrane was washed in 400ml wash buffer (0.1% SDS and 0.1*SSC) twice and subject to phosphorus-signal detection by typhoon phosphoimager (GE Healthcare). The signals were quantified by software ImageJ (NIH).

Time-point experiment for monitoring DSB formation in single cell cycle.

Overnight yeast culture in YPD were inoculated in 1L YPGS (1% yeast extract, 2% peptone, 2% glycerol and 1% succinic acid, pH5.5) containing 300ug/ml G418 and incubated in 30 degree overnight with vigorous shaking. 200ml culture was taken out and placed into sterile flask when OD of the culture reached 0.7-0.8. Cells in the 800ml culture was synchronized in G1 with alpha factor (0.1ug/ml) for 3hr (G1-S experiment) and those in 200ml culture was synchronized in G2/M with nocodazole (150ug/ml) (G2/M experiment). After synchronization, 100ml culture from each treatment was taken into ice-cold bottle containing sodium azide and 0.2M EDTA solution with the final concentration of 0.1% and 20mM for making cell plugs (before induction sample). 1ml culture was also taken and centrifuged. The pellet was suspended in 70% ethanol for FACS analysis. The rest culture was spun down and pellets were washed once and released into fresh YPGS medium containing 2% galactose and 4uM estradiol to induce Cre recombinase. Alpha factor was added into the G1-S experiment and nocodazole added to G2/M experiment. After 3hr induction, samples were taken for FACS and make cell plugs (after induction sample). In the G1/S experiment, the rest of the culture was spun down and the pellet was washed twice with autoclaved water to remove alpha factor. The cells were then suspended in fresh YPD containing pronase. Samples for each time-points were taken and processed right away after all time-points were taken to make cell plugs as mentioned above.

Time-point experiment using conditional Sae2 system

Overnight culture in YPD was inoculated in YPGS as mentioned above. Alpha factor was added to 0.1ug/ml when OD reached 0.6-0.8. After 3hr of G1 arrest, Galactose and estradiol was added to final concentration of 2% and 4uM respectively to induce Sae2-Ebd in G1-arrested stage. After 3hr induction, cells were spun down and washed twice. Pellets were released into fresh YPGS medium containing 2% galactose, 4uM estradiol and pronase (12.5ug/ml). The time-points were taken from 0 min after release to 5.5hr after release. For the experiment in which cells are arrested in G2/M in the end, nocodazole was also added at 150ug/ml at the time-point of 0min.

2D neutral/neutral and neutral/alkaline gels for analyzing broken ends in strains containing *URA3*-PAL

Plugs containing yeasts were prepared as described above. Each plug (about 40ul) was washed in 30ml 1*TE for 1hr twice, 1*TE containing 1mM PMSF for 1hr, 1*TE for 1hr and Millipore water for 1hr before being equilibrated in 2*Orange digestion buffer (Thermo Fisher Fermentas) and digested in 1*Orange buffer with 50unit AflII. Loading the 2D neutral/neutral and neutral/alkaline gel electrophoresis and performing Southern blotting hybridization is described in Yu Zhang et al., 2013. The probe used for this hybridization targets *LYS2* region centromere-proximal to repeat.

2D neutral/neutral and neutral/neutral gel electrophoresis for analyzing replication and repair intermediates.

2D gel electrophoresis for analyzing complex DNA structures was carried out as described in previous publication (Brewer and Fangman, 1987). For experiments comparing structures in *SAE2* and *Δsae2* background, overnight culture with OD 0.6-0.8 was synchronized in G1 with alpha factor (0.1ug/ml) for 3hr before being washed by autoclaved water twice and released into fresh YPD liquid for collecting samples at timepoints. For experiments with inducible Sae2, cells were inoculated in YPGS (10% yeast extract, 20% peptone, 20% glycerol, 10% succinate, pH5.5) to grow overnight. Culture was arrested with alpha factor as same time and concentration as mentioned above. After 3hr of arresting by alpha factor, galactose and estradiol were added to a concentration of 2% and 4mM respectively to induce Sae2 for 2 and half hour. Cells then were washed by autoclaved water twice and released into fresh YPGS with galactose and estradiol. In the inducible Sae2 experiment with nocodazole addition, nocodazole was added when cells were released into fresh medium. Cells were harvested and genomic DNA was extracted as described previously in Fiedman and Brewer, 1995. DNA samples were digested by AflII for *Alu*-PAL and *URA3*-PAL and double digestion by BoxI and Bst1107I for *IS50*-PAL. Digested DNA was loaded in 2D gel electrophoresis as described in Yu Zhang et al., 2013. DNA was firstly loaded in 0.4% agarose gel and run in 1*TBE under 55V for 22hr. The gel was sliced out and placed horizontally and embedded in second dimensional agarose gel of 1.2%. The gel was run in 1*TBE buffer under 8.5V/cm for 12hr in 4 degree. DNA was

transferred to nylon membrane for Southern blot hybridization. The probe targeting *LYS2* region centromere-proximal to repeats was used in hybridization.

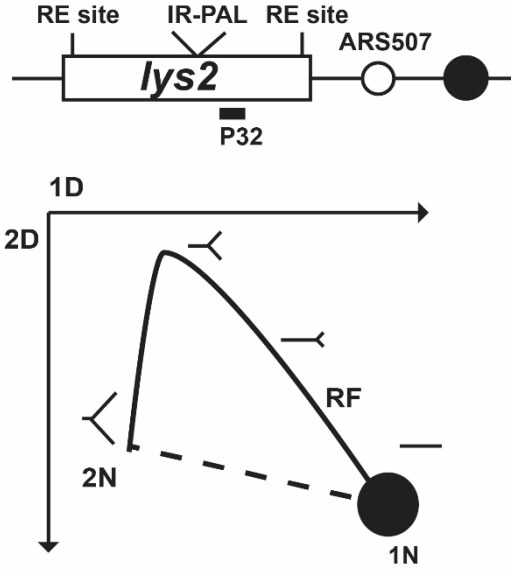

Figure 15. 2-dimensional gel to analyze the structure of intermediates of replication fork. Replicating DNA was extracted, digested with restriction enzyme and separated in the first dimension (1D) by size followed by the separation of size and complexity in the second dimension (2D). The 1N indicates the unreplicated linear molecule. Take *URA3*-PAL for example, 1N is 6kb. 2N indicates the molecule that also finishes replication. The peak of the arc-shape indicates the molecules that half-replicated that are most branched molecules.

RNA extraction and qRT-Realtime PCR

Yeast cells were inoculated in 10ml synthetic complete medium and incubated in 30degree overnight. On the second day, cells were washed by autoclaved water twice and split equally into the fresh 50ml synthetic complete medium and synthetic medium minus uracil. The cultures were shaked in 30 degree incubator for 4hr before taking samples for embedding cells in low-melt agarose

plugs for DSB analysis and for RNA extraction. RNA was extracted using the YeaStar RNA kit (Zymo Research), treated with DNase I followed by purification using DNA-free RNA kit (Zymo Research). RNA samples were then used to set up RT-qPCR using qScript One-Step SYBR Green RT-qPCR (Quanta). *Act1* was amplified as a housekeeping control. Primer information is shown as following: *Act1* rt5-AACCGCTGCTCAATCTTC; *Act1* Primer 2-CAATACCGGCAGATTCCAA; *URA3*-rt5-GAACGTGCTGCTACTCATC; *URA3*-rt3-ACTCCAGTAATTCCTTGGTG.

Restriction digestion in plugs for DSB detection

Plugs were washed and digested as mentioned above. To detect the ARS507-distal breaks, BsrGI was used; for the detection of ARS507-proximal breaks, AflII was used. After digestion, plugs were equilibrated in the running buffer 1*TBE for 20min before loading to the 0.8% agarose gel. Gel electrophoresis was performed under 60V for 18hr before gel was processed to transfer the DNA from gel to nylon membrane for Southern blotting hybridization.

References

Amler, L.C., and Schwab, M. (1989). Amplified N-myc in human neuroblastoma cells is often arranged as clustered tandem repeats of differently recombined DNA. Molecular and cellular biology *9*, 4903-4913.

Beggs, J.D. (2005). Lsm proteins and RNA processing. Biochemical Society transactions *33*, 433-438.

Bishop, A.C., Ubersax, J.A., Petsch, D.T., Matheos, D.P., Gray, N.S., Blethrow, J., Shimizu, E., Tsien, J.Z., Schultz, P.G., Rose, M.D.*, et al.* (2000). A chemical switch for inhibitor-sensitive alleles of any protein kinase. Nature *407*, 395-401.

Blanco, M.G., Matos, J., Rass, U., Ip, S.C., and West, S.C. (2010). Functional overlap between the structure-specific nucleases Yen1 and Mus81-Mms4 for DNA-damage repair in S. cerevisiae. DNA repair *9*, 394-402.

Bloom, J., and Cross, F.R. (2007). Multiple levels of cyclin specificity in cell-cycle control. Nature reviews Molecular cell biology *8*, 149-160.

Brewer, B.J., and Fangman, W.L. (1987). The localization of replication origins on ARS plasmids in S. cerevisiae. Cell *51*, 463-471.

Chang, J.H., Kim, J.J., Choi, J.M., Lee, J.H., and Cho, Y. (2008). Crystal structure of the Mus81-Eme1 complex. Genes & development *22*, 1093-1106.

Chung, W.H., Zhu, Z., Papusha, A., Malkova, A., and Ira, G. (2010). Defective resection at DNA double-strand breaks leads to de novo telomere formation and enhances gene targeting. PLoS genetics *6*, e1000948.

Ciccia, A., Constantinou, A., and West, S.C. (2003). Identification and characterization of the human mus81-eme1 endonuclease. The Journal of biological chemistry *278*, 25172-25178.

Connelly, J.C., and Leach, D.R. (1996). The sbcC and sbcD genes of Escherichia coli encode a nuclease involved in palindrome inviability and genetic recombination. Genes to cells : devoted to molecular & cellular mechanisms *1*, 285-291.

Cote, A.G., and Lewis, S.M. (2008). Mus81-dependent double-strand DNA breaks at in vivo-generated cruciform structures in S. cerevisiae. Molecular cell *31*, 800-812.

Cromie, G.A., Millar, C.B., Schmidt, K.H., and Leach, D.R. (2000). Palindromes as substrates for multiple pathways of recombination in Escherichia coli. Genetics *154*, 513-522.

Darmon, E., Eykelenboom, J.K., Lincker, F., Jones, L.H., White, M., Okely, E., Blackwood, J.K., and Leach, D.R. (2010). E. coli SbcCD and RecA control chromosomal rearrangement induced by an interrupted palindrome. Molecular cell *39*, 59-70.

Davis, A.P., and Symington, L.S. (2004). RAD51-dependent break-induced replication in yeast. Molecular and cellular biology *24*, 2344-2351.

de los Santos, T., Hunter, N., Lee, C., Larkin, B., Loidl, J., and Hollingsworth, N.M. (2003). The Mus81/Mms4 endonuclease acts independently of double-Holliday junction resolution to promote a distinct subset of crossovers during meiosis in budding yeast. Genetics *164*, 81-94.

Deem, A., Barker, K., VanHulle, K., Downing, B., Vayl, A., and Malkova, A. (2008). Defective break-induced replication leads to half-crossovers in Saccharomyces cerevisiae. Genetics *179*, 1845-1860.

Deem, A., Keszthelyi, A., Blackgrove, T., Vayl, A., Coffey, B., Mathur, R., Chabes, A., and Malkova, A. (2011). Break-Induced Replication Is Highly Inaccurate. Plos Biol *9*.

Dickie, P., Morgan, A.R., and McFadden, G. (1987). Cruciform extrusion in plasmids bearing the replicative intermediate configuration of a poxvirus telomere. J Mol Biol *196*, 541-558.

Eykelenboom, J.K., Blackwood, J.K., Okely, E., and Leach, D.R. (2008). SbcCD causes a double-strand break at a DNA palindrome in the Escherichia coli chromosome. Molecular cell *29*, 644-651.

Ezekiel, U.R., and Zassenhaus, H.P. (1993). Localization of a cruciform cutting endonuclease to yeast mitochondria. Molecular & general genetics : MGG *240*, 414-418.

Farah, J.A., Hartsuiker, E., Mizuno, K., Ohta, K., and Smith, G.R. (2002). A 160-bp palindrome is a Rad50.Rad32-dependent mitotic recombination hotspot in Schizosaccharomyces pombe. Genetics *161*, 461-468.

French, S.L., Sikes, M.L., Hontz, R.D., Osheim, Y.N., Lambert, T.E., El Hage, A., Smith, M.M., Tollervey, D., Smith, J.S., and Beyer, A.L. (2011). Distinguishing the roles of Topoisomerases I and II in relief of transcription-induced torsional stress in yeast rRNA genes. Molecular and cellular biology *31*, 482-494.

Fricke, W.M., and Brill, S.J. (2003). Slx1-Slx4 is a second structure-specific endonuclease functionally redundant with Sgs1-Top3. Genes & development *17*, 1768-1778.

Galgoczy, D.J., and Toczyski, D.P. (2001). Checkpoint adaptation precedes spontaneous and damage-induced genomic instability in yeast. Molecular and cellular biology *21*, 1710-1718.

Gallo-Fernandez, M., Saugar, I., Ortiz-Bazan, M.A., Vazquez, M.V., and Tercero, J.A. (2012). Cell cycle-dependent regulation of the nuclease activity of Mus81-Eme1/Mms4. Nucleic acids research *40*, 8325-8335.

Gordenin, D.A., Lobachev, K.S., Degtyareva, N.P., Malkova, A.L., Perkins, E., and Resnick, M.A. (1993). Inverted DNA repeats: a source of eukaryotic genomic instability. Molecular and cellular biology *13*, 5315-5322.

Guenthoer, J., Diede, S.J., Tanaka, H., Chai, X., Hsu, L., Tapscott, S.J., and Porter, P.L. (2012). Assessment of palindromes as platforms for DNA amplification in breast cancer. Genome research *22*, 232-245.

Havas, K., Flaus, A., Phelan, M., Kingston, R., Wade, P.A., Lilley, D.M., and Owen-Hughes, T. (2000). Generation of superhelical torsion by ATP-dependent chromatin remodeling activities. Cell *103*, 1133-1142.

Holbeck, S.L., and Strathern, J.N. (1997). A role for REV3 in mutagenesis during double-strand break repair in Saccharomyces cerevisiae. Genetics *147*, 1017-1024.

Huertas, P., Cortes-Ledesma, F., Sartori, A.A., Aguilera, A., and Jackson, S.P. (2008). CDK targets Sae2 to control DNA-end resection and homologous recombination. Nature *455*, 689-692.

Inagaki, H., Ohye, T., Kogo, H., Tsutsumi, M., Kato, T., Tong, M., Emanuel, B.S., and Kurahashi, H. (2013). Two sequential cleavage reactions on cruciform DNA structures cause palindrome-mediated chromosomal translocations. Nature communications *4*, 1592.

Ip, S.C., Rass, U., Blanco, M.G., Flynn, H.R., Skehel, J.M., and West, S.C. (2008). Identification of Holliday junction resolvases from humans and yeast. Nature *456*, 357-361.

Joseph, P., Guiseppi, A., Sorokin, A., and Denizot, F. (2004). Characterization of the Bacillus subtilis YxdJ response regulator as the inducer of expression for the cognate ABC transporter YxdLM. Microbiology *150*, 2609-2617.

Kambach, C., Walke, S., Young, R., Avis, J.M., de la Fortelle, E., Raker, V.A., Luhrmann, R., Li, J., and Nagai, K. (1999). Crystal structures of two Sm protein complexes and their implications for the assembly of the spliceosomal snRNPs. Cell *96*, 375-387.

Kato, T., Franconi, C.P., Sheridan, M.B., Hacker, A.M., Inagakai, H., Glover, T.W., Arlt, M.F., Drabkin, H.A., Gemmill, R.M., Kurahashi, H.*, et al.* (2014). Analysis of the t(3;8) of hereditary renal cell carcinoma: a palindrome-mediated translocation. Cancer genetics *207*, 133-140.

Keeney, S., Giroux, C.N., and Kleckner, N. (1997). Meiosis-specific DNA double-strand breaks are catalyzed by Spo11, a member of a widely conserved protein family. Cell *88*, 375-384.

Kehrer-Sawatzki, H., Udart, M., Krone, W., Baden, R., Fahsold, R., Thomas, G., Schmucker, B., and Assum, G. (1997). Mutational analysis and expression studies of the neurofibromatosis type 2 (NF2) gene in a patient with a ring chromosome 22 and NF2. Human genetics *100*, 67-74.

Kim, H.M., Narayanan, V., Mieczkowski, P.A., Petes, T.D., Krasilnikova, M.M., Mirkin, S.M., and Lobachev, K.S. (2008). Chromosome fragility at GAA tracts in yeast depends on repeat orientation and requires mismatch repair. The EMBO journal *27*, 2896-2906.

Klapholz, S., Waddell, C.S., and Esposito, R.E. (1985). The role of the SPO11 gene in meiotic recombination in yeast. Genetics *110*, 187-216.

Kleff, S., Kemper, B., and Sternglanz, R. (1992). Identification and characterization of yeast mutants and the gene for a cruciform cutting endonuclease. The EMBO journal *11*, 699-704.

Kramer, K.M., and Haber, J.E. (1993). New telomeres in yeast are initiated with a highly selected subset of TG1-3 repeats. Genes & development *7*, 2345-2356.

Kufel, J., Allmang, C., Petfalski, E., Beggs, J., and Tollervey, D. (2003). Lsm Proteins are required for normal processing and stability of ribosomal RNAs. The Journal of biological chemistry *278*, 2147-2156.

Kurahashi, H., Shaikh, T., Takata, M., Toda, T., and Emanuel, B.S. (2003). The constitutional t(17;22): another translocation mediated by palindromic AT-rich repeats. American journal of human genetics *72*, 733-738.

Kuwahara, Y., Tanabe, C., Ikeuchi, T., Aoyagi, K., Nishigaki, M., Sakamoto, H., Hoshinaga, K., Yoshida, T., Sasaki, H., and Terada, M. (2004). Alternative mechanisms of gene amplification in human cancers. Genes, chromosomes & cancer *41*, 125-132.

Lander, E.S., Linton, L.M., Birren, B., Nusbaum, C., Zody, M.C., Baldwin, J., Devon, K., Dewar, K., Doyle, M., FitzHugh, W.*, et al.* (2001). Initial sequencing and analysis of the human genome. Nature *409*, 860-921.

Lemoine, F.J., Degtyareva, N.P., Lobachev, K., and Petes, T.D. (2005). Chromosomal translocations in yeast induced by low levels of DNA polymerase a model for chromosome fragile sites. Cell *120*, 587-598.

Li, Y., Cross, F.R., and Chait, B.T. (2014). Method for identifying phosphorylated substrates of specific cyclin/cyclin-dependent kinase complexes. Proceedings of the National Academy of Sciences of the United States of America *111*, 11323-11328.

Llorente, B., Smith, C.E., and Symington, L.S. (2008). Break-induced replication - What is it and what is it for? Cell Cycle *7*, 859-864.

Lobachev, K.S., Gordenin, D.A., and Resnick, M.A. (2002). The Mre11 complex is required for repair of hairpin-capped double-strand breaks and prevention of chromosome rearrangements. Cell *108*, 183-193.

Lobachev, K.S., Shor, B.M., Tran, H.T., Taylor, W., Keen, J.D., Resnick, M.A., and Gordenin, D.A. (1998a). Factors affecting inverted repeat stimulation of recombination and deletion in Saccharomyces cerevisiae. Genetics *148*, 1507-1524.

Lobachev, K.S., Shor, B.M., Tran, H.T., Taylor, W., Keen, J.D., Resnick, M.A., and Gordenin, D.A. (1998b). Factors affecting inverted repeat stimulation of recombination and deletion in Saccharomyces cerevisiae. Genetics *148*, 1507-1524.

Lobachev, K.S., Stenger, J.E., Kozyreva, O.G., Jurka, J., Gordenin, D.A., and Resnick, M.A. (2000). Inverted Alu repeats unstable in yeast are excluded from the human genome. The EMBO journal *19*, 3822-3830.

Lydeard, J.R., Jain, S., Yamaguchi, M., and Haber, J.E. (2007). Break-induced replication and telomerase-independent telomere maintenance require Pol32. Nature *448*, 820-823.

Malkova, A., and Haber, J.E. (2012). Mutations Arising During Repair of Chromosome Breaks. Annu Rev Genet *46*, 455-473.

Malkova, A., and Ira, G. (2013). Break-induced replication: functions and molecular mechanism. Curr Opin Genet Dev *23*, 271-279.

Malkova, A., Ivanov, E.L., and Haber, J.E. (1996). Double-strand break repair in the absence of RAD51 in yeast: a possible role for break-induced DNA replication. Proceedings of the National Academy of Sciences of the United States of America *93*, 7131-7136.

Malkova, A., Signon, L., Schaefer, C.B., Naylor, M.L., Theis, J.F., Newlon, C.S., and Haber, J.E. (2001). RAD51-independent break-induced replication to repair a broken chromosome depends on a distant enhancer site. Genes & development *15*, 1055-1060.

Mangano, R., Piddini, E., Carramusa, L., Duhig, T., Feo, S., and Fried, M. (1998). Chimeric amplicons containing the c-myc gene in HL60 cells. Oncogene *17*, 2771-2777.

Mayes, A.E., Verdone, L., Legrain, P., and Beggs, J.D. (1999). Characterization of Sm-like proteins in yeast and their association with U6 snRNA. The EMBO journal *18*, 4321-4331.

Mayle, R., Campbell, I.M., Beck, C.R., Yu, Y., Wilson, M., Shaw, C.A., Bjergbaek, L., Lupski, J.R., and Ira, G. (2015). DNA REPAIR. Mus81 and converging forks limit the mutagenicity of replication fork breakage. Science *349*, 742-747.

McDonald, J.P., Levine, A.S., and Woodgate, R. (1997). The Saccharomyces cerevisiae RAD30 gene, a homologue of Escherichia coli dinB and umuC, is DNA damage inducible and functions in a novel error-free postreplication repair mechanism. Genetics *147*, 1557-1568.

Mendenhall, M.D., and Hodge, A.E. (1998). Regulation of Cdc28 cyclin-dependent protein kinase activity during the cell cycle of the yeast Saccharomyces cerevisiae. Microbiology and molecular biology reviews : MMBR *62*, 1191-1243.

Mortensen, U.H., Bendixen, C., Sunjevaric, I., and Rothstein, R. (1996). DNA strand annealing is promoted by the yeast Rad52 protein. Proceedings of the National Academy of Sciences of the United States of America *93*, 10729-10734.

Murnane, J.P. (2006). Telomeres and chromosome instability. DNA repair *5*, 1082-1092.

Narayanan, V., Mieczkowski, P.A., Kim, H.M., Petes, T.D., and Lobachev, K.S. (2006). The pattern of gene amplification is determined by the chromosomal location of hairpin-capped breaks. Cell *125*, 1283-1296.

Neiman, P.E., Burnside, J., Elsaesser, K., Hwang, H., Clurman, B.E., Kimmel, R., and Delrow, J. (2006). Analysis of gene expression, copy number and palindrome formation with a Dt40 enriched cDNA microarray. Sub-cellular biochemistry *40*, 245-256.

Neiman, P.E., Elsaesser, K., Loring, G., and Kimmel, R. (2008). Myc oncogene-induced genomic instability: DNA palindromes in bursal lymphomagenesis. PLoS genetics *4*, e1000132.

Pennaneach, V., Putnam, C.D., and Kolodner, R.D. (2006). Chromosome healing by de novo telomere addition in Saccharomyces cerevisiae. Molecular microbiology *59*, 1357-1368.

Pomeranz Krummel, D.A., Oubridge, C., Leung, A.K., Li, J., and Nagai, K. (2009). Crystal structure of human spliceosomal U1 snRNP at 5.5 A resolution. Nature *458*, 475-480.

Prakash, S., Johnson, R.E., and Prakash, L. (2005). Eukaryotic translesion synthesis DNA polymerases: specificity of structure and function. Annual review of biochemistry *74*, 317-353.

Rattray, A.J., Shafer, B.K., McGill, C.B., and Strathern, J.N. (2002). The roles of REV3 and RAD57 in double-strand-break-repair-induced mutagenesis of Saccharomyces cerevisiae. Genetics *162*, 1063-1077.

Rooks, H., Clark, B., Best, S., Rushton, P., Oakley, M., Thein, O.S., Cuthbert, A.C., Britland, A., Ruf, A., and Thein, S.L. (2012). A novel 506kb deletion causing epsilongammadeltabeta thalassemia. Blood cells, molecules & diseases *49*, 121-127.

Ruskin, B., and Fink, G.R. (1993). Mutations in POL1 increase the mitotic instability of tandem inverted repeats in Saccharomyces cerevisiae. Genetics *134*, 43-56.

Saini, N., Ramakrishnan, S., Elango, R., Ayyar, S., Zhang, Y., Deem, A., Ira, G., Haber, J.E., Lobachev, K.S., and Malkova, A. (2013a). Migrating bubble during break-induced replication drives conservative DNA synthesis. Nature *502*, 389-392.

Saini, N., Zhang, Y., Nishida, Y., Sheng, Z., Choudhury, S., Mieczkowski, P., and Lobachev, K.S. (2013b). Fragile DNA motifs trigger mutagenesis at distant chromosomal loci in saccharomyces cerevisiae. PLoS genetics *9*, e1003551.

Saugar, I., Vazquez, M.V., Gallo-Fernandez, M., Ortiz-Bazan, M.A., Segurado, M., Calzada, A., and Tercero, J.A. (2013). Temporal regulation of the Mus81-Mms4 endonuclease ensures cell survival under conditions of DNA damage. Nucleic acids research *41*, 8943-8958.

Schwartz, E.K., and Heyer, W.D. (2011). Processing of joint molecule intermediates by structure-selective endonucleases during homologous recombination in eukaryotes. Chromosoma *120*, 109-127.

Schwartz, E.K., Wright, W.D., Ehmsen, K.T., Evans, J.E., Stahlberg, H., and Heyer, W.D. (2012). Mus81-Mms4 functions as a single heterodimer to cleave nicked intermediates in recombinational DNA repair. Molecular and cellular biology *32*, 3065-3080.

Sheridan, M.B., Kato, T., Haldeman-Englert, C., Jalali, G.R., Milunsky, J.M., Zou, Y., Klaes, R., Gimelli, G., Gimelli, S., Gemmill, R.M.*, et al.* (2010). A palindrome-mediated recurrent translocation with 3:1 meiotic nondisjunction: the t(8;22)(q24.13;q11.21). American journal of human genetics *87*, 209-218.

St Charles, J., and Petes, T.D. (2013). High-resolution mapping of spontaneous mitotic recombination hotspots on the 1.1 Mb arm of yeast chromosome IV. PLoS genetics *9*, e1003434.

Stark, H., Dube, P., Luhrmann, R., and Kastner, B. (2001). Arrangement of RNA and proteins in the spliceosomal U1 small nuclear ribonucleoprotein particle. Nature *409*, 539-542.

Symington, L.S. (2002). Role of RAD52 epistasis group genes in homologous recombination and double-strand break repair. Microbiology and molecular biology reviews : MMBR *66*, 630-670, table of contents.

Tanaka, H., Bergstrom, D.A., Yao, M.C., and Tapscott, S.J. (2005). Widespread and nonrandom distribution of DNA palindromes in cancer cells provides a structural platform for subsequent gene amplification. Nature genetics *37*, 320-327.

Tanaka, H., Bergstrom, D.A., Yao, M.C., and Tapscott, S.J. (2006). Large DNA palindromes as a common form of structural chromosome aberrations in human cancers. Human cell *19*, 17-23.

Tanaka, H., Cao, Y., Bergstrom, D.A., Kooperberg, C., Tapscott, S.J., and Yao, M.C. (2007). Intrastrand annealing leads to the formation of a large DNA palindrome and determines the boundaries of genomic amplification in human cancer. Molecular and cellular biology *27*, 1993-2002.

Taylor, E.R., and McGowan, C.H. (2008). Cleavage mechanism of human Mus81-Eme1 acting on Holliday-junction structures. Proceedings of the National Academy of Sciences of the United States of America *105*, 3757-3762.

Tiefenbach, T., and Junop, M. (2012). Pso2 (SNM1) is a DNA structure-specific endonuclease. Nucleic acids research *40*, 2131-2139.

Wagstaff, J.E., Klapholz, S., Waddell, C.S., Jensen, L., and Esposito, R.E. (1985). Meiotic exchange within and between chromosomes requires a common Rec function in Saccharomyces cerevisiae. Molecular and cellular biology *5*, 3532-3544.

Waldman, A.S., Tran, H., Goldsmith, E.C., and Resnick, M.A. (1999). Long inverted repeats are an at-risk motif for recombination in mammalian cells. Genetics *153*, 1873-1883.

Wang, H., Li, Y., Truong, L.N., Shi, L.Z., Hwang, P.Y., He, J., Do, J., Cho, M.J., Li, H., Negrete, A.*, et al.* (2014). CtIP maintains stability at common fragile sites and inverted repeats by end resection-independent endonuclease activity. Molecular cell *54*, 1012-1021.

Wilson, M.A., Kwon, Y., Xu, Y., Chung, W.H., Chi, P., Niu, H., Mayle, R., Chen, X., Malkova, A., Sung, P.*, et al.* (2013). Pif1 helicase and Poldelta promote recombination-coupled DNA synthesis via bubble migration. Nature *502*, 393-396.

Zhang, Y., Saini, N., Sheng, Z., and Lobachev, K.S. (2013). Genome-wide screen reveals replication pathway for quasi-palindrome fragility dependent on homologous recombination. PLoS genetics *9*, e1003979.

Zhu, H., Shang, D., Sun, M., Choi, S., Liu, Q., Hao, J., Figuera, L.E., Zhang, F., Choy, K.W., Ao, Y.*, et al.* (2011). X-linked congenital hypertrichosis syndrome is associated with interchromosomal insertions mediated by a human-specific palindrome near SOX3. American journal of human genetics *88*, 819-826.

Zhu, Z., Chung, W.H., Shim, E.Y., Lee, S.E., and Ira, G. (2008). Sgs1 helicase and two nucleases Dna2 and Exo1 resect DNA double-strand break ends. Cell *134*, 981-994.

Ford, M., and Fried, M. (1986). Large inverted duplications are associated with gene amplification. Cell 45, 425-430.

Chapter 4. Other accomplishment

4.1. Summary

During my graduate studies, I also participated in the research focusing on understanding the mechanism underlying HO-endonuclease-induced break-induced replication (BIR) in collaboration with Dr. Anna Malkova's laboratory at the University of Iowa, Department of Biology.

In the yeast experimental system we employed, one truncated copy of Chr III contains a HO-endonuclease site at the MATa locus and a full-length of Chr III, serving as the repair template in BIR, contains a mutant uncleavable MATα-inc allele. In the process of BIR, the 3' end of resected broken molecule from HO-induced double strand break at the truncated copy of Chr III (recipient) invades into the MATα-inc sequences and copies approximately 100kb DNA to the right telomere on the full-length Chr III (donor). During the progression of BIR, joint molecules might form between broken recipient and donor chromosomes and lead to detrimental consequences if the structures are not resolved. Therefore resolvases that process toxic recombination intermediates are required in both meiosis and mitosis (Zakharyevich et al., 2012; Mullen et al., 2001).

Srs2 helicase is responsible for resolving recombination intermediates in multiple pathways in yeast. Mutation of Srs2 leads to the hyper-recombination phenotype indicating that the Srs2 is inhibiting the channeling of stalled replication fork into recombination products (Aguilera and Klein, 1988). It is also shown sensitivity is more severe in diploid *srs2Δ* strain than in haploid mutant in response

to DNA damages, such as MMS, UV- and gamma-irradiation. It is proposed that Srs2 is involved in resolving toxic recombination intermediates during DNA repair.

In this study, using 2-D gel electrophoresis, I demonstrated that in the *srs2* mutant strains, DNA structures with high complexity and mass were accumulated during HO-induced BIR This toxic intermediates are likely products from recombination between donor and recipient chromosomes. I also found that structure-specific endonucleases Mus81-Mms4 and Yen1 can resolve the toxic joints molecules in the *srs2* mutant strains to promote BIR progression.

4.2 Introduction

Homologous recombination (HR) is an important mechanism to repair double-strand DNA breaks (DSBs). It initiates by invasion of a broken DNA into the region of homology using it as a template for repair synthesis that allows restoration of the broken DNA in a faithful manner. The potential problem, however, is that this leads to the formation of joint molecules (structures containing the broken and intact DNA molecules), which require proper resolution, and are detrimental for the cell when remained unresolved. A classic example of toxicity arising from joint molecules came from the observation in meiosis in cells where in the absence of Holliday Junction resolvases, joint molecules accumulate leading to the meiotic failure (Zakharyevich et al., 2012). Similarly, resolvases are required in mitotic cells to prevent toxic accumulation of recombination and replication intermediates in *sgs1* helicase or *top3* topoisomerase mutants (Mullen et al., 2001).

Therefore, recombination is potentially dangerous since it can lead to trapping of broken and intact chromosomes together, and should be properly regulated in both meiotic and vegetative cells.

Srs2 helicase is a major regulator of recombination in yeast. Mutations in *SRS2* were originally discovered as suppressors of the UV sensitivity of *rad6* and *rad18* mutants (Aboussekhra et al., 1989; Lawrence and Christensen, 1979). In addition, the absence of Srs2 led to a hyper-recombination phenotype, which suggested that the role of Srs2 is to prevent channeling of stalled replication intermediates into recombination that can be toxic for the cell (Aguilera and Klein, 1988). This was further supported by the synthetic lethality of *srs2Δ* in combination with *sgs1Δ*, *rad54Δ,* and several other mutations that was suppressed by deletion of *RAD51* eliminating recombination (Gangloff et al., 2000; Klein, 2001). Intriguingly, toxic recombination appeared especially detrimental when involved homologous chromosomes since the defect of Srs2 alone was reported to cause sickness or even lethality in diploid and disomic cells, but not in haploids (Keyamura et al., 2016). This suggested that Srs2 is especially important for preventing accumulation of recombination intermediates that can trap homologous chromosomes together. What remained unknown is the identity of the DNA lesions that give rise to these toxic DNA intermediates. It was suggested that they were not DSBs, but other lesions, possibly ssDNA gaps, that were channeled into recombination in the absence Srs2 (Aboussekhra et al., 1989; Keyamura et al., 2016). The idea that toxic intermediates formed between homologs are especially detrimental was further supported by the observation that diploid *srs2Δ* mutants

were much more sensitive than haploids to various types of DNA damage, including UV, MMS and gamma radiation (Aboussekhra et al., 1989). All this genetic evidence, led to the proposal that the main role of Srs2 is in preventing channeling of DNA damage into recombination that can trap chromosomes and lead to cell death.

To perform its anti-recombination function, Srs2 is recruited by PCNA when it is sumoylated by Siz1 at K127 and K164 in response to replication stalling (Papouli et al., 2005; Pfander et al., 2005). The recruitment of Srs2 prevents channeling of ssDNA gaps into recombination, and therefore promotes other types of repair, for example translesion DNA synthesis. The suppression of *srs2Δ* phenotypes by *rad51Δ* suggested that Srs2 performs its anti-recombination function via stripping off Rad51 from ssDNA, which was confirmed by *in vitro* experiments (Krejci et al., 2003; Veaute et al., 2003). This "strippase activity" requires two domains of Srs2: the translocase and Rad51-interacting domains. The translocase domain of Srs2 resides in N- terminal portion of the protein and can be disrupted by a K41A mutation, inactivating ATPase activity of the protein (Krejci et al., 2004). Rad51-interaction (BRC) domain (862-914 bp) is essential for strippase activity of Srs2 (Colavito et al., 2009). Another biochemical function of Srs2 is in its helicase activity. Srs2 can *in vitro* unwind various DNA substrates, including linear DNA duplexes and D-loops (Marini and Krejci, 2012). *In vivo*, Srs2 helicase activity is required to prevent expansions of trinucleotide repeats and of rNMP induced mutagenesis (Bhattacharyya and Lahue, 2004; Potenski et al., 2014). It remains

unclear, however, whether helicase activity of Srs2 is also important for the regulation of recombination.

The studies described above suggest an anti-recombination function of Srs2. Paradoxically, Srs2 appears to have also a pro-recombination function because it is required for the successful repair of DSB proceeding by homologous recombination. In particular, Srs2 promotes DSB repair by synthesis-dependent strand annealing (SDSA) and limits crossover outcomes (Ira et al., 2003). Two models explaining the anti-crossover role of Srs2 were proposed. The first model suggested that Srs2 removes Rad51 from the second non-invading (catching) DSB end and thus prevents formation of a Holliday junction, an intermediate required for crossing-over (Mitchel et al., 2013). According to the second model, Srs2 prevents crossovers by unwinding of D-loops via its helicase activity (Ira et al., 2003). Another study suggested a role of Srs2 in DNA damage checkpoint recovery after DSB repair (Vaze et al., 2002). This function was deduced from observation of massive cell death following completion of DSB repair by Southern blot. In most extreme case, 98% of *srs2Δ* cells died despite of successful completion of DSB repair by single strand annealing, as detected by southern blot analysis. It was later reported, however, that Rad51 remained bound to the chromatin in areas surrounding the repair region and the death was explained by inability of Srs2 to remove Rad51 from the repaired chromosomes (Yeung and Durocher, 2011). DSB-induced death was also observed in cells undergoing break-induced replication (BIR), but the cause of this death was not explained (Lydeard et al., 2010). Together, these studies proposed a pro-recombinational role of Srs2 in DSB repair.

The goal of this study is to test an alternative hypothesis that Srs2 plays an anti-recombination role that ensures successful DSB repair. In particular, we postulated that the loss of viability observed in *srs2* mutants results from toxic joint molecules formed by long ssDNA regions created in the course of DSB repair. In fact, the pathways promoting accumulation of long ssDNA (SSA, BIR and ectopic GC) were most sensitive to the absence of Srs2. We tested this idea by using an experimental system where an HO-induced DSB was repaired by BIR involving two copies of chromosome III sharing more than 100 kb of homology. This repair is associated with the accumulation of ssDNA resulting both from extensive resection and from asynchrony between leading and lagging strand synthesis. We report that in the absence of Srs2, 30% of the cells produce viable BIR outcomes while 70% die. This massive death results from accumulation of unresolved toxic joint molecules that are likely formed by invasion of long ssDNA located behind the migrating DNA replication bubble into the intact donor, which leads to trapping of donor and recipient chromosomes together and interferes with BIR completion. Two main activities of Srs2, strippase and helicase, counteract toxic joint intermediates by preventing their formation and promoting their disruption, respectively. We also demonstrate that the structure-specific endonucleases Mus81 and Yen1 disrupt toxic joint molecules formed in the absence of Srs2, thus promoting cell survival. Together, we demonstrate that during DSB repair Srs2 prevents channeling of long ssDNA regions into formation of toxic joint molecules, which is similar to the anti-recombination role that Srs2 was proposed to play during replication, and which remained poorly characterized.

4.3 Results and discussion

To study the role of Srs2 in BIR we used a budding yeast experimental system where a DSB is repaired by BIR involving homologous chromosomes (Figure 16Ai) (Deem et al., 2008). In this system, a galactose-inducible DSB is initiated by HO endonuclease at the *MAT***a** locus of the truncated copy of chromosome III, while the full-length donor copy of chromosome III contains an uncleavable *MATα-inc* allele and serves as the template for DSB repair. Elimination of all but 46 bp of homology on one side of the break on the recipient molecule via replacement with *LEU2* and telomere sequences results in efficient DSB repair through BIR. Initiation of BIR in this system is preceded by extensive 5′-to-3′ resection of the DSB at *MAT***a**, followed by strand invasion of the 3′ single-strand end into the donor chromosome at a position proximal to the Y*α-inc* sequences and the subsequent copying of approximately 100 kb of donor DNA to the right telomere (Figure 16A). BIR and alternative repair pathways or chromosome loss can be followed based on maintenance of markers located at all arms of recombining molecules (Figure 16B).

Here, using this BIR assay, we observed that *srs2Δ* mutant cells exhibited a large decrease in viability, from ~90% in wild type cells to only 30% in mutant cells (Figure 16C); however, BIR remained the predominant repair outcome among *srs2Δ* survivors (Figure 16B, D). Massive death observed in *srs2Δ* mutants was unusual for our experimental system, where the presence of two copies of chromosome III, one of which remains unbroken, allows the cells to survive even in situations when a second, broken chromosome is unrepaired and lost, e.g. in

rad52Δ mutants (Malkova et al., 1996) (Figure 16B). Thus, the loss of viability suggested that initiation of BIR in the absence of Srs2 compromises not only the broken chromosome but also the intact donor serving as a template for repair. To test this idea we analyzed BIR progression using chromosome-separating CHEF gel electrophoresis and observed two striking defects in *srs2Δ*. First, the amount of BIR product measured 8 h after DSB induction was nearly 5-fold less than in wild type (Figure 16E, F). Second, while the unbroken Chr3 template molecule in wild type cells remained constant throughout the course of BIR, in *srs2Δ* the amount of template chromosome drastically decreased. At 8 h, the amount of the donor entering the gel was only 48% of the initial amount before DSB induction in *srs2Δ* as compared to 96% in *SRS2* (Figure15E, F).

We hypothesized that decrease of donor molecules in the agarose gel in *srs2Δ* results from accumulation of recombination intermediates. This was tested using 2D gel electrophoresis of BglII digested genomic DNA obtained from *SRS2* and *srs2Δ* cells undergoing BIR. We have previously used this method to demonstrate that BIR is carried out by a replication bubble, and ssDNA accumulates during asynchronous synthesis of leading and lagging strands (Saini et al., 2013). Following 2D electrophoresis, DNA digested with BglII or KpnI (see legend to Figure 16G) was hybridized with radioactively labeled probes specific to various positions located 0kb, 24kb and 85kb centromere-distal to the DSB position (Figure 16G). BIR in wild type cells was associated with the formation of bubble-arc replication intermediate that was previously described (Saini et al., 2013). In *srs2Δ*, the bubble-intermediate (blue arrow) was barely detectable while another

more prominent BIR intermediate was observed. This intermediate consisted of heterogeneous DNA molecules that were more branched and heavier than those forming the bubble intermediate (red arrow) and we will refer to this intermediate as 'the rubble' (Figure 16G).

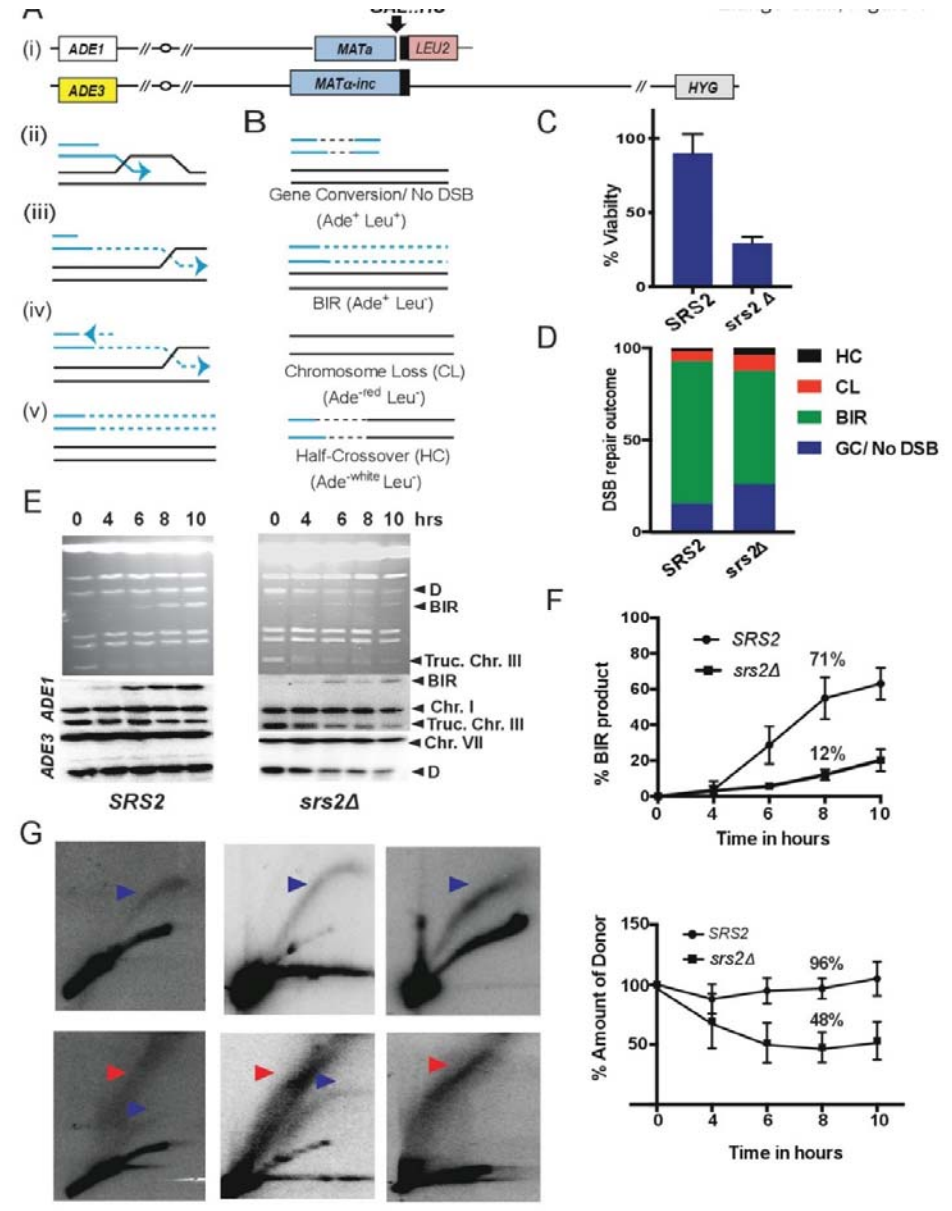

Figure 16. Srs2 prevents accumulation of toxic joints molecules during BIR.

(A) (i) BIR is initiated by DSB introduced by HO endonuclease at *MAT***a** locus in yeast disomic for Chromosome III. (ii) Broken recipient chromosome (blue)

invades unbroken homologous donor (black). (iii and iv) Repair DNA synthesis is initiated (iii) and progresses (iv) by a migrating bubble. (v) Conservative inheritance of newly synthesized DNA. (B) DSB repair outcomes with corresponding phenotypes (in parenthesis). (C) Cell viability following DSB induction (%). (D) Distribution of DSB repair outcomes in *SRS2* (WT) and *srs2Δ* based on their phenotypes (refer (B)). (E) BIR kinetics analyzed by CHEF using cells taken at indicated time points following DSB induction. Upper panel: CHEF gels stained with Ethidium Bromide. Subsequent panels below show Southern blot analysis using *ADE1*-specific, and *ADE3*-specific probes as indicated. (F) Quantification of BIR product (top) and of donor chromosome entering the gel (bottom). (G) 2D gels analysis of BIR intermediates in *SRS2* (top panel) and *srs2Δ* (bottom panel) at 7h following DSB induction. Genomic DNA was digested with KpnI to detect intermediates at 0kb and with BglII to detect intermediates at 24kb and 85kb. Intermediates were detected using probes specific to the following positions on Chr III: 0kb (left panel), 24kb (middle panel) and 85kb (right panel) away from the DSB. Blue arrowheads denote bubble arc intermediate and red arrowheads denote 'rubble' structure. Mean and standard deviation are shown representing ≥ 3 independent experiments.

We propose that long stretches of ssDNA generated during BIR by resection and DNA synthesis promote formation of additional joint structures located behind the migrating BIR bubble and interfere with BIR completion. Leaving these structures unresolved may lead to cell death. This hypothesis was tested by EM analysis of whole genome from DNA extracted from *srs2Δ* and *SRS2* cells, digested with BglII and enriched for ssDNA-containing fragments by passing through a BND cellulose column (Figure 18A, B). We observed a significant increase (P=0.0003) of branched DNA molecules, which included 4-way and 3-way junctions in *srs2Δ* (100/3860 molecules) as compared to *SRS2* cells (47 out of 3395 molecules). This was consistent with accumulation of joint molecules in *srs2Δ*. As expected, the level of branched molecules was very low in in a no-cut control.

Based on the survival of 30% of *srs2Δ* cells, we hypothesized that in the absence of Srs2 toxic joint molecules can be resolved by structure-specific nucleases, Mus81-Mms4 or Yen1, known to process Holliday junctions (HJ), and other branched intermediates (reviewed in (Schwartz and Heyer, 2011)). To test this possibility we first deleted *MUS81* in *srs2Δ* strains, and observed that it led to further decrease of cell viability upon DSB induction: from 30% in *srs2Δ* to only 10% in *srs2Δ mus81Δ* (Figure 18C). Deletion of *MUS81* itself does not affect repair or viability following BIR induction (Figure 18C) (Wilson et al., 2013). In addition, the amount of BIR product accumulated in *srs2Δ mus81Δ* at 8 hours following the break (as detected by CHEF) was 10 fold lower as compared to *srs2Δ* (Figure 18D). Based on these results, we propose that Mus81 resolves some of the toxic joint molecules accumulated in the absence of Srs2. In support of this conclusion, we found that the structures observed by 2D gel electrophoresis of BIR intermediates accumulated in *srs2Δ mus81Δ* looked different from the rubble structures. In particular, the intermediates accumulated in *srs2Δ mus81Δ*, contained molecules of larger mass than those in the "rubble" structure and were reminiscent of the spike structures that were previously reported for joint molecules in meiosis (yellow arrows) (Figure 18F-G) (Hunter and Kleckner, 2001; Schwacha and Kleckner, 1994, 1995). Overall, we propose that joint molecules (seen as spikes on 2D gels) are formed in the absence of Srs2, but some of them are resolved by Mus81 endonuclease, and this allows formation of viable BIR outcomes. We

envision that 'rubbles' represent the transitional structures where some of joint molecules were resolved.

Another feature of BIR is a very high level of repair-associated mutation (Deem et al., 2011). The level of frameshift mutagenesis was measured using a *lys2* frameshift reporter placed at three position (0kb, 16kb, and 36kb) along the track of BIR (Deem et al., 2011). We observed that when compared to wild type (*SRS2*), mutagenesis decreased among *srs2Δ* BIR outcomes two-fold at all positions (Figure S2A). However, it was still very high when compared to S-phase replication. The frequency of base substitutions, measured at the *ura3-29* reporter gene inserted in at 36kb position, was reduced 4x and 10x for two different orientations of the reporter, respectively (Figure S2B). Overall, in the absence of Srs2 BIR remained mutagenic, but the level of mutagenesis decreased.

The role of another structure specific endonuclease Yen1 was not evident based on the viability data of *yen1Δ srs2Δ* double mutant (Figure 18C). This could be explained by the very late activation of Yen1 in the cell cycle. In order to test the ability of Yen1 to resolve toxic DNA structures formed in *srs2Δ,* we used a constitutively active allele $Yen1^{ON}$ (Blanco et al., 2014). We observed that expression of $Yen1^{ON}$ largely suppressed the defect of *srs2Δ* and *srs2Δ mus81Δ* mutant cells, which suggested that $Yen1^{ON}$ is capable of processing toxic intermediates formed in these mutants and the resolution of these intermediates helps survival (Figure 18C). Consistently, $Yen1^{ON}$ *srs2Δ mus81Δ* accumulated a 'rubble intermediate' (similar to the one observed in *srs2Δ*) instead of a 'spike structure' that was observed in *srs2Δ mus81Δ* (Figure 18H-J). Interestingly,

expression of Yen1^{ON} in wild-type cells resulted in decreased BIR and an increase in chromosome loss (CL) and half-crossover (HC) events (Figure 18E). However, the formation of chromosome loss (CL) and half-crossover (HC) events were very rare following BIR initiation in Yen1^{ON} *srs2Δ* strains (Figure 18E).

Overall, we propose that the absence of Srs2 leads to formation of HJ-like structures (seen as 'spikes') that can be resolved by Mus81 or by Yen1. This resolution leads to the formation of heterogeneous rubbles (transitional structures), and some of them are fully resolved producing survivors.

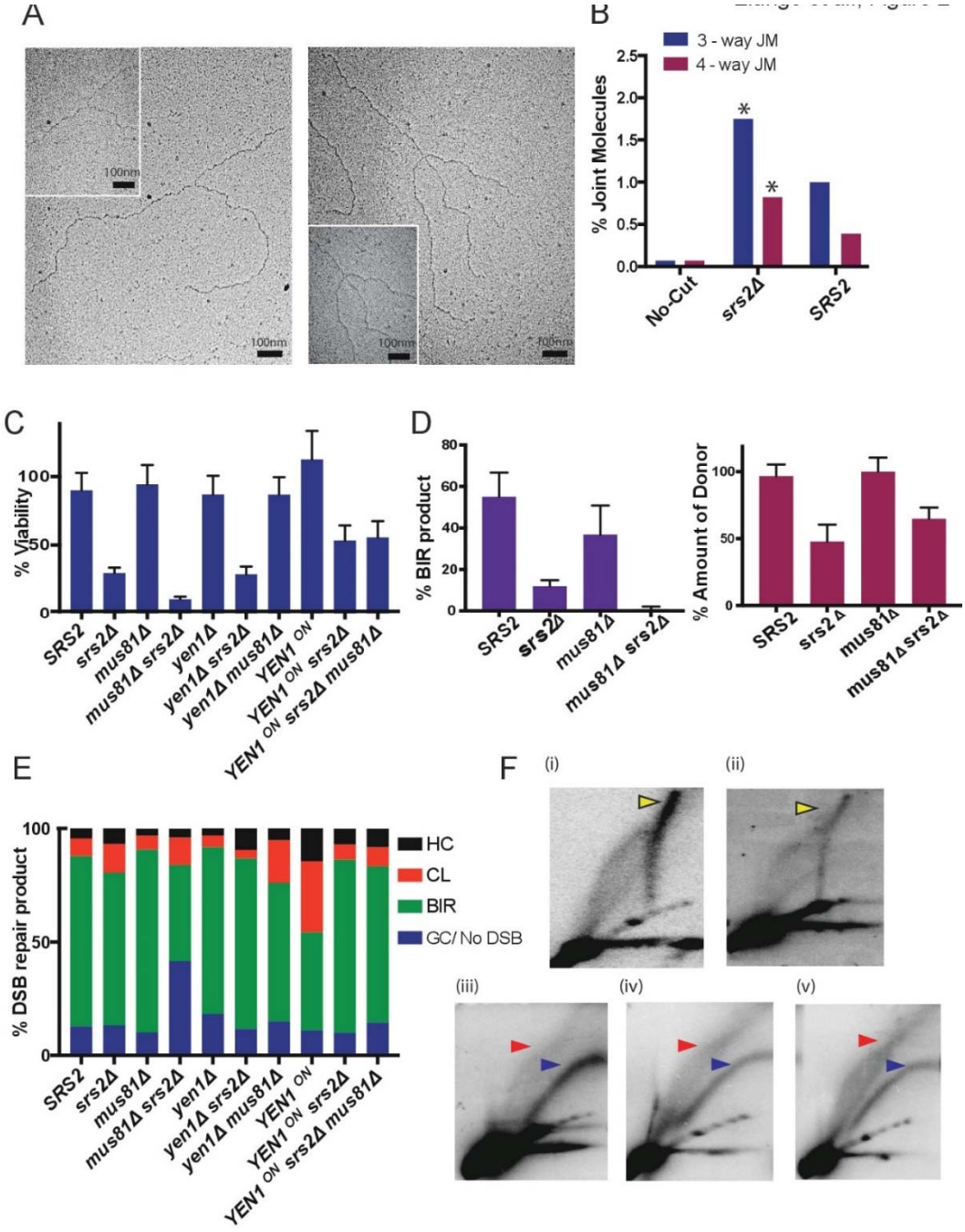

Figure 17. Structure-specific endonucleases resolve toxic BIR intermediates. (A) Representative images of DNA fragments containing 3-way and 4-way junctions in *srs2*Δ identified by EM analysis of genomic DNA isolated 7 hours following induction of BIR. (B) The fraction of DNA fragments containing 3-way and 4-way junctions in yeast (*SRS2* and *srs2Δ*) undergoing BIR; NC: no-cut control. The ** and * asterisk indicates a p-value of 0.0066 and 0.0379 respectively (C) Cell viability following BIR induction in various mutants, including *srs2Δ, mus81Δ, yen1Δ,* and also in cells containing $YEN1^{ON}$ construct. (D) Quantification

of BIR product (left) and of the donor chromosome (right) at 8h following initiation of BIR. (E) Distribution of DSB repair outcomes following BIR initiation in various mutants shown in (C). 2D gel analysis of BIR intermediates in *srs2Δ mus81Δ* using probes specific to 24kb position (F) and 85kb position (G) away from the DSB site. (H-J) shows 2D intermediates detected by 24kb probe in *Yen1*^{ON} (H), *srs2Δ Yen1*^{ON} (I), *srs2Δ mus81Δ Yen1*^{ON} (J) strains. Yellow and blue arrowhead denotes 'spike' and bubble intermediates respectively. Red arrowhead denotes 'rubble' intermediate. Mean and standard deviation were calculated based on ≥ 3 independent experiments.

We propose that Srs2 promotes BIR by counteracting toxic intermediates via the two anti-recombinational activities of Srs2: a "strippase" activity, which removes Rad51 from ssDNA thus preventing joint molecule formation and through its helicase activity which physically disrupts the toxic joint intermediates (reviewed in Niu and Klein, 2016). To test this idea we examined the effects of mutations in two Srs2 domains: (i) the ATPase domain (*srs2-K41A)* required for stripping Rad51 and DNA unwinding; and (ii) the BRC domain (*srs2-BRCΔ*) required for Rad51 interaction and for efficient stripping of Rad51 from ssDNA (Figure 18A). The effect of *srs2-K41A* mutation on BIR was similar to that of *srs2Δ* with respect to cell survival (Figure 18B), and the amount of BIR product formation (Figure 18C-D). In addition, similar to *srs2Δ,* a large fraction of the *srs2-K41A* donor chromosome molecules failed to enter the agarose gel following DSB induction (Figure 18D), and accumulated rubble intermediates as monitored by 2D gel electrophoresis (Figure 18F). Thus, the ATPase activity of Srs2, which is required for both its strippase and helicase activities, is necessary for BIR.

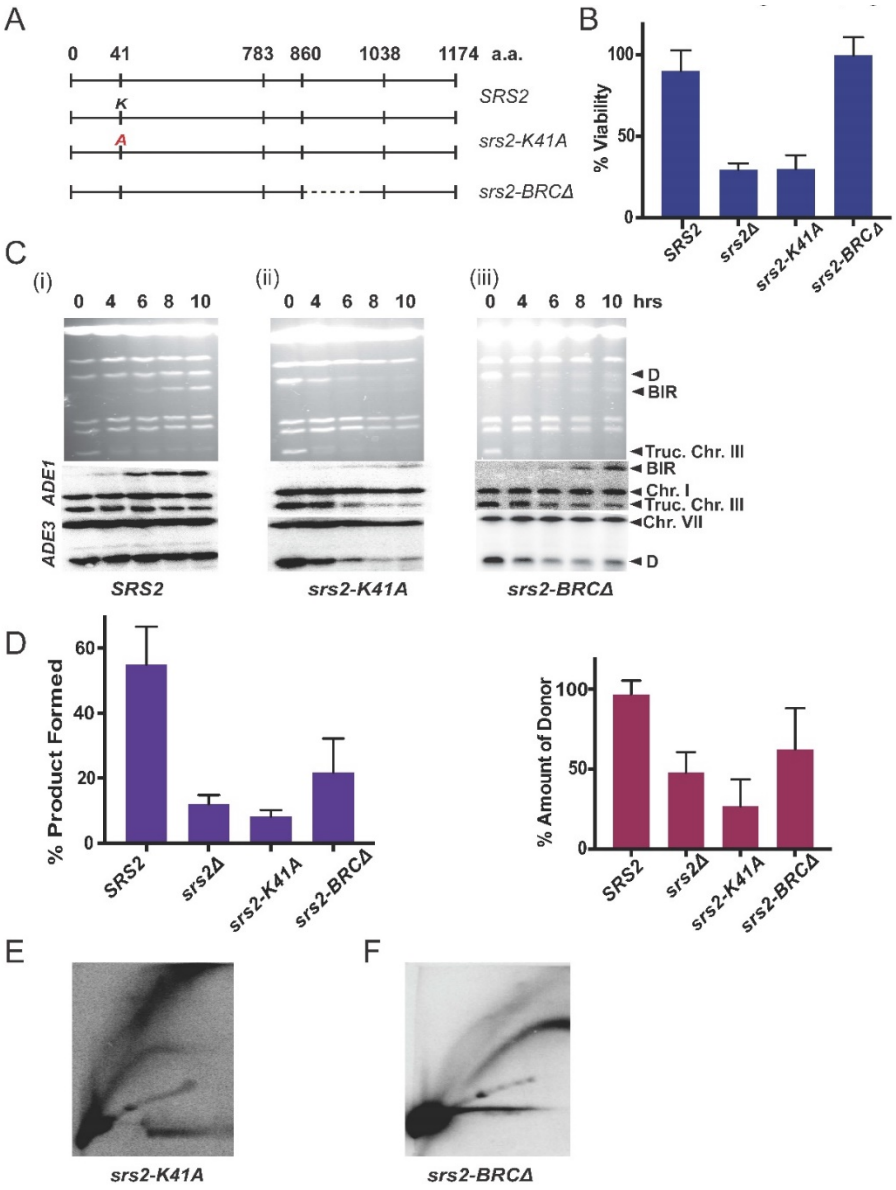

Figure 18. The defects in the helicase and strippase activities of Srs2 interfere with BIR progression. (A) The schematic of Srs2 (WT) and of srs2 mutations *srs2-K41A* and *srs2-BRCΔ*. "A" represents the position where lysine is replaced by arginine resulting in the ATPase (strippase and helicase) defect. Dotted line denotes deletion *srs2-BRC* domain (B) Cell viability following DSB induction in *SRS2*, *srs2Δ, srs2-K41A, siz1Δ* and *siz1Δ srs2-BRCΔ* .(C) BIR kinetics analyzed by CHEF in strains with various alleles of *SRS2* stained with Ethidium Bromide. (D) Quantification of the amount of BIR product (left) and of donor entering the gel (right) measured at 8 hours after DSB repair initiation. (E) 2D analysis of BIR in *srs2-K41A* and (F) *srs2-BRCΔ*. A probe 24kb away from the DSB was used. See Fig. 1 for all other details. Blue and red arrowheads denote bubble arc intermediate

and ‘rubble’ structure respectively. Mean and standard deviation were calculated based on ≥ 3 independent experiments.

Next we tested the importance of the BRC domain region occupying 862-914 bp of *SRS2* in BIR (Figure 18A). We expected that the absence of this region would affect the ability of Srs2 to remove Rad51 from the filament but not its helicase activity (Colavito et al., 2009; Marini and Krejci, 2012). The genetic analysis performed in this mutant demonstrated that successful BIR that was similar to that observed in *SRS2* cells with the viability of ~90% (Figure 18B; Figure 19A), and with BIR outcomes comprising 90% of the survivors (Figure 19B). At the same time, the physical analysis of BIR using CHEF indicated slower kinetics of BIR with only 22% of BIR product accumulated in *srs2-BRCΔ* at 8 h versus 55% in *SRS2* cells (Figure 18D). Also, a significant fraction of the template chromosome molecules failed to enter the agarose gel during CHEF analysis in the middle of BIR time course. These defects were indicative of branched structure accumulation. Indeed, 2D gel electrophoresis detected ‘rubble’ intermediates in *srs2-BRCΔ* cells (Figure 18G). Based on these results we propose that in *srs2-BRCΔ* where Srs2 does not remove the excess of Rad51 from the filament, toxic intermediates are still formed but they are eventually removed by the helicase activity of Srs2, allowing slower but efficient repair and survival. Based on these results we propose that Srs2 works in two steps. First, it prevents formation of toxic intermediates using its strippase (translocase) activity and second, the helicase activity of Srs2 removes those intermediates that were nevertheless formed.

We hypothesized that the need for the helicase activity of Srs2 could be bypassed by having less stable Rad51 nucleofilament. Toward this goal, we used the *rad55Δ* mutant where Rad51 filament is inherently unstable. Deletion of *RAD55* leads to profound defect in BIR as the great majority of cells lose the broken chromosome (Figure 19A, B) due to problem in strand invasion resulting from a defective Rad51 filament. Importantly, deletion of *RAD55* in *srs2Δ* led to complete recovery of BIR and cell viability (Figure 19A, B). The viability of *srs2Δ rad55Δ* cells was 90%, which is much higher than in *srs2Δ* (30%), and 75% of the survivors in *srs2Δ rad55Δ* resulted from BIR, which was significantly higher compared to *rad55Δ* single mutant (17%). Similarly, combining *rad55Δ* and the helicase dead mutant *srs2-K41A* led to high cell viability (to ~90%) and efficient BIR (~ 90% of BIR) (Figure 19A, B). This result was further confirmed by 2D gel electrophoresis, where normal BIR bubble-arc, and no rubble intermediates were observed in *rad55Δ srs2Δ* (Figure 19E-F). These results suggest that when the formation of toxic intermediates is precluded by instability of Rad51 filament, the helicase activity of Srs2 is less needed for the completion of BIR than in the case of "excessive" and stable Rad51 filament. While the efficiency of BIR in *srs2Δ rad55Δ* mutants appears to be much better than in single *srs2Δ* or *rad55Δ* mutants, the kinetics of BIR product formation in *srs2Δ rad55Δ* is significantly slower than in wild type cells, with respectively 23% versus 55% of product accumulated 8 h

following DSB induction (Figure 19C-D). Nevertheless, most *srs2Δ rad55Δ* cells successfully completed BIR.

Recent reports demonstrated that a mutant within ssDNA binding protein Rpa1 (*rfa1-t33)* is defective in BIR and this defect may result from decreased Rad51 loading (Ruff et al., 2016). Thus we tested whether similar to *rad55Δ*, *rfa1-t33* can suppress low viability of *srs2Δ* When *rfa1-t33* and *srs2Δ* were combined, we observed that the viability of double mutant was much higher as compared to *srs2Δ* (Figure 19A). Moreover the proportion of cells completing BIR was significantly increased as compared to *rfa1-t33* (Figure 19B). These results suggested that the defect in the Rad51 filament in *rfa1-t33* bypassed the defect of *srs2Δ* in BIR. Finally, the low viability following BIR initiation in *srs2Δ* was partially suppressed by *fun30Δ*, which likely resulted from the decrease of DSB resection in this mutant (Figure S2 A, B). Overall, our results suggest that the need for Srs2 can be bypassed by compromising Rad51 filament formation at ssDNA regions accumulated during BIR.

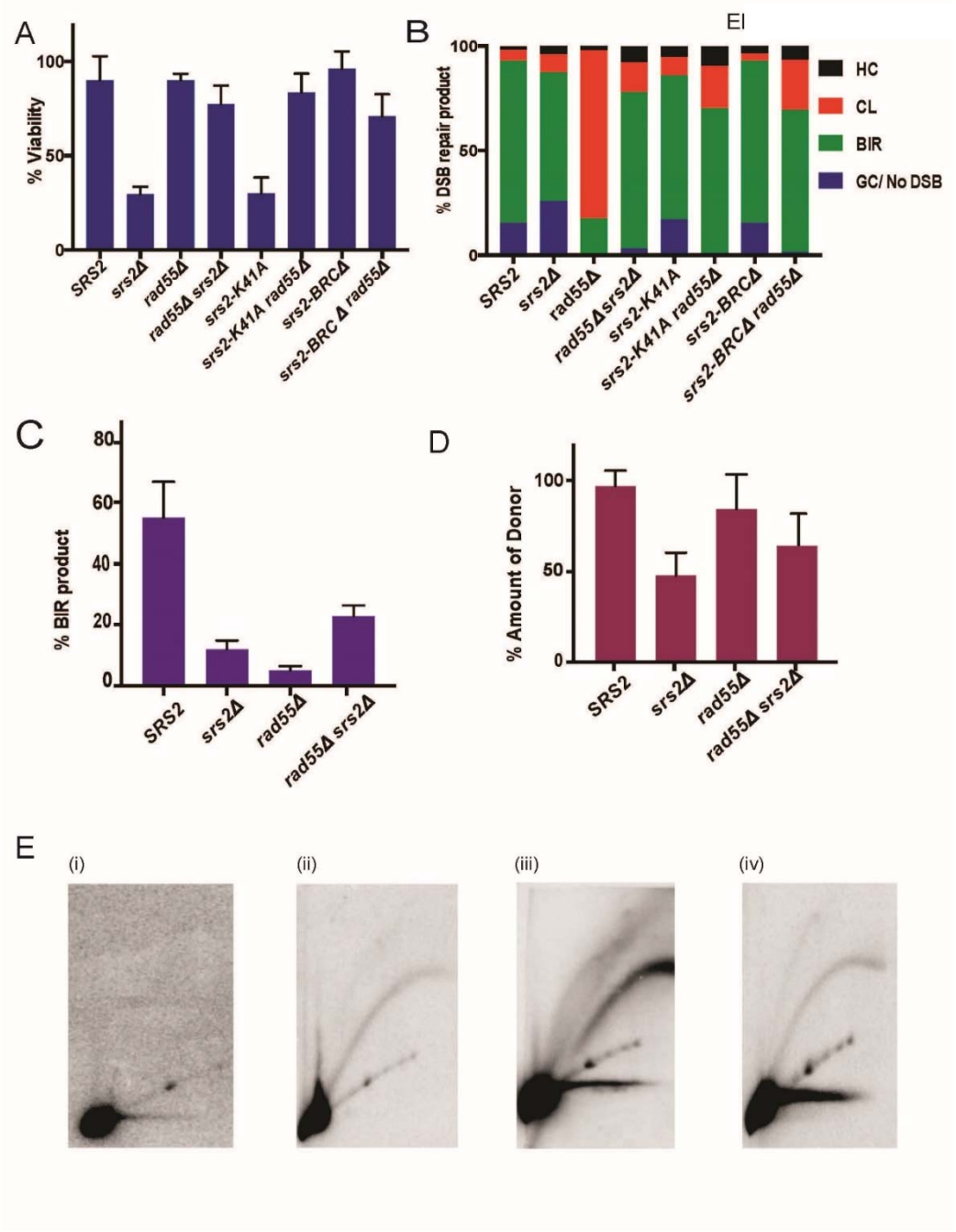

Figure 19. Destabilization of Rad51 filament bypasses the requirement for Srs2 during BIR. Cell viability (A) and distribution of repair outcomes (B) following DSB induction in *rad55Δ, rfa1* and *srs2Δ* mutants. Quantification of BIR product (C) and of the donor entering the gel (D) measured at 8 hours following DSB repair initiations and of the donor entering the gel. 2D gel analysis of BIR intermediates in *rad55* and *srs2* mutants. The mutants are (E) *rad55Δ* (F) *rad55Δ srs2Δ* (G) *srs2-BRCΔ* and (H) *srs2-BRCΔ rad55Δ.* See Fig.1 for other details. Blue and red arrowheads denote bubble arc intermediate and 'rubble' structure

respectively. Mean and standard deviation were calculated based on ≥ 3 independent experiments.

Next, we asked whether the detox function of Srs2 that we described for BIR is necessary for other pathways of DSB repair, gene conversion and single strand annealing (SSA). Gene conversion was tested in a simple ectopic recombination system, where Srs2 was shown previously to play important roles (Figure 20A). In this assay, a DSB induced within a 1.9 kb *MAT***a** sequence inserted at the *ARG5,6* locus on Chr5 is repaired by gene conversion with homologous *MAT***a**-inc sequence on Chr3 (Figure 20A)(Ira et al., 2003; Vaze et al., 2002). Repair in this assay proceeds by SDSA with rare (<5%) crossover outcomes. It was previously reported that the efficiency of repair, measured 8 h after DSB by Southern blot analyses of the digested genomic DNA, was decreased in the absence of Srs2 from ~85% to about ~20-25%. Importantly, cell viability following DSB induction in *srs2Δ* was reduced to just several percent (Vaze et al., 2002); Figure 20B). Here we analyzed the repair in the same system by CHEF electrophoresis, and observed that even at 12 h after DSB, the intensity of the repaired chromosome remained at less than ~10% level (Figure 20C), indicating branched structures that prevent normal DNA migration within agarose gels. Also, similar to our observations in BIR system, *srs2-BRCΔ* did not affect cell viability following DSB (Figure 20B), indicative of the important role of Srs2 helicase activity for survival.

As with BIR, the viability of double mutant *srs2Δ rad55Δ* during ectopic GC was significantly improved as compared to *srs2Δ* or *rad55Δ* single mutants (Figure

20B). This data suggests that destabilization of Rad51 filament by *rad55Δ* improved SDSA repair in *srs2Δ*. This supported the idea that the detox function of Srs2 is required for the successful completion of gene conversion. While the efficiency of GC in *srs2Δ rad55Δ* mutants appears to be much better than in single *srs2Δ* or *rad55Δ,* GC in this double mutant showed a dramatically increased level of crossover outcomes when compared to single mutants (Figure 20C, D). Thus, while repair is improved in *srs2Δ rad55Δ* cells, it comes at the cost of very high level of crossover that is thought to drive genomic instability and loss of heterozygosity. Recent analysis of purified Srs2 suggests that its D-loop unwinding activity can account for its anti-crossover activity (Heyer W-D, personal communication). As previously reported in a different system, the anti-crossover activity of Srs2 is largely dependent on its recruitment to SUMO-modified PCNA. Here we tested Siz1 SUMO ligase, which sumoylates K127 and K164 residues of PCNA and also tested the requirement of lysine at 164 position of PCNA (*pol30-K164R*) (Papouli et al., 2005; Pfander et al., 2005). The mutations affecting this sumoylation (*siz1Δ, pol30-K164R,* as well as the *pol30-K127R,K164R* double mutant) had little effect on viability, but caused a modest increase in CO outcomes (Figure 20B, 19D). In addition, we observed that *siz1Δsrs2-BRCΔ* was viable as well. *T*hese data together indicated that that recruitment of Srs2 to recombination intermediates to promote efficient repair, and specifically the recruitment of Srs2 helicase to toxic joint molecules is distinct from anti-crossover function of Srs2.

In BIR, *siz1Δ* showed no phenotype (Figure 18B, C) and this is expected considering that disruption of the D-loop would rather counteract than help any D-

loop migration mechanism during BIR. Interestingly, this point was supported by another observation: even though *srs2-BRCΔ* restored BIR in *rad55Δ*, the extent of restoration was less as compared to *srs2Δ* (Figure 19B*)*. Since the Rad51 filaments formed in *srs2Δ* and *srs2-BRCΔ* in *rad55Δ* background were likely similar, we envision that the higher frequency of chromosome losses observed in *srs2-BRCΔ rad55Δ* likely resulted from the reversal of the D-loop using the helicase activity of Srs2 (Figure 19A, B). In addition, we observed that *siz1Δ* did not affect cell viability and the level of BIR in *srs2-BRCΔ* (Figure 18B, C)*,* which suggested that the helicase activity of Srs2 disrupting toxic intermediates was Siz1-independent. Overall, our data demonstrate that the detox role of Srs2 is required not only for BIR but also for the success of such a major DSB repair pathway as gene conversion.

We further hypothesized that the absence of the detox function of Srs2 was also responsible for the death that was previously observed in *srs2Δ* following DSB repair by SSA. In that system, DSB was introduced by HO endonuclease into the *LEU2* gene on chromosome III and could repair by SSA with a partial *LEU2* copy (*U2*) located 25 kb away (Vaze et al., 2002) (Figure 20F). The induction of this repair in *srs2Δ* resulted in loss of viability in 98% of cells. Nevertheless, the authors observed an efficient formation of the repair product 6 h after the DSB detected by Southern blot analysis of the genomic DNA following its restriction digest and separation by gel electrophoresis. Here we analyzed the repair in the same cells using CHEF gel electrophoresis and observed that there were no intact, repaired chromosomes even after 12 h following DSB induction (Figure 20H). We

propose that despite the initiation of repair (previously detected by Southern blot analysis of restriction enzyme digested DNA within partial *leu2* repeats) the intact full chromosomes are never formed in *srs2Δ* cells. The inability of chromosomes to enter the agarose gel suggests formation of branched intermediate structures similar to BIR assay. Thus, we propose that Srs2 plays important detox role during SSA as well. In support of our model, removal of *RAD51* eliminates the need for Srs2 in SSA (Vaze et al., 2002). In addition, *srs2-BRCΔ* did not affect cell viability following DSB (Figure 20G), indicative of the crucial role that Srs2 helicase (rather than strippase) plays in survival.

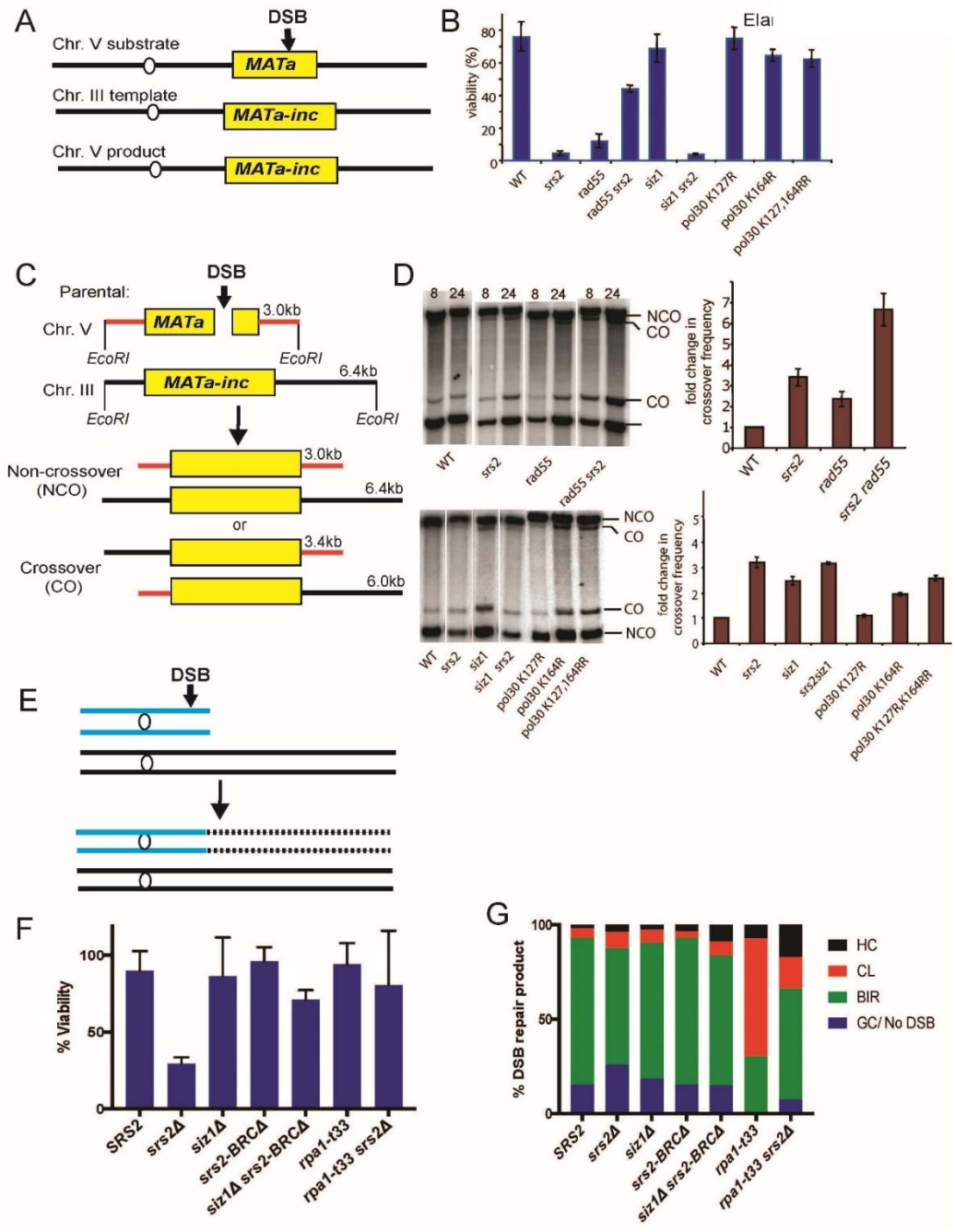

Figure 20. Anti-toxic function of SRS2 during ectopic gene conversion (GC) and single-strand annealing (SSA). (A) Ectopic gene conversion is initiated by DSB introduced by HO endonuclease at *MAT***a** inserted at the *ARG5,6* locus on chromosome V and proceeds by using homologous *MATa*-inc sequence on chromosome III as a template. (B) Cell viability reflecting the efficiency of GC in various mutant backgrounds. (C) The schematic of assay to distinguish crossover from non-crossover products of gene conversion. (D) CHEF analysis of ectopic GC in wild-type (*SRS2*; left) and *srs2Δ* (right) Upper panel: CHEF gels stained with

ethidium bromide. Lower panels: Southern blot analysis using a probe specific to RMD6 gene on chromosome V (E) Crossover and non-crossover GC products detected by Southern blot analysis (left, top and bottom panels) and the effect of various mutant backgrounds on the frequency of crossover formation (right, top and bottom panels).(F) The schematic of SSA system in YMV80 strains where DSB is induced at *leu2* by HO endonuclease on Chr. III and repaired by SSA using *U2* as a template on the chromosome. (G) Cell viability in *SRS2* and various *srs2* mutants. (H) Upper panel: Ethidium Bromide stained CHEF gels showing analysis of repair by SSA in *SRS2* (wild-type) (left) and *srs2Δ* (right) strains. Lower panels: Southern blot analysis using *ADE1* probe on Chr.III. Mean and standard deviation were calculated based on ≥ 3 independent experiments.

Srs2 regulates spontaneous and DSB-induced recombination, but its specific roles in the regulation of these different types of recombination remain controversial. In particular, during replication Srs2 plays an anti-recombination role by preventing channeling of ssDNA gaps into homologous recombination (reviewed in (Niu and Klein, 2016)). Conversely, during DSB repair, the role of Srs2 appears to promote recombination (Ira et al., 2003; Vaze et al., 2002; Yeung and Durocher, 2011). The details of this latter function remain under debate, and several possible pro-recombination functions of Srs2 have been postulated. Our results presented here led us to propose a unifying anti-recombination role for Srs2 during replication and DSB repair: it prevents channeling of ssDNA into formation of toxic joint molecules. In the case of problems associated with replication, the lethal intermediates are more detrimental when formed between homologous chromosomes than with sister-chromatids (Aboussekhra et al., 1989) . The better survival following inter-sister recombination might be either thanks to rapid repair reducing chances of forming toxic intermediates or due to the presence of special proteins (e.g. Sgs1) capable of unwinding inter-sister toxic intermediates (Gangloff

et al., 2000). The simultaneous breakage of both sister chromatids by HO endonuclease makes inter-sister repair unavailable, thereby giving rise to toxic inter-homolog intermediates.

We observed that ssDNA regions formed during BIR are prevented from channeling into toxic joint intermediates via two main activities of Srs2: (i) by its strippase activity that eliminates excess of Rad51 from ssDNA regions formed during BIR, thus preventing formation of toxic joint molecules (Figure 21A, B); and (ii) by its helicase activity disrupting toxic joint molecules when they are formed (Figure 21C). The strippase activity of Srs2 requires its ATPase and Rad51 interaction domains and is critical for the achieving the optimal quality of Rad51 filament that allows efficient strand invasion of the 3' end into homolog, but prevents toxic invasions in the areas located behind the BIR bubble. When toxic joint molecules are formed, they are unwound by the helicase activity of Srs2, which requires its ATPase, but not Rad51-interaction domain. Since we were able to detect by EM the presence of branched DNA structures even in wild type (*SRS2*) cells we envision that toxic molecules could be formed, at least transiently, in wild type (*SRS2*) cells. This was supported by detection of the rubble structures by 2D analysis, albeit at the residual level, in wild type cells. This supports the idea that helicase activity of Srs2 likely plays an important anti-toxic role even in the presence of strippase.

Overall, we propose that both activities of Srs2, strippase and helicase, are important for the success of DSB repair. Helicase can remove extensive toxic intermediates formed in the absence of Srs2 strippase activity (Figure 21C), but it comes at a price of slower BIR kinetics. Alternatively, when Rad51 filament is unstable (i.e. in *rad55Δ* or *rfa1* mutants), the requirement for Srs2 helicase activity is bypassed. Interestingly, however, we observed that the kinetics of BIR in *srs2Δ rad55Δ* was slower than in wild type cells. This observation suggested that the properties of the Rad51 filament formed in the double mutant differed from that in wild type. Specifically, the slower kinetics could result from the decreased strand invasion due to instability of Rad51 filament in *rad55Δ* observed even in the absence of Srs2. Nevertheless, most cells successfully completed BIR, which could be explained by the absence of the D-loop reversal mediated by the helicase activity of Srs2 that could otherwise interrupt those BIR events that were successfully initiated.

We propose that joint molecules formed in the absence of Srs2, can be resolved by Mus81-Mms4 or active Yen1 (Figure 21B). This explains a higher viability in *srs2Δ* cells possessing Mus81 or Yen1^{ON}. The viable outcomes formed as a result are similar to the BIR outcomes in wild type (*SRS2*) cells. However, the decreased level of frameshifts observed among viable *srs2Δ* BIR outcomes suggest that in the absence of Srs2 BIR progresses slower, while the reduction of base substitution is suggestive of less of ssDNA accumulated in *srs2Δ* as compared to

wild type cells. This could be because a significant portion of ssDNA is involved in formation of toxic joint intermediates, or due to more synchrony between leading and lagging DNA strand synthesis due to slower BIR progression. In the latter case, this may contribute to formation of double-stranded Holliday-junction (HJ)-like structures which could represent better substrates for Mus81 and Yen1. It is also possible that BIR events associated with accumulation of longer tracts of ssDNA are more likely to die due to formation of toxic intermediates.

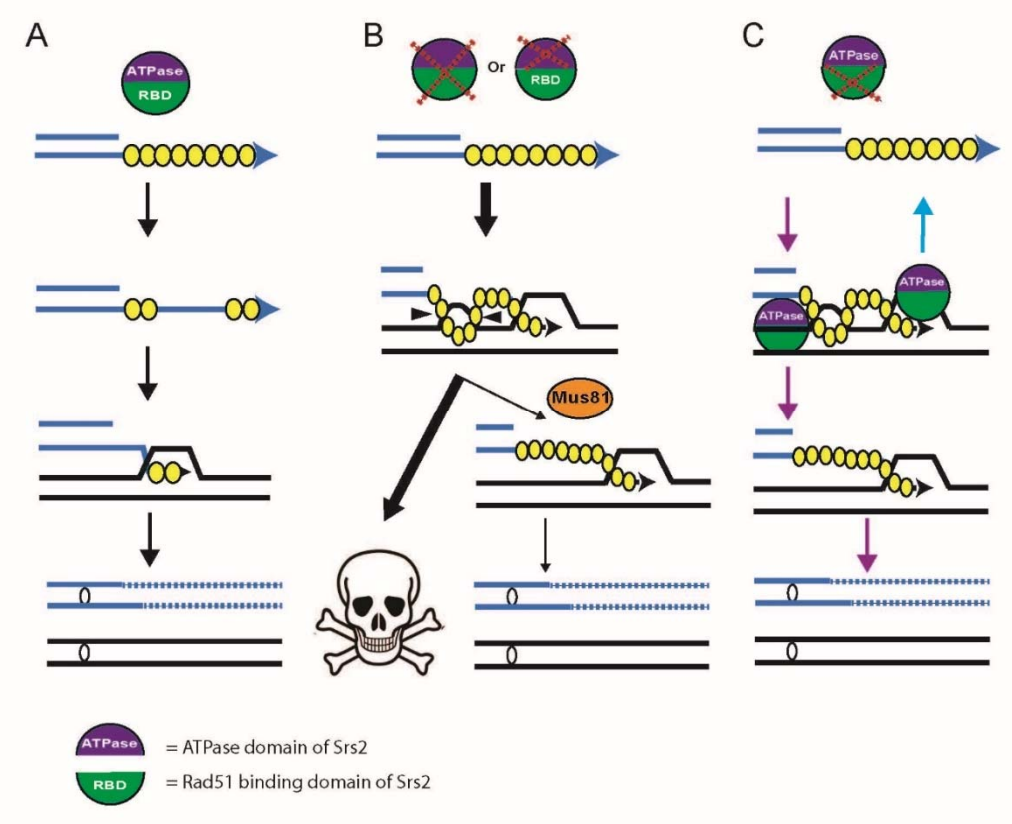

Figure 21. The model of the role of Srs2 during DSB repair. (A)The strippase activity of Srs2 requiring both the ATPase domain (purple semi-circle) and the Rad51 binding domain (RBD) (green) removes excess of Rad51 (yellow circles) from the pre-synaptic filament, which prevents formation of toxic intermediates behind the migrating BIR replication bubble, and ensures efficient BIR. (B) The absence of Srs2 or of its ATPase activity (Srs2-K41A) excess Rad51 bound to long ssDNA leads to formation of toxic intermediates, which predominantly lead to cell

death (denoted by the skull), but can be resolved by Mus81-Mms4, which allows BIR completion and cell survival. (C) In the absence of the Rad51 binding domain, the strippase role of Srs2 is defective, resulting in accumulation of toxic intermediates, which can be reversed via helicase activity of Srs2, which remains intact. In addition, the anti-crossover function of Srs2 can reverse BIR intermediates via D-loop unwinding.

Besides the survival, our conclusions that Mus81 and Yen1 resolve toxic joint molecule was also based on the change of the pattern of the branched DNA structures detected by 2D gel electrophoresis. In particular, we observed that the "spike structures" observed in *mus81Δ srs2Δ* were substituted in *srs2Δ* or in *srs2Δ mus81Δ* Yen1^{ON} by the "rubble". We propose that the "rubble" represented a sum of heterogeneous products resulting from processing of HJ-like structures by Mus81 or Yen1. Importantly, the components of the rubble are highly branched, and therefore are in need for further processing to produce linear molecules. It is also possible that the resolved outcomes can form toxic joint molecules again. Overall, the persistence of the rubble in *srs2Δ* cells suggests that the majority of toxic intermediates remain unresolved, consistent with the observed death of 70% of cells.

Another interesting observation is that constitutive expression of Yen1 in *SRS2* cells led to frequent formation of half-crossovers and chromosome losses, known to result from the resolution of normal BIR intermediates. This suggested that when Yen1^{ON} is active at G2, it interferes with BIR progression and leads to formation of abnormal repair outcomes. This can explain why Yen1 is not normally active at G2, which is the time of the cell cycle when BIR and many other types of

homologous recombination take place. Interestingly, the expression of Yen1^{ON} in cells lacking Srs2 produced significantly less of chromosome loss and half-crossovers events as compared to *SRS2* cells. This suggests that resolution of toxic intermediates accumulated in *srs2Δ* can produce aberrant chromosomes that cannot support viability in the absence of intact donor chromosome. It has been proposed that Mus81 can resolve toxic intermediates that may spontaneously accumulate in *srs2Δ* cells without induced DNA damage (Keyamura et al, 2016). This supports our unifying idea that Srs2 plays the same anti-recombination role during replication and DSB-repair, while Mus81 in both situations resolves toxic intermediates formed in the absence of Srs2.

Our results obtained in ectopic gene conversion system allowed us to further characterize the anti-crossover role of Srs2. In particular, it has been proposed that Srs2 fulfills its anti-crossover function either by unwinding D-loops by its helicase activity (Ira et al., 2003) or by dislodging Rad51 by its strippase activity from the non-invading (catching) DSB end, which precludes the formation of HJ, and therefore prevents crossovers (Mitchel et al., 2013). According to the latter model, *rad55Δ* should destabilize Rad51 filament on the catching end, and therefore should lower crossover frequency in *srs2Δ*. Contrary to this, the frequency of crossovers in *srs2Δ rad55Δ* was higher as compared to *srs2Δ*. Based on these results, we favor the first model that Srs2 helicase discourages crossover formation via D-loop unwinding. While the exact reason for very high level of crossover in *srs2Δ*

rad55Δ cells is not known, it is possible that Rad52 annealing role may increase in this mutant leading to more frequent second capture. In addition, we observed that while anti-crossover activity of Srs2 depends on PCNA sumoylation by Siz1, the anti-toxic activity of Srs2 investigated in our GC and BIR systems does not, which distinguishes these two activities from each other.

This situation appears somewhat different for the repair of ssDNA gaps formed during S-phase DNA replication where Srs2 is recruited to the sumoylated PCNA (Papouli et al., 2005; Pfander et al., 2005). In this case, the absence of Siz1 suppresses UV sensitivity of *rad18Δ,* because ssDNA gaps can be channeled into recombination due to absence of Srs2 recruitment. However, in this situation Srs2 should be able to unwind toxic intermediates via its helicase activity.

Here we reported that Srs2 prevents channeling of ssDNA formed during BIR into toxic joint molecules. Since ssDNA is often formed in association with other types of DSB repair as well, we propose that Srs2 plays a similar role in other DSB repair pathways. In fact, we observed that repaired chromosomes were virtually undetectable following SSA and ectopic GC. Remarkably, the successful formation of the initial repair fragments was reported in both of these pathways (Vaze et al., 2002). Nevertheless, the failure of the repaired chromosomes to enter the CHEF gel is indicative of branched toxic joint molecules that can be formed by ssDNA regions generated by resection that proceeded outside of the D-loop area in a case of ectopic GC and outside of annealing region in a case of SSA. These toxic

intermediates could be formed by the invasion of ssDNA at ectopic positions, at locations of the Ty or delta elements, which can explain a low viability following DSB induction in haploid cells. In fact, using the same SSA system, demonstrated that long ssDNA regions formed in a course of DSB resection can invade at ectopic positions which slightly decreased cell viability even in the presence of Srs2 (Jain et al., 2016). It is likely that the absence of Srs2 can significantly exacerbate this problem. Finally, Jain et al., 2016 suggested that at least some of the break initiated in their SSA system could be repaired in that system by BIR instead of SSA. Therefore, the important anti-toxic role of Srs2 that we described for BIR, could be applicable here as well.

Based on the detox role of Srs2 in BIR we predict that Srs2 is also important for the alternative telomere lengthening (ALT), a BIR-like pathway in yeast and humans extending telomeres in the absence of telomerase (reviewed in (Dilley and Greenberg, 2015)). ALT is responsible for telomere maintenance in 10-15% of cancers and involves key BIR players. We predict that the absence of Srs2 results in trapping of chromosomes participating in ALT. Therefore, human counterparts of Srs2 may serve as anti-cancer targets in ALT cells. While there is no distinct mammalian ortholog of Srs2 in mammals, several functional homologs, including *FBH1*, *RecQL5*, *PARI* and *RTEL*, have been identified (reviewed in (Niu and Klein, 2016)). Testing their potential anti-toxic role in DSB repair and ALT is an exciting direction towards our understanding of how recombination is regulated in humans.

While this manuscript was prepared for submission, another study focused on Srs2 was published (Vasianovich et al., 2017). This study continued a traditional

view of pro-recombination role of Srs2 in DSB repair by suggesting that dislodging of Rad51 by Srs2 is needed for successful filling-in of ssDNA gaps. This model however does not explain our observation that cell survival following DSB induction is dependent on helicase rather than strippase activity of Srs2. The pro-recombination model also does not explain why in our experiments DSBs would be lethal in diploids and disomes that contain intact copies of a broken chromosome and should not depend therefore on the success of DSB repair for survival. Finally, we demonstrate that Mus81 and Yen1 resolve toxic joint molecules, which promotes cell survival following DSB induction in *srs2Δ* mutants, and which cannot be explained by the (Vasianovich et al., 2017) model. Here we report that toxic recombination intermediates accumulated in the absence of Srs2 promote trapping of whole chromosomes, including those originally intact that serve as donors for DSB repair that explains *srs2Δ* cells death after DSB. We demonstrate an important role played by Srs2 helicase activity in removing toxic joint molecules, which explains why the presence of helicase activity is sufficient for cell survival even in the absence of strippase activity. Overall, we propose a unifying idea that Srs2 plays the same anti-recombination role during DSB repair and replication: it counteracts toxic joint molecules.

My contribution to this work. For the experiments mentioned above, I performed 2-D gel electrophoresis obtained results for Figure 16G, 17F, 18E, 18F and 19E and prepared DNA for electron microscopy analysis (Fig17A, SF3 A-E).

Appendix B

B1 Experimental Procedures

All yeast strains were isogenic to AM1003 (Deem et al., 2008), which is disomic for chromosome III with a genotype as follows: *hmlΔ::ADE1*/*hmlΔ::ADE3 MAT***a**-*LEU2*-tel/*MAT*α-inc *hmrΔ*::*HPH FS2Δ::NAT*/*FS2 leu2/leu2-3,112 thr4 ura3-52 ade3::GAL::HO ade1 met13*.

AM3110 was derived from AM1003 in two steps. First, multiple copies of *TEF1/BSD* were inserted into *SNT1* similar to (Saini et al., 2013). Second, p304-BrdU cassette was integrated into *TRP1* similar to (Saini et al., 2013). All strains used in BIR assay were derivatives of AM3110. Strains used for the ectopic GC assays are derivatives of tGI354 (Ira et al., 2003). Strains used in SSA assay were derivatives of YMV80 (Vaze et al., 2002). Derivatives containing *srs2-BRCΔ* were created using *delitto perfetto* approach (Storici and Resnick, 2003) and confirmed by sequencing. Strains containing *srs2*::*KANMX, pol30-K127R::KanMX, pol30-K164R::KanMX* and *sizl::KANMX* were constructed by transformation with PCR-derived *KANMX* module similar (Wilson et al., 2013). Strains containing *mus81::ble*^{r}, *srs2*::*ble*^{r} and *rad55*::*ble*^{r} were constructed by transformation with PCR-derived phleomycin-resistant (ble^r) cassette (Gueldener et al., 2002) flanked by terminal sequences matching the first and last 80bp of the open reading frame of *MUS81, SRS2* and *RAD55* gene respectively. *pol30-K127R::KanMX, pol30-K164R::KanMX* strains were constructed by transformation with PCR-derived

fragments amplified using genomic DNA of corresponding mutant strains described in (Pfander et al., 2005).

Growth media contained rich medium yeast extract–peptone–dextrose (YEPD) and synthetic medium specific bases and amino-acids omitted as specified and were made as described in (Deem et al., 2011) and (Chung et al., 2010).

The kinetics and efficiency of BIR, ectopic GC and SSA was analyzed by CHEF gel electrophoresis followed by Southern hybridization similar to (Saini et al., 2013) using the following probes: *ADE1and ADE3*-specific probes for the analysis of BIR and SSA (Deem et al., 2008); probes specific to Chr. V (*RMD6*-specific) were used for the analysis of ectopic GC. Images were analyzed using a GE typhoon FLA 7000. The measurement of crossover frequency was performed similar to (Ira et al., 2003). Two-dimensional (2D) gel electrophoresis was performed similar to (Saini et al., 2013). Prior to 2D electrophoresis, the genomic DNA was digested by KpnI to analyze BIR intermediates at 0kb, and by BglII for 24kb and 85kb positions. The detection of intermediates at 0kb, 24kb, and 85kb positions was performed using *TAF2, PWP2* and *CDC39* -specific probes, respectively.

Cell viability following DSB induction was determined by plating cells on YEPD and YEP-Gal media similar to (Deem et al., 2008) and calculated by dividing the number of colony-forming units (CFUs) on YEP-Gal by the number of

CFUs on YEPD. A minimum of three plating experiments was performed to calculate the averages and standard deviations for viability. To characterize the DSB repair outcomes, the colonies formed on YEP-Gal plates were replica plated onto appropriate omission media to determine the fraction of DSB repair events with the following phenotypes: Ade^{+} Leu^{+} (GC), $Ade^{-white}Leu^{-}$ (HC), Ade^{-red} Leu^{-} (CL), and Ade^{+} Leu^{-}, similar to (Deem et al., 2008). The rate of Lys^{+} mutagenesis was determined similar to (Deem et al., 2008). The rate of Ura^{+} mutagenesis was determined similar to (Saini et al., 2013) except that appropriate concentration of cells were plated on YEPD media and on media omitting uracil before (0 h) and after (7 h) DSB induction.

EM analysis of BIR intermediates was performed as described in (Neelsen et al., 2014). The DNA samples were prepared following a protocol similar to that used for the preparation for the samples the 2D analysis (Saini et al., 2013). Briefly, samples were collected 7 h following DSB induction and crosslinked using psoralen to preserve branched intermediates. Genomic DNA was extracted and processed for 2D analysis as previously described in (Saini et al., 2013) and (Oh et al., 2009). For No DSB control, 2% galactose was added simultaneously with 0.015mg/ml nocodazole. After 4 hours when cells were arrested at G2, samples were collected similar to the sample collection for 2D. DNA was extracted and digested with BglII. Following enrichment using BND cellulose, EM samples were prepared by spreading the DNA on carbon-coated grids in the presence of benzyl-dimethyl-alkylammonium chloride and visualized by platinum rotary shadowing. Images

were acquired on a transmission electron microscope (JEOL 1200 EX) with side-mounted camera (AMTXR41 supported by AMT software v601) and analyzed with ImageJ (National Institutes of Health).

B2 Supplemental information

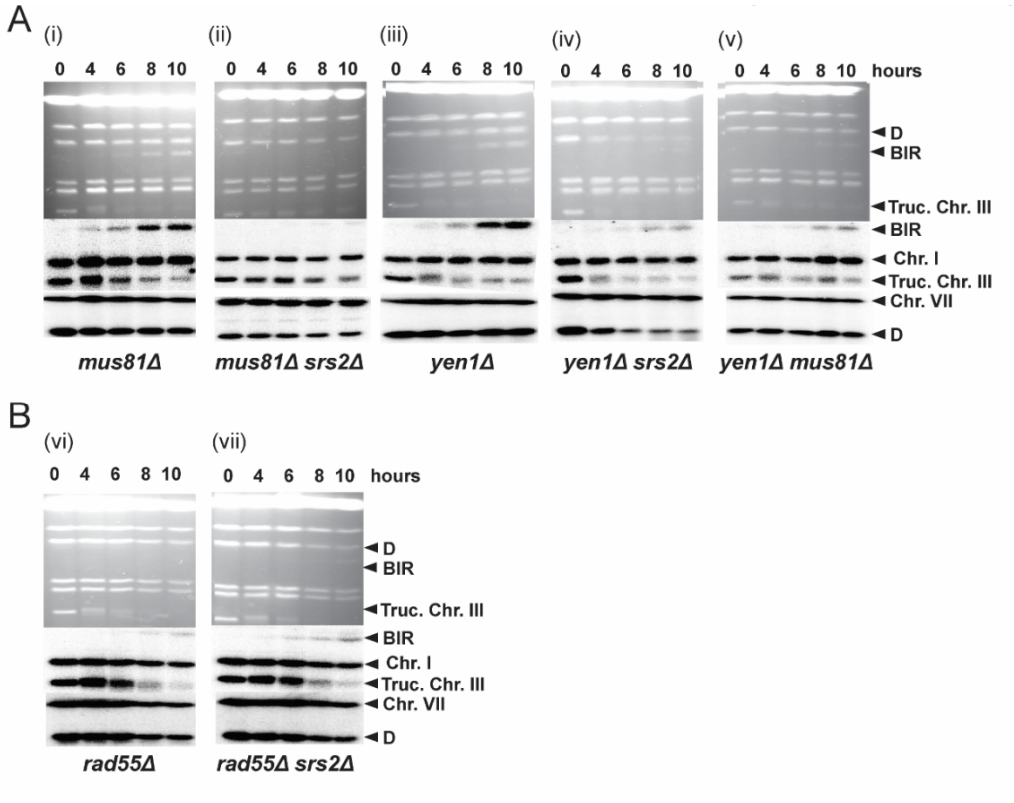

Supplemental Figure 1. Physical analysis of BIR in various mutants. (A) CHEF gel analysis of BIR in (i) *mus81Δ,* (ii) *mus81Δ srs2Δ,* (iii) *yen1Δ,* (iv) *yen1Δ srs2Δ,* (v) *yen1Δ mus81Δ*, (vi) *rad55Δ,* and (vii) *rad55Δsrs2Δ.*

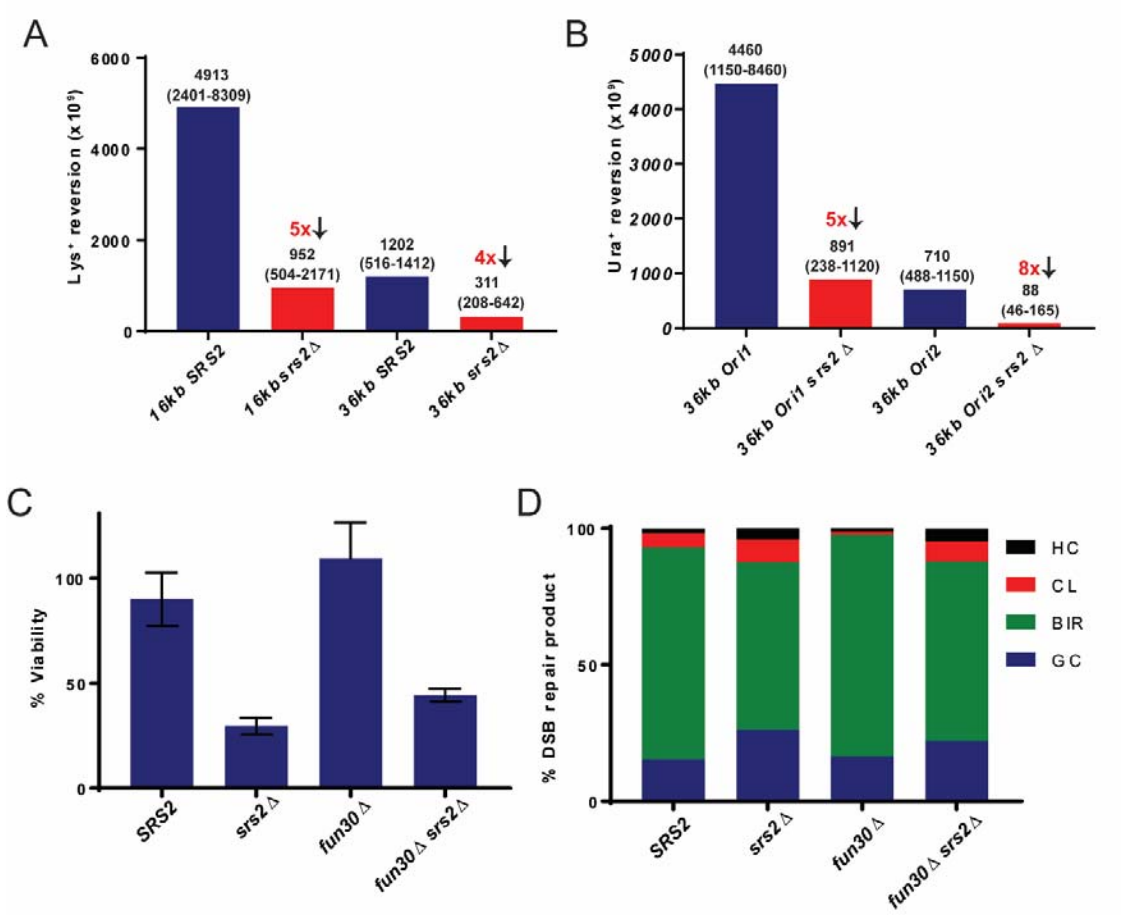

Supplemental Figure 2. Mutagenesis analysis in *SRS2* and *srs2Δ* (A) Analysis of frameshift-mutagenesis in *SRS2* and *srs2Δ* at positions16kb and 26kb away from DSB. *SRS2* (wild-type) data are from (Deem et al., 2011). (B) Analysis of base-substitution mutagenesis in *SRS2* and *srs2Δ* in two orientations (Ori1 and Ori2; (Saini et al., 2013).) at a position 36kb away from the DSB. (C) Cell viability and (D) DSB repair outcomes following BIR induction in resection deficient mutants. Rates are reported as the median value with range of experiments in parenthesis representing a minimum of three individual experiments.

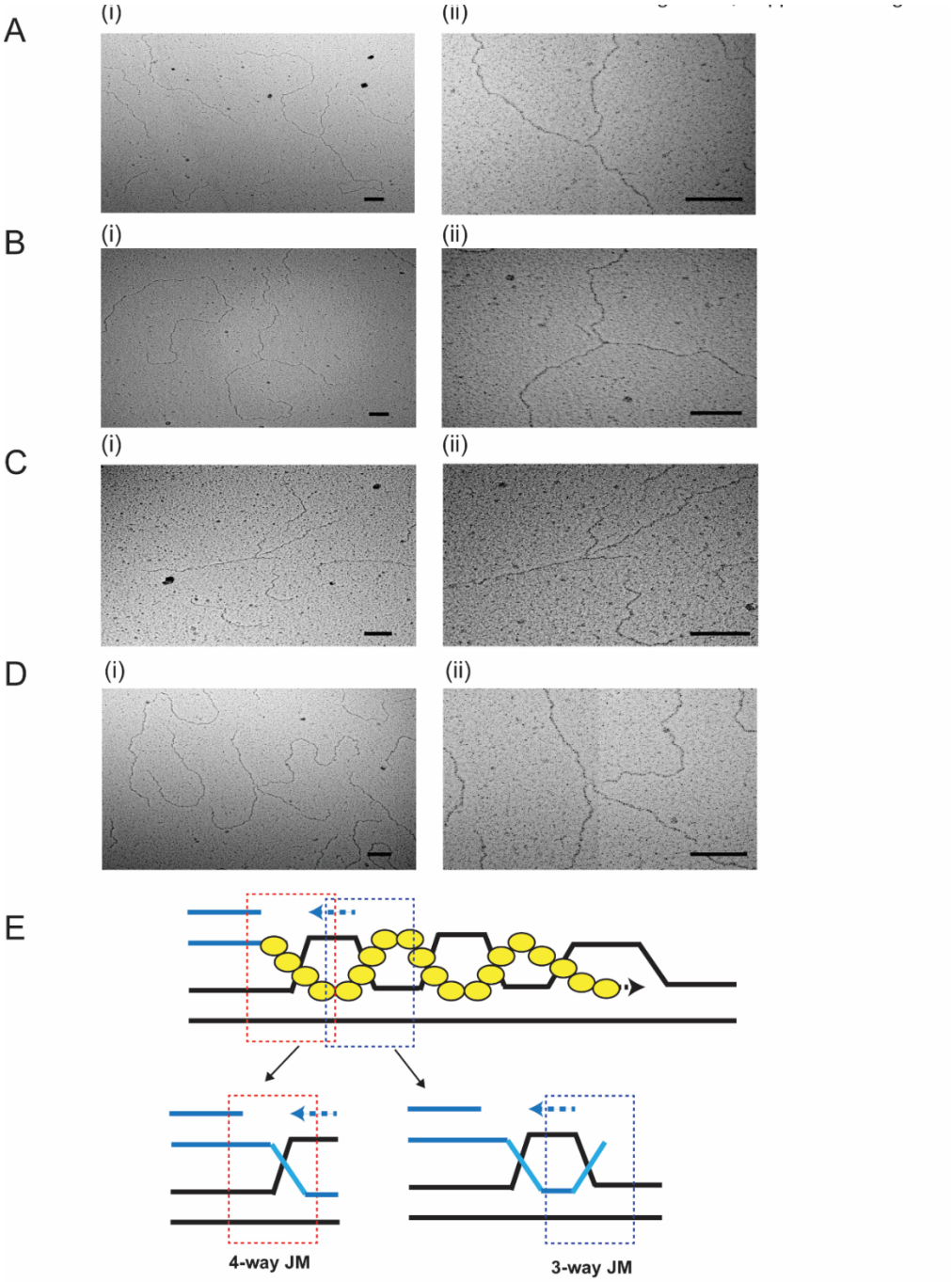

Supplemental Figure 3. Representative images for EM analysis. (A) and (B) 3-way junction in *srs2Δ* and (C) and (D) 4-way junction in *srs2Δ*. Total views of the indicated joint molecule structures are shown in (i) and enlarged views are shown in (ii) (E) Schematic showing 4-way (red dotted rectangle) and 3-way joint molecules (blue dotted rectangle) that could be formed from the 'rubble' intermediate during BIR.

Supplemental Table S1. List of strains

Strain Name	Genotype	Reference
AM3110	*hmlΔ::ADE1/hmlΔ::ADE3 MAT**a**-LEU2-tel/MATα-inc hmrΔ::HPH FS2Δ::NAT/FS2 leu2/leu2-3,112 thr4 ura3-52 ade3::GAL::HO ade1 met13 trp1::p304-BrdU snt1::(TEF1/BSD)$_5$*	This study
AM3257	AM3110 *but srs2::KANMX*	This study
AM3350	AM3110, *but srs2-K41A*	This study
AM3601	AM3110, but *srs2-BRCΔ*	This study
AM3332	AM3110, but *mus81:: ble^r*	This study
AM3610	AM3332, but *srs2::KANMX*	This study
AM3312	AM3110, but yen1::HPHMX	This study
AM3322	AM3312, but *srs2::KANMX*	This study
AM3451	AM3312, but *mus81::ble^r*	This study
AM3572	AM3110 but *Yen1^{ON}*	This study
AM3654	AM3572, but *srs2::KANMX*	This study
AM3658	AM3654, but *mus81:: ble^r*	This study
AM3391	*AM3257 but Matα-inc-LEU2-tel*	This study
AM3457	AM3110 but *rad55:: ble^r*	This study
AM3462	AM3457, but *srs2::KANMX*	This study
AM3485	AM3350, but *rad55::ble^r*	This study
AM3489	AM3601, but *rad55::ble^r*	This study

Supplemental Table S1 continued

AM3340	AM3110, but *rfa1-t33*	This study
AM3362	AM3340, but *srs2::KANMX*	This study
AM3768	AM3110, but *siz1::KANMX*	This study
AM3864	AM3601, but *siz1::KANMX*	This study
AM1291	AM1003, but *lys2::insA$_4$* reporter inserted at 16kb position	(Deem et al., 2011)
AM3205	AM1291, but *srs2:: KANMX*	This study
AM1482	AM1003, but *lys2::insA$_4$* reporter inserted at 36kb position	(Deem et al., 2011)
AM3206	AM1482 but, *srs2:: KANMX*	This study
AM2944	AM1003, but *ura3-29* reporter inserted at 36kb in Orientation 1	(Saini et al., 2013)
AM3201	AM2944, but *srs2::ble^r*	This study
AM2951	AM1003, but *ura3-29* reporter inserted at 36kb in Orientation 2	(Saini et al., 2013)
AM3200	AM2951, but *srs2:: ble^r*	This study
tGI354	*hmlΔ::ADE1 MAT**a**-inc hmrΔ::ADE1 ade1 leu2-3,112 lys5 trp1::hisG ura3-52 ade3::GAL::HO arg5,6::GAL::MAT**a***	(Vaze et al., 2002)
tGI383	tGI354, but *srs2::LEU2*	(Vaze et al., 2002)
tGI572	tGI354, but *rad55::LEU2*	This study

Supplemental Table S1 continued

yDS178	tGI354, but but *srs2::TRP1 rad55::LEU2*	This study
yAP47	tGI354, but *siz1::KanMX*	This study
yAP53	tgi383, but *siz1::KanMX*	This study
yGI96	tGI354, but *pol30-K127R::KanMX*	This study
yGI99	tGI354, but *pol30-K164R::KanMX*	This study
yGI102	yGI96, but *K164R::KanMX*	This study
AM3918	tGI354, but *srs2-BRCΔ*	This study
AM3967	AM3918, but *siz1::KanMX*	This study
YMV80	*hmlΔ::ADE1 mataΔ::hisG hmrΔ::ADE1 leu2-cs ade3::GAL::HO ade1 lys5 ura3-52*	(Vaze et al., 2002)
YMV88	YMV80, but *srs2::KANMX*	(Vaze et al., 2002)
AM3724	YMV80, but *srs2-BRCΔ*	This study

Table S2. Analysis of electron microscopy samples

[a] 3-way and 4-way joint molecule DNA structures

	3-way JM[a]	**4-way JM[a]**	**linear**	**Total**
No-Cut	1	1	1401	1403
srs2Δ	68 **	32*	3760	3860
SRS2	34	13	3348	3395

References

Aboussekhra, A., Chanet, R., Zgaga, Z., Cassier-Chauvat, C., Heude, M., and Fabre, F. (1989). RADH, a gene of Saccharomyces cerevisiae encoding a putative DNA helicase involved in DNA repair. Characteristics of radH mutants and sequence of the gene. Nucleic Acids Res *17*, 7211-7219.

Aguilera, A., and Klein, H.L. (1988). Genetic control of intrachromosomal recombination in Saccharomyces cerevisiae. I. Isolation and genetic characterization of hyper-recombination mutations. Genetics *119*, 779-790.

Aguilera, A., and Klein, H.L. (1989). Yeast intrachromosomal recombination: long gene conversion tracts are preferentially associated with reciprocal exchange and require the RAD1 and RAD3 gene products. Genetics *123*, 683-694.

Bhattacharyya, S., and Lahue, R.S. (2004). Saccharomyces cerevisiae Srs2 DNA helicase selectively blocks expansions of trinucleotide repeats. Mol Cell Biol *24*, 7324-7330.

Blanco, M.G., Matos, J., and West, S.C. (2014). Dual control of Yen1 nuclease activity and cellular localization by Cdk and Cdc14 prevents genome instability. Mol Cell *54*, 94-106.

Chung, W.H., Zhu, Z., Papusha, A., Malkova, A., and Ira, G. (2010). Defective resection at DNA double-strand breaks leads to de novo telomere formation and enhances gene targeting. PLoS Genet *6*, e1000948.

Colavito, S., Macris-Kiss, M., Seong, C., Gleeson, O., Greene, E.C., Klein, H.L., Krejci, L., and Sung, P. (2009). Functional significance of the Rad51-Srs2 complex in Rad51 presynaptic filament disruption. Nucleic Acids Res *37*, 6754-6764.

Deem, A., Barker, K., Vanhulle, K., Downing, B., Vayl, A., and Malkova, A. (2008). Defective break-induced replication leads to half-crossovers in Saccharomyces cerevisiae. Genetics *179*, 1845-1860.

Deem, A., Keszthelyi, A., Blackgrove, T., Vayl, A., Coffey, B., Mathur, R., Chabes, A., and Malkova, A. (2011). Break-induced replication is highly inaccurate. PLoS Biol *9*, e1000594.

Dilley, R.L., and Greenberg, R.A. (2015). ALTernative Telomere Maintenance and Cancer. Trends Cancer *1*, 145-156.

Gangloff, S., Soustelle, C., and Fabre, F. (2000). Homologous recombination is responsible for cell death in the absence of the Sgs1 and Srs2 helicases. Nat Genet *25*, 192-194.

Gueldener, U., Heinisch, J., Koehler, G.J., Voss, D., and Hegemann, J.H. (2002). A second set of loxP marker cassettes for Cre-mediated multiple gene knockouts in budding yeast. Nucleic Acids Res *30*, e23.

Hunter, N., and Kleckner, N. (2001). The single-end invasion: an asymmetric intermediate at the double-strand break to double-holliday junction transition of meiotic recombination. Cell *106*, 59-70.

Ira, G., Malkova, A., Liberi, G., Foiani, M., and Haber, J.E. (2003). Srs2 and Sgs1-Top3 suppress crossovers during double-strand break repair in yeast. Cell *115*, 401-411.

Jain, S., Sugawara, N., and Haber, J.E. (2016). Role of Double-Strand Break End-Tethering during Gene Conversion in Saccharomyces cerevisiae. PLoS Genet *12*, e1005976.

Keyamura, K., Arai, K., and Hishida, T. (2016). Srs2 and Mus81-Mms4 Prevent Accumulation of Toxic Inter-Homolog Recombination Intermediates. PLoS Genet *12*, e1006136.

Klein, H.L. (2001). Mutations in recombinational repair and in checkpoint control genes suppress the lethal combination of srs2Delta with other DNA repair genes in Saccharomyces cerevisiae. Genetics *157*, 557-565.

Krejci, L., Macris, M., Li, Y., Van Komen, S., Villemain, J., Ellenberger, T., Klein, H., and Sung, P. (2004). Role of ATP hydrolysis in the antirecombinase function of Saccharomyces cerevisiae Srs2 protein. J Biol Chem *279*, 23193-23199.

Krejci, L., Van Komen, S., Li, Y., Villemain, J., Reddy, M.S., Klein, H., Ellenberger, T., and Sung, P. (2003). DNA helicase Srs2 disrupts the Rad51 presynaptic filament. Nature *423*, 305-309.

Lawrence, C.W., and Christensen, R.B. (1979). Metabolic suppressors of trimethoprim and ultraviolet light sensitivities of Saccharomyces cerevisiae rad6 mutants. J Bacteriol *139*, 866-876.

Le Breton, C., Dupaigne, P., Robert, T., Le Cam, E., Gangloff, S., Fabre, F., and Veaute, X. (2008). Srs2 removes deadly recombination intermediates independently of its interaction with SUMO-modified PCNA. Nucleic Acids Res *36*, 4964-4974.

Lydeard, J.R., Lipkin-Moore, Z., Sheu, Y.J., Stillman, B., Burgers, P.M., and Haber, J.E. (2010). Break-induced replication requires all essential DNA replication factors except those specific for pre-RC assembly. Genes Dev *24*, 1133-1144.

Malkova, A., Ivanov, E.L., and Haber, J.E. (1996). Double-strand break repair in the absence of RAD51 in yeast: a possible role for break-induced DNA replication. Proc Natl Acad Sci U S A *93*, 7131-7136.

Marini, V., and Krejci, L. (2012). Unwinding of synthetic replication and recombination substrates by Srs2. DNA Repair (Amst) *11*, 789-798.

Mitchel, K., Lehner, K., and Jinks-Robertson, S. (2013). Heteroduplex DNA position defines the roles of the Sgs1, Srs2, and Mph1 helicases in promoting distinct recombination outcomes. PLoS Genet *9*, e1003340.

Mullen, J.R., Kaliraman, V., Ibrahim, S.S., and Brill, S.J. (2001). Requirement for three novel protein complexes in the absence of the Sgs1 DNA helicase in Saccharomyces cerevisiae. Genetics *157*, 103-118.

Neelsen, K.J., Chaudhuri, A.R., Follonier, C., Herrador, R., and Lopes, M. (2014). Visualization and interpretation of eukaryotic DNA replication intermediates in vivo by electron microscopy. Methods Mol Biol *1094*, 177-208.

Niu, H., and Klein, H.L. (2016). Multifunctional Roles of Saccharomyces cerevisiae Srs2 protein in Replication, Recombination and Repair. FEMS Yeast Res.

Oh, S.D., Jessop, L., Lao, J.P., Allers, T., Lichten, M., and Hunter, N. (2009). Stabilization and electrophoretic analysis of meiotic recombination intermediates in Saccharomyces cerevisiae. Methods Mol Biol *557*, 209-234.

Papouli, E., Chen, S., Davies, A.A., Huttner, D., Krejci, L., Sung, P., and Ulrich, H.D. (2005). Crosstalk between SUMO and ubiquitin on PCNA is mediated by recruitment of the helicase Srs2p. Mol Cell *19*, 123-133.

Pfander, B., Moldovan, G.L., Sacher, M., Hoege, C., and Jentsch, S. (2005). SUMO-modified PCNA recruits Srs2 to prevent recombination during S phase. Nature *436*, 428-433.

Potenski, C.J., Niu, H., Sung, P., and Klein, H.L. (2014). Avoidance of ribonucleotide-induced mutations by RNase H2 and Srs2-Exo1 mechanisms. Nature *511*, 251-254.

Ruff, P., Donnianni, R.A., Glancy, E., Oh, J., and Symington, L.S. (2016). RPA Stabilization of Single-Stranded DNA Is Critical for Break-Induced Replication. Cell Rep *17*, 3359-3368.

Saini, N., Ramakrishnan, S., Elango, R., Ayyar, S., Zhang, Y., Deem, A., Ira, G., Haber, J.E., Lobachev, K.S., and Malkova, A. (2013). Migrating bubble during break-induced replication drives conservative DNA synthesis. Nature *502*, 389-392.

Schwacha, A., and Kleckner, N. (1994). Identification of joint molecules that form frequently between homologs but rarely between sister chromatids during yeast meiosis. Cell *76*, 51-63.

Schwacha, A., and Kleckner, N. (1995). Identification of double Holliday junctions as intermediates in meiotic recombination. Cell *83*, 783-791.

Schwartz, E.K., and Heyer, W.D. (2011). Processing of joint molecule intermediates by structure-selective endonucleases during homologous recombination in eukaryotes. Chromosoma *120*, 109-127.

Storici, F., and Resnick, M.A. (2003). Delitto perfetto targeted mutagenesis in yeast with oligonucleotides. Genet Eng (N Y) *25*, 189-207.

Vasianovich, Y., Altmannova, V., Kotenko, O., Newton, M.D., Krejci, L., and Makovets, S. (2017). Unloading of homologous recombination factors is required for restoring double-stranded DNA at damage repair loci. EMBO J *36*, 213-231.

Vaze, M.B., Pellicioli, A., Lee, S.E., Ira, G., Liberi, G., Arbel-Eden, A., Foiani, M., and Haber, J.E. (2002). Recovery from checkpoint-mediated arrest after repair of a double-strand break requires Srs2 helicase. Mol Cell *10*, 373-385.

Veaute, X., Jeusset, J., Soustelle, C., Kowalczykowski, S.C., Le Cam, E., and Fabre, F. (2003). The Srs2 helicase prevents recombination by disrupting Rad51 nucleoprotein filaments. Nature *423*, 309-312.

Wilson, M.A., Kwon, Y., Xu, Y., Chung, W.H., Chi, P., Niu, H., Mayle, R., Chen, X., Malkova, A., Sung, P.*, et al.* (2013). Pif1 helicase and Poldelta promote recombination-coupled DNA synthesis via bubble migration. Nature *502*, 393-396.

Yeung, M., and Durocher, D. (2011). Srs2 enables checkpoint recovery by promoting disassembly of DNA damage foci from chromatin. DNA Repair (Amst) *10*, 1213-1222.

Zakharyevich, K., Tang, S., Ma, Y., and Hunter, N. (2012). Delineation of joint molecule resolution pathways in meiosis identifies a crossover-specific resolvase. Cell *149*, 334-347.

PUBLICATIONS

Fragile DNA motifs trigger mutagenesis at distant chromosomal loci in saccharomyces cerevisiae. Saini N, Zhang Y, Nishida Y, Sheng Z, Choudhury S, Mieczkowski P, Lobachev KS.PLoS Genet. 2013

A reversible histone H3 acetylation cooperates with mismatch repair and replicative polymerases in maintaining genome stability. Kadyrova LY, Mertz TM, Zhang Y, Northam MR, Sheng Z, Lobachev KS, Shcherbakova PV, Kadyrov FA.PLoS Genet. 2013

Genome-wide screen reveals replication pathway for quasi-palindrome fragility dependent on homologous recombination. Zhang Y, Saini N, Sheng Z, Lobachev KS.PLoS Genet. 2013

Rtt107 Is a Multi-functional Scaffold Supporting Replication Progression with Partner SUMO and Ubiquitin Ligases. Hang LE, Peng J, Tan W, Szakal B, Menolfi D, Sheng Z, Lobachev K, Branzei D, Feng W, Zhao X. Mol Cell. 2015

Detox role of Srs2 in double-strand break repair: preventing and unwinding of toxic joint molecules. Elango R., Sheng Z., DeCata J., Ibrahim Y., Ira G. Lobachev KS and Malkova A. 2017 (in preparation)

Three distinct pathways for double-strand break formation at palindromic repeats in yeast. Sheng Z, Saini N, Mieczkowski P.A., Lobachev, KS. 2017 (in preparation)

Bidirectional break-induced replication involving sister-chromatids is triggered by breakage at palindromes. Sheng Z, Guo W, Lobachev KS. 2017 (in preparation)